國 立 交 通 大 學

交通運輸研究所

博 士 論 文

No.064

汽機車混合車流模擬—新細胞自動機模型之研發

Car/Motorcycle Mixed Traffic Modeling: A New Cellular Automaton Approach

指導教授：藍武王博士、邱裕鈞博士

研 究 生：林日新

中 華 民 國 九 十 九 年 六 月

汽機車混合車流模擬—新細胞自動機模型之研發

Car/Motorcycle Mixed Traffic Modeling: A New Cellular Automaton Approach

研 究 生：林日新　　Student: Zih-Shin Lin

指導教授：藍武王博士　　Advisors: Dr. Lawrence W. Lan

邱裕鈞博士　　Dr. Yu-Chiun Chiou

國 立 交 通 大 學

交 通 運 輸 研 究 所

博 士 論 文

A Dissertation

Submitted to Institute of Traffic and Transportation

College of Management

National Chiao Tung University

in Partial Fulfillment of the Requirements

for the Degree of Doctor of Philosophy

in

Management

June 2010

Taipei, Taiwan, Republic of China

中 華 民 國 九 十 九 年 六 月

汽機車混合車流模擬-新細胞自動機模型之研發

研 究 生：林日新　　指導教授：藍武王博士、邱裕鈞博士

國立交通大學交通運輸研究所

摘要

細胞自動機模型可分類為一種微觀的數值模擬車流模型，近年來世界各地學者曾提出多種不同的細胞自動機車流模型，用以模擬現實生活中各種複雜的交通現象。但由於目前細胞自動機模型主要應用相對稀疏之格點系統，導致其無法應用於都市之交通模擬，因此本研究提出一種全新的細胞自動機模型，以克服上述限制，並將細胞自動機模型之應用範圍擴展至都市交通之模擬。

本研究基本上可分為三部份，首先，本研究提出一個具細微格點系統之細胞自動機模型，以提昇進行交通模擬時之模型解析度，並有效反應微觀的交通車流特性。與現有其它細胞自動機車流模型相較，本研究所提出細微格點系統之細胞自動機模型主要有三項明顯差異；首先本研究提出「共有單元」的概念做為描述不同車輛尺寸及不同道路寬度的共同基本單元，而一單獨細胞單位及網格則分別定義為車輛及道路之基本單元。其次本研究提出立體通用交通參數之觀念，如此於進行交通模擬時可將不同車輛尺寸及不同道路寬度之影響納入評估。以上述細微格點系統之細胞自動機模型為基礎，本研究並建議採用線段線性變化之車輛速度變化方式，接下來本研究並將車輛之減速能力亦納入交通模擬之分析範圍，以改正現有多數細胞自動機模型模擬結果中普遍存在的一個重要瑕疵，亦即當車輛遭遇障礙物或抵達塞車車陣之後緣時會有不合理的急速剎車行為。本研究所構思的減速機制事實上源起於 1950 年代美國學者 Pipes 及 Forbes 等人所提出原始車流理論。後續模擬結果證實，本研究所提出之減速機制已成功改正現有細胞自動機模型上述車輛不合理減速現象。

其次，本研究建立於應用上述細微格點系統之細胞自動機模型進行交通模擬時擷取區域路段交通參數數據之有效方法。模擬結果亦證實透過

上述方式所擷取之區域路段交通參數資料除可成功印證德國知名學者 Kerner 於 2004 年所提出之三相車流理論外，並可描述三種車流車相間之相變化。

在本研究的第三部份中，藉由上述改良之細微格點系統，對由汽車及機車所組成之混合車流形態之交通特性進行模擬及分析。模擬結果證實，本研究所提出之細胞自動機模型可模擬一些重要的都市交通之混合車流現象，如機車於塞車車陣中之橫向移動或由車陣後方兩輛並排車輛間空隙鑽入車陣之複雜行為。

雖然現有之細胞自動機車流模型仍廣受認同，但仍持續有人質疑其應用範圍多限縮於高速公路交通模擬，且無法由微觀角度成功描述細微之車輛行為。反之，透過模擬結果分析，可印證本研究所提出新細胞自動機模型之優越性，因其成功地克服一般現有細胞自動機車流模型之適用限制，將可用以分析實際生活中多變的交通現象。基於本研究所提出新細胞自動機模型具有高解析度及高應用彈性等優點，未來各種不同的交通現象，如由不同種類車輛所組成之混合車流形態及複雜的都市交通現象，無論由巨觀或微觀觀點，皆可藉之進行分析模擬。期待本研究所建立新細胞自動機模型未來成為細胞自動機模型發展歷程中之一項重要突破，並加速交通模擬技術之發展。預期未來各種不同之交通管制策略於實際採用前將可應用本研究所建立新細胞自動機模型於事前評估其效果。

關鍵字：細微細胞自動機模型、時空交通參數、混合車流、機車

Car/Motorcycle Mixed Traffic Modeling: A New Cellular Automaton Approach

Student: Zih-Shin LIN

Advisors: Dr. Lawrence W. LAN
Dr. Yu-Chiun CHIOU

Institute of Traffic and Transportation
National Chiao Tung University

Abstract

Recently, various cellular automaton (hereinafter referred to as CA) models that can be categorized as one branch from the microscopic viewpoint, were developed to describe the phenomena of real traffic flows characterized with complex dynamic behaviors. However, the coarse cell unit adopted in existing CA models makes them extremely difficult to implement urban traffic simulation. Therefore in this study, a novel CA model is developed, in order to release this restriction and henceforth expands the application of CA model to urban traffic scenarios.

This study basically can be divided into three-folds. First, as the onset, a CA model with refined cell/site system is developed in order to enhance the simulation resolution and henceforth to efficiently gauge the microscopic traffic characteristics. Here three important amendments, as compared with traditional CA models, are carried out. First of all, the concept *"common unit"* is defined to serve as the basic unit for simulating both roads of various widths and vehicles in various sizes, where *"cell"* and *"site"* represent the basic unit for vehicle and roadway space respectively. Following that, the 3-D generalized traffic parameters are defined so as to take vehicular and/or roadway widths into consideration. Coupled with this refined cell/site system, piecewise-linear speed variation is introduced into CA simulations. Following this, limited deceleration which in essence arising from Pipes and/or Forbes' car-following concept, is also proposed for the sake of rectifying one common defect in most existing CA models—unrealistic abrupt deceleration as vehicles

encounter stationary obstacles or upstream front of traffic jams. It is evidenced that the proposed refined CA model successfully fixed the unrealistic deceleration behaviors.

Next, the methodology for deriving local traffic parameters when implementing our refined CA models is also defined. The simulation results show that through the derived local traffic parameters, the renowned three-phase traffic patterns, as proposed by Kerner (2004), and the phase transitions among them can be successfully simulated.

In the third part of this study, based upon the aforementioned refined CA model, mixed traffic comprised by cars and motorcycles are analyzed. The simulations reveal that the proposed CA model successfully gauges some important traffic characteristics of urban traffic, such as the unique transverse drift behaviors of motorcycles when break inside traffic jams and the lateral drift behavior for motorcycles breaking into two moving cars from the upstream front of traffic jam.

Aside from their popularity, the existing CA models in the past were continuously criticized for their significantly biased application to freeway traffic and their failure to uncover delicate vehicular behavior from microscopic viewpoint. On the other hand, our simulations evidence the superiority of the proposed novel CA model since it successfully liberates the above-mentioned restriction and is able to capture the violate traffic phenomena in real world. Based upon the enhanced resolution and the increased flexibility of the proposed CA model, analysis of different traffic contexts, such as the mixed traffic comprised by vehicles of various sizes and sophisticated traffic phenomena in urban area, either from microscopic or macroscopic perspective, will be practical in the future. Thus the proposed novel CA model can be deemed as a breakthrough progress in development of CA model and shed some light for the future analysis of traffic modeling. It is looking forward that via the proposed CA model different traffic control strategies for separate traffic contexts can be efficiently evaluated before practical implementation.

Keywords: Refined Cellular Automaton Model, Spatiotemporal Traffic Parameters, Mixed Traffic Flows, Motorcycles

誌謝

六年前得知被錄取博士班的那一刻，心中充滿著雀躍與期待。離開學校已十六個年頭，校園裏的一切是如此熟悉又如此陌生。然一路走來，途中佈滿了層層關卡，心情也隨著關關考驗的來臨而起起伏伏。修完了學分，在忐忑中通過了博士候選人資格考試，原以為可以稍微鬆口氣，但隨著研究進行，多少夜深人靜的假日晚上，獨自埋首程序除錯或撰寫期刊論文，往往不覺已近天明，其間的甘苦如人飲水，冷暖自知。而期刊論文發表的喜悅，亦非筆墨所能言盡。

首先感謝民航局的各級長官，同意我以在職進修方式攻讀博士學位。其次感謝交大交研所的各位老師，錄取一個非交通管理背景的工程師，讓我能重回學術殿堂，重溫快樂的學生生活。在學期間，承蒙恩師藍武王老師及邱裕鈞老師細心指導，讓我學習到周延的思考以及任何細節都不能忽略的研究精神。藍老師嚴謹的教學態度及律己甚嚴的治學精神，惠我良多，未來的職場生涯必將受用無窮。邱老師的殷殷督促及對於研究方向及論文寫作的指導，使我的論文得以順利完成，誠摯感謝。在職進修的研究生活緊湊忙碌，尤其公務繁重經常影響研究與期刊投稿的進度，感謝藍老師及邱老師的包容與體諒，容忍我緩慢的研究進度，讓我得以兼顧學業與工作。

此外，承蒙學長姐及學弟妹許多協助。感謝志誠學長及 Gary，沒有他們完成模擬程式基本架構的建立，不可能有後續混合車流模式的發展。志誠學長對於模擬結果及圖表繪製的協助，是投稿國際期刊得以被快速接受的重要關鍵之一。資格考戰友承憲、群明、文斌、立欽無私地將蒐集所得資料與讀書心得與我分享，使我得以順利通過資格考試，易詩、世昌學長及承憲、姿慧、士軒、永祥、香怡、建樺等學弟妹於修課時的協助，民航局的工作伙伴玉成、洸洋及本雄於在學期間公務上的配合，在此一併致謝。此外，還要感謝可愛的姪女 Patricia 及侄子 Timothy 於定稿時英文文法校正的協助，使我的論文更臻完善。

我要將這篇論文獻給在背後默默支持我的家人，特別是愛妻素卿，雖身為職業婦女公務繁重，但在我就學期間仍承擔大部份家務及兩個青春期兒子的教養工作，讓我無後顧之憂地完成學業。當課業或研究遇到瓶頸心情低落時，她的鼓勵及安慰往往是我重新出發的動力來源。感謝兩個兒子博源和博仁的包容，因為在他們成長的重要階段，我無法全程陪伴。最

後；感謝老爸、老媽與老姐、老弟對我的鼓勵。他們期待我畢業已經夠久了。

六年來的時光點滴在心頭，感謝所有支持我、關心我的人，期許自己在未來的日子能平安喜樂、福慧雙修。

CONTENTS

LIST OF FIGURES

LIST OF TABLES

CHAPTER 1 INTRODUCTION

1.1 Motivation

Understanding vehicular moving behaviors provides the fundamental rationales for planning, designing, controlling and managing the road systems. In order to avoid the time- and money-consuming field observations, numerical implementation can be used as an efficient instead for providing precious reference and guidance. Therefore, along with the rapid progress of digital technology since early fifties, numerous traffic simulation models have been plentifully proposed.

Generally, existing traffic models can be roughly separated into three branches; depending on the level of detail or resolution of traffic been derived—macroscopic, microscopic and mesoscopic models. The coarsest ones are the macroscopic models which include the traffic flow models and fluid-dynamical models. Traffic flow models analyze the relationships between speed, density and volume (May, 1990). Fluid-dynamical models, on the other hand, analogize vehicular flow to fluids and assume that aggregate behavior of drivers is dominated by the surrounding traffic conditions. Lighthill and Whitham (1955) and Richard (1956) developed the most prominent one-order fluid-dynamical models. Subsequently, high-order fluid-dynamical models were developed by other researchers; for example, Payne (1971), Liu *et al* (1998) and Zhang (1998).

The microscopic traffic flow models, in contrast, describe the interaction between individual vehicle and other vehicles. Car-following models are the most pertinent models to explicate the one-dimensional movements in a longitudinal lane such that the following vehicle adjusts its speed to maintain desirable or safe distance headway to the lead vehicle. Stimulus-response models are perhaps the most prominent models developed in the 1950s and 1960s by the General Motors (GM) research group, because the same principles is still being applied and/or extended nowadays by scholars worldwide, for example, that by May (1990), Brackstone and McDonald (1999), Lan and Yeh (2001), etc.

The third branch, the mesoscopic models, serves as the linkage to fill the gap between the aggregate level approach of macroscopic models and the

individual viewpoint in the microscopic ones. Mesoscopic models aim to describe the behavior of small groups of vehicles. Examples of these models are the cluster models, gas-kinetic models and the cell transmission models. Prigogine & Herman (1971) proposed the kinetic equation of vehicular traffic and summarized the possible alternate forms of the relaxation term. Hoogendoorn and Bovy (1999) proposed a traffic flow model describing multilane heterogeneous (i.e. unconstrained and constrained) traffic flow. Various kinetic models were subsequently proposed by many researchers, such as Paveri-Fontana (1975), Phillips (1979), and more recently Nelson (1995), and Nelson and Sopasakis (1998). Daganzo (1993, 1994) proposed the cell transmission model (CTM model for short) and since then have been popularly utilized for traffic simulation.

Recently, various CA models that can be categorized as one branch from the microscopic perspective have been developed to describe the phenomena of real traffic flows with complex dynamic behaviors, owing to their capacity for reflecting complicated traffic patterns via comparatively concise numerical algorithms. Nagel and Schreckenberg (1992) proposed their famous pioneer model (referred as for NaSch model hereinafter) to reproduce the basic features of real traffic. In their model, the road is divided into squared cells of length 7.5 meters. Each cell can either be empty or occupied by at most one car (i.e., the size of a car is viewed as one cell). Space, speed, acceleration and even time are treated as discrete variables. The state of the road at one certain instant is derived from one time-step ahead by applying acceleration, braking, randomization and driving rules for all cars at the same instant (i.e., parallel dynamics). Obviously, such a coarse description is an extreme simplification of real world conditions; therefore, a considerable number of modified NaSch models has been developed in the past decade. For instance, Nagel (1996, 1998) employed the concept of stochastic CA and treated each particle with randomized-integer speed between zero and maximum speed. Rickert *et al* (1996) examined a simple two-lane CA model and pointed out some important parameters that define the shape of the fundamental diagram (flow-density); Chowdhury *et al* (1997) generalized the NaSch model by introducing a particle-hopping model for two-lane traffic with two different vehicle speeds (fast and slow); Barlović *et al* (1998), in contrast to the constant randomization in the NaSch model, introduced a velocity-dependent randomization (VDR) parameter. Although the VDR model is a simple generalization of the NaSch

model, it is capable of revealing some complex traffic dynamics, i.e., the existence of wide phase separated jams and metastable free-flow states. Nagel *et al* (1998) further proposed different CA rules to govern vehicular lane-change behavior. More Recently, Boris Kerner (2002, 2004), a German traffic physician, introduced a three-phase traffic theory that consists of free flow, synchronized flow, and wide-moving jam phases. The latter two phases exist in congested states in which downstream front of the synchronized flow phase is often fixed at a bottleneck while the wide-moving jam will propagate through the position where bottleneck locates. To explore the emergence of such traffic patterns, Kerner and partners tried to describe the complex spatiotemporal behaviors based on empirical freeway traffic analysis. (Kerner *et al*, 2004)

Over the years, most conventional CA models were developed for depicting the traffic phenomena on freeways. However, most of times these models were limited to the simulation of pure traffic scenarios in which vehicles have identical size. Few has been devoted to the analysis of urban traffic such as mixed traffic that is comprised by vehicles in various sizes; such as heavy vehicles (e.g., bus, truck), light vehicles (car) and of course, smaller two-wheel ones (motorcycle, bicycle). It is evidenced that the coarse cell system in existing CA models makes it extremely impossible to reflect various vehicle sizes and the slight speed variation of vehicles on urban streets. Thus inevitably refined cell system must be established beforehand if one ever tries to successfully simulate the urban traffic.

In addition to the refined cell system, some unique behaviors must also be scrupulously considered in places where both cars and motorcycles are introduced. Unlike heavy or light vehicles that normally move within a specific longitudinal lane and sometimes change lanes for overtaking or turning, motorcycles do not move in a specified lane. As the result, conventional flow models may not satisfactorily elucidate the motorcycles' moving behaviors. Because motorcycles are the most popular transportation mode in Taiwan as well as in some other Asian countries, it is important to gain better insights of the motorcycles' moving behaviors, from both academic and practical perspectives.

1.2 Research Objectives

The final goal of this study is to develop an effective CA model capable of simulating urban traffic with different vehicle kinds and/or sizes introduced. To fulfill this, the intended multiple purposes of this study can be outlined sequentially as follows.

A To introduce refined grid system to facilitate the implementation of CA into urban traffic simulation

A refined *"cell unit"* is first proposed for developing the novel CA model. Henceforth, the rules governing the forward movement and lateral shift of vehicles that come into different sizes and their incurred interactions can be conscientiously elucidated. Along with this, the general 3-D traffic parameters, including density, traffic flow and spatiotemporal averaged speed will also be introduced.

B To establish CA update rules for describing vehicular movements

The primitive CA update rules are devised in reference to that proposed in existing CA efforts. In addition, revised CA update rules will be developed to rectify the common defect prevailed in existing CA models, i.e., abrupt deceleration when vehicles encounter stationary obstacles or approach upstream front of traffic jams, as to reflect more precisely the real driving behaviors in real world.

C To define means to measure local traffic parameters

Methodology for deriving local traffic parameters in the proposed refined CA model will be created. Accordingly, macroscopic traffic parameters such as traffic flow, density and speed in various traffic conditions (i.e., with bottleneck, lane-drop, signalized intersection, etc.) can be well derived whereas the local traffic parameters from microscopic approach that describing the incurred complex spatiotemporal traffic patterns and the transitions among them, either on highways or urban streets, can also be obtained.

D To develop sophisticated CA model capable of simulating car/motorcycle mixed traffic

Simulation of various traffic scenarios, such as different car/motorcycle ratios that prevailed in urban streets via the refined CA models will be

implemented. The relevant CA update rules for delineating complicated behaviors of motorcycles will be defined as well. It is expected that some important spatiotemporal characteristics thereof can be successfully obtained.

1.3 Research Framework

To cope with the research purposes, as mentioned, the research framework is demonstrated in the flowchart as shown in Figure 1-1. Each step therein is elaborated in the followings.

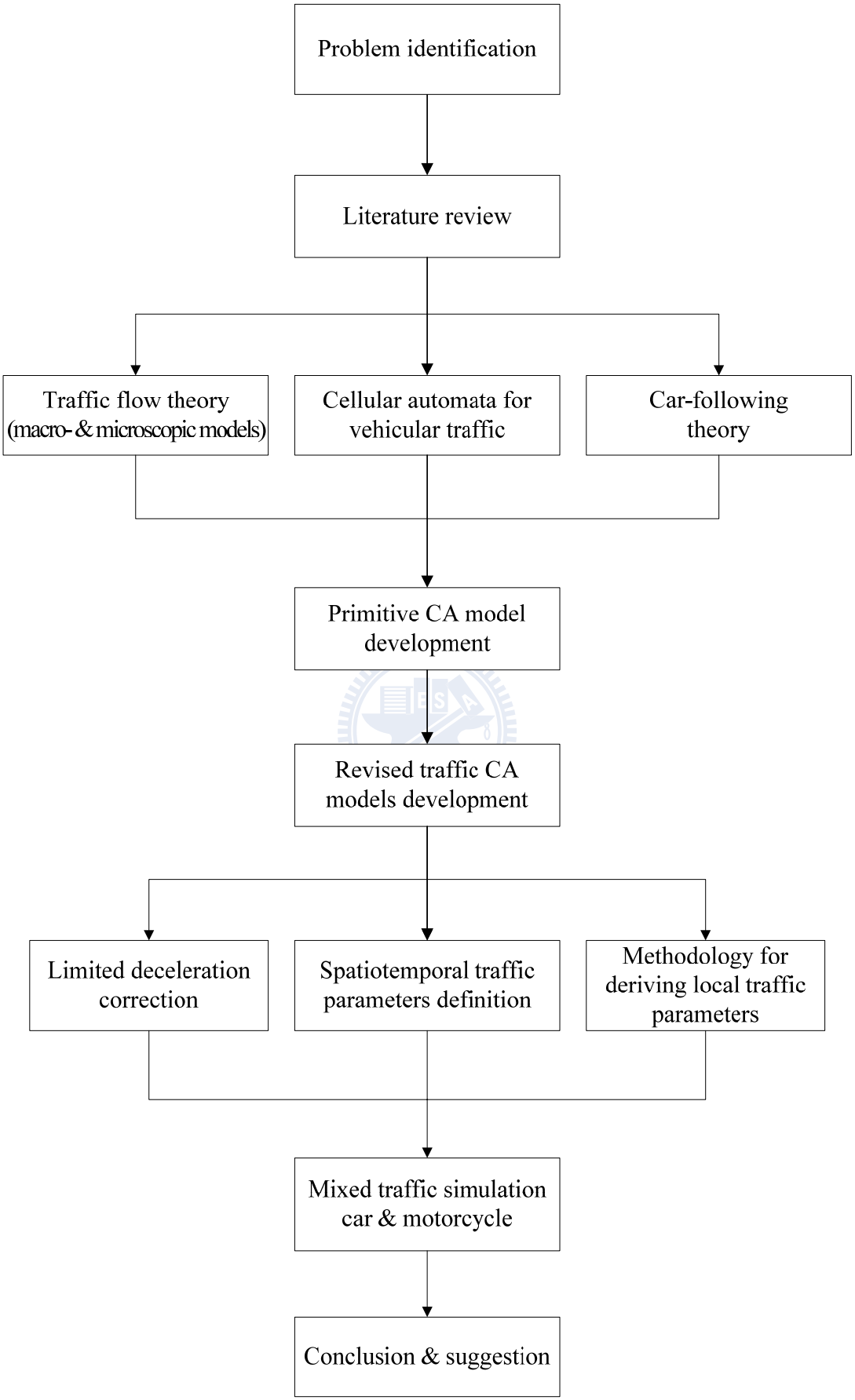

Figure 1-1. Research framework

(1) Problem identification

The first step is to identify the purposes and scope of this study, and to address problems that need to be explored.

(2) Literature review

The second step is to review related researches in traffic flow theories, including macroscopic, microscopic, mesoscopic models and the car-following theory, especially the existing CA models. This puts the current status of traffic modeling in perspective and identifies the potential defects of existing traffic models that impede their implementation for urban traffic simulation.

(3) Development of basic refined CA models

In this step a refined CA model is proposed, introducing drivers' heterogeneity into simulation. As the first groundwork, a refined *"common unit"* is defined so as to fulfill the required *"resolution"* for urban traffic simulations. Along with that, several spatiotemporal traffic parameters are thereby devised. Second, referring to traditional CA models, some basic forward and lane-change rules that govern vehicular movements are developed. The refined CA model, coupled with these basic CA update rules, is capable of capturing the essential features of traffic flows, including those found in previous works. Thirdly, to cope with the real vehicular performance behavior with required precision, the basic model is extended further to mandate vehicles equipped with piecewise linear speed variation as well as limited deceleration capacity. It shows that this amendment can reflect the genuine driver behavior in real world and is capable of revealing Kerner's three-phase traffic patterns. By end of this step, the methodology for deriving local traffic parameter in the proposed refined CA model will also be developed.

(4) Development of sophisticated CA models

Upon the refined CA model developed in step 3, simulations for mixed traffic with diverse compositions of cars and motorcycles are carried out. For this, CA update rules, especially lateral movement update rules besides the lane-change rules, must be addressed according to the attributes of each individual vehicle and the traffic situations around it. Therefore a

sophisticated CA model to elucidate the erratic motorcycle behavior in mixed traffic contexts is devised. In addition to the conventional moving forward and lane-change rules, the sophisticated CA model also explicates the lateral drift behavior for cars moving in the same lane, the lateral drift behavior for motorcycles breaking between two moving cars, and the transverse crossing behavior for motorcycles through the gap between two stationary cars in the same lane. Fundamental diagrams and space-time trajectories for vehicles with various car-motorcycle mixed ratios are demonstrated and compared with existing effort..

(5) Conclusions and recommendations

After the exhaustive and deliberate explorations, the findings in the model formulation and validation will be summarized. The strengths and weaknesses of the proposed model will then be discussed, followed by some recommendations for future study.

1.4 Chapters Organization

This thesis is organized as follows. Chapter one briefly describes existing traffic flow models and illustrates the motives for proposing the new CA model, followed by a brief circumscription of research objectives, research framework of this study. Chapter two overviews previous works and the diverse existing traffic flow models, especially the progress of CA models in latest two decades. Chapter three examines first the main defect of existing CA models, in particular, the deficiency for urban traffic simulation is pointed out and the potential cause is discussed; following is a detail illustration of the developed refined CA model. Chapter four describes the methodology for measuring local traffic parameters via the proposed CA model. Chapter five further proposes the sophisticated CA model for mixed traffic comprised by cars and motorcycles. Chapter six summarizes, concludes and addresses issues for future studies.

CHAPTER 2 LITERATURE REVIEW

Conventional traffic flow models can be roughly separated into macroscopic, microscopic and mesoscopic models, as the level of detail in simulation ranges from the coarsest to the finest, respectively. Macroscopic models describe traffic flow as fluid flow and hence analyze traffic phenomena at a high level of aggregation (for example, number of vehicles per hour that pass a certain spot) without considering its constituent parts (the vehicles), Microscopic models describe the behaviors of the entities making up the traffic flow (the vehicles) as well as their interactions in detail. On the other hand, mesoscopic models are at an intermediate level of detail, oftentimes aiming at description of vehicles in groups instead the interactions among individual vehicles. All these approaches, especially the prominent car-following theory and related vehicular traffic theory are reviewed in this chapter.

2.1 Macroscopic Approaches

Macroscopic traffic models were virtually originated from fluid dynamics in which traffic flow is treated as continuous chain and behaves analogous to fluid flow. Thus, the continuity equation for traffic flow can be derived via the well-known Reynolds transport theorem. Therefore, relationship among some important traffic parameters, such as traffic flow, density and average speed from global perspective can be derived. The basic philosophy thereof, the renowned law of conservation of mass flow, is illustrated as below.

2.1.1 Conservation law for traffic flow

The general form of Reynolds transport theorem that familiar to scholars in fluid dynamics field is enclosed as Equation 2-1.The LHS of Equation (2-1) represents the variation rate of a moving system B at time-step t from Lagrangian viewpoint (i.e., a coordinate system following the movement of system B), whereas the RHS thereof represents the summation of variations inside a fixed control volume (CV) and the influx/outflux across the control surface (CS) at same time-step, i.e., from Eulerian viewpoint, as shown in Figure 2-1. The parameter b is defined as elementary unit of system B.

$$\frac{DB}{Dt} = \oiint_{cs} b(\rho V \cdot dA) + \frac{\partial}{\partial t} \iiint_{cv} (b\rho) dV \tag{2-1}$$

where

$$B = \iiint_{system} b\rho dV \tag{2-2}$$

When B is set as mass (or say, b equals to unity), and the mass of system B is assumed to be unchanged (in traffic theory, this implies that there is no vehicular exit or access for system B), Equation (2-1) is transformed into the so-called equation of conservation for mass flow—the continuity equation, shown as Equation (2-3).

$$\frac{\partial}{\partial t} \iiint_{cv} \rho dV + \oiint_{cs} \rho V \cdot dA = 0 \tag{2-3}$$

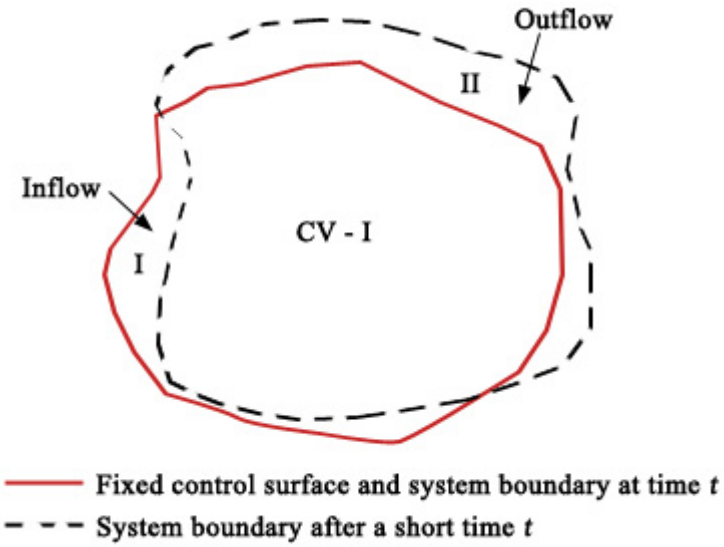

Figure 2-1. A general description of relationship among fixed control volume, control surface and a moving system for defining Reynolds transport theorem.

2.1.2 Lighthill-Whitham-Richards (LWR) model

For traffic prevailed on freeway, since longitudinal movement is the main concern, the continuity equation is further simplified into a two-dimensional equation with two independent variables—location x at an instant of time t. Upon this, Lighthill and Whitham (1955) first conjectured that density is the function of the two above-mentioned independent

variables—$\rho=\rho(x,t)$. After that, they adopted the traditional formula for estimating fluid flow rate q (Equation 2-4). Thus the continuity equation in form of first order partial differential equation (PDE) can be derived as Equation (2-5):

$$q = \rho v \tag{2-4}$$

$$\frac{\partial \rho(x,t)}{\partial t} + \frac{\partial q(x,t)}{\partial x} = 0 \tag{2-5}$$

An additional hypothesis was inspired by the q-ρ profile from the theoretical fundamental diagram of traffic (FD, see Figure 2-2) to assume that flow is the function of density only (Equation (2-6)); therefore Equation (2-5) can be reduced as Equation (2-7).

$$q = q(\rho) \tag{2-6}$$

$$\frac{\partial \rho(x,t)}{\partial t} + \frac{\partial q(\rho(x,t))}{\partial x} = 0 \tag{2-7}$$

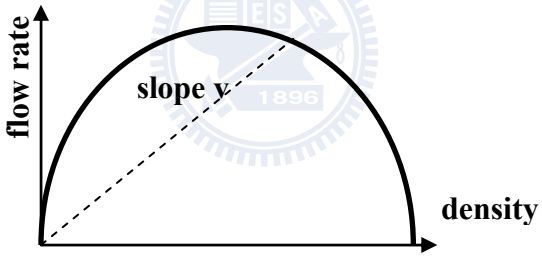

Figure 2-2. The theoretical fundamental diagram of traffic.

Since now there is only one dependent variable—the vehicles' density ρ in the derived equation; it becomes possible to obtain the analytic solution of this PDE if its initial and boundary conditions are both given and, finally leading to a solvable traffic flow model.

In the LWR theory, a traffic disturbance is propagated by kinematic waves at a speed

$$\text{Kinematic waves (KW)} \quad c = \frac{dq(\rho)}{d\rho} \tag{2-8}$$

According to Equation 2-8 and Figure 2.2, one can find that the KW velocity is positive on the part of the fundamental diagram where the flow rate

increases with density, and it is negative on the part of the fundamental diagram where the flow rate decreases with density.

Besides the effort of Lighthill and Whitham, one year later Richards (1956) published a similar model. Therefore, this model is usually referred to as the Lighthill-Whitham-Richards (LWR) model.

2.1.3 Other macroscopic models

Obviously LWR model is an over-simplification of traffic phenomena, since it assumes a homogeneous and deterministic traffic flow and it implies smooth and concave functionso for both speed and density. Therefore in the past three decades, many efforts were devoted in improving the LWR model. Most notable studies in this regard include the work by Bick and Newell (1960) for two-lane bidirectional road, by Munjal and Pipes (1971) for multi-plane freeways and those by Liu *et al* (1998) and Zhang (2005) of high-order similar models. In the same spirit, some other proposed systems of finite different equations (FPE) to model freeway traffic, such as Payne (1971) and Daganzo (1995). Wong and Wong (2002) further formulated a multi-class traffic flow model as an extension of LWR model with heterogeneous drivers.

2.2 Mesoscopic Approaches

Mesoscopic models bridge the gap between macroscopic and microscopic models by combining the aggregate traffic flow variables with some assumptions on the interactions among vehicles. Mesoscopic models normally describe the traffic entities at a high level of detail whilst their behaviors and interactions are described at a lower level of detail.

The mesoscopic models can take varying forms. One form is vehicles grouped into packets, which are routed through the network (Leonard *et al*, 1989). Each packet of vehicles acts as one entity and its speed on each road (link) is derived from a speed-density function defined for that link as well as the density on the link at the moment of entry. The density on a link is defined as the number of vehicles per kilometer per lane. A speed-density function relates the speed of vehicles on the link to the density.

The second approach is the gas-kinetic traffic models. Analogous to gas kinetic theory, in these models traffic flow is treated as a gas of interacting

particles where each particle represents a vehicle. As such, instead of describing the traffic dynamics of individual vehicle, gas-kinetic traffic flow models describe the dynamics of the velocity distribution functions of vehicles in the traffic stream. Recent application of gas-kinetic traffic flow models can be referred to Hoogendoorn (1999) and Klar & Wegener (1999).

Another mesoscopic paradigm is that vehicles are grouped into cells which control their behaviors. The cells traverse the link and vehicles can enter and leave cells when needed, but not to overtake. The speed of the vehicles is determined by the cell, not the individual driver's decision. One famous approach in this regard is the cell transmission (CTM) model proposed by Daganzo (1993, 1994). In that, the LWR continuum model is discretized into cells. The road is represented by a number of small sections (cells). The simulation model keeps tracking the number of vehicles in each cell, and in each time-step it calculates the number of vehicles that cross the boundaries between adjacent cells. The flow from one cell to the other depends on how many vehicles can be sent by the upstream cell and how many can be received by the downstream cell. The amount of vehicles that can be sent is a function of the density in the upstream cell whereas the number can be received depends on the density in the receiving cell. The lagged cell transmission model (Daganzo, 1999) is a refinement of this scheme, where the amount of vehicles a cell can receive (from the adjacent upstream cell) is also affected by the density some time earlier in the cell.

One new category in this regard is the hybrid model which tries to introduce concurrently the macroscopic and microscopic model into simulation. For example, Leclercq and Moutari (2007) proposed to take the advantage of different approaches and tried to develop a combined algorithm which includes both macroscopic model (based on Eulerian coordinate) such as LWR model and the microscopic model (based on Lagrangian coordinate) in order to provide more efficient traffic simulations on large road networks. However, they agreed that there are two important questions have to be addressed first when developing a hybrid model: (a) How closely are the microscopic and macroscopic models to be coupled? (b) How to synchronize or to translate boundary conditions, when passing from one traffic representation to another? For this they also tried to define the translations of boundary conditions at interfaces in the primitive hybrid model they proposed.

2.3 Microscopic Approaches

The microscopic models describe the interrelationship of individual vehicle's movement as well as its interaction with other vehicles. In these models of vehicular traffic, attention is focused on individual vehicle that is represented by a *"particle"*. Car-following models are the most pertinent ones to explicate the one-dimensional movements in a longitudinal lane such that the following vehicle adjusts its speed to maintain desirable or safe distance headway to the lead vehicle. Stimulus-response model is perhaps the most prominent one developed in the 1950s and 1960s by the General Motors (GM) research group, which is still being applied or extended (e.g., Brackstone & McDonald, 2000; Chakroborty & Kikuchi, 1999; Lan & Yeh, 2001). The car-following models are summarized as follows.

2.3.1 Concept of "car following"

The terminology *"car following"* on a motorway means the behavior of a driver who, through control of the brake and accelerator, tends to maintain an acceptable distance behind the lead vehicle in the same lane. Therefore, for each individual vehicle, an equation of motion is defined, which is the analogue of the Newton's equation for each individual particle in a system of interacting particles. In Newtonian mechanics, the acceleration may be regarded as the response of the particle to the stimulus it receives in the form of force which includes both the external force as well as those arising from its interaction with all the other particles in the system.

2.3.2 Stimulus-response relationship

The basic philosophy of the car-following theories can be summarized by the relationship:

$$[response]_n \propto [stimulus]_n \tag{2-9}$$

Each driver can respond to the surrounding traffic conditions only by accelerating or decelerating the vehicle. Different equations of motion were proposed in various car-following models, arising from their differences in postulating the nature of stimulus. In general, the Newtonian kinetics is adopted as the basic principle for movement:

$$\ddot{x}_n = f_{sti}(v_n, \Delta x_n, \Delta v_n) \tag{2-10}$$

where the function f_{sti} represents the stimulus received by the n^{th} vehicle. Different car-following model interprets the function f_{sti} differently. In the following, several car-following models are illustrated.

2.3.3 Pipes' car-following theory

The very first car following model can be traced back to the primary model proposed by Pipes (1953). He introduced the concept of minimum (safety) space headway, as shown below:

$$\Delta x_n(t) = (\Delta x)_{safe} + \tau * v_n(t) = x_{n+1}(t) - x_n(t) \quad (2\text{-}11)$$

where τ is a parameter that sets the time scale of the model

$v_n(t) = \dot{x}_n(t)$ is the speed of n^{th} vehicle at instant t

$n+1$ represents the vehicle in right front

Accordingly, one may derive the acceleration/deceleration of each vehicle by differentiating, with respect to time, on both sides of the Equation (2-11).

$$\ddot{x}_n(t) = \frac{1}{\tau}[\dot{x}_{n+1}(t) - \dot{x}_n(t)] \quad (2\text{-}12)$$

This model encapsulates two basic assumptions: (a) The higher the speed of the vehicle the larger should be the distance-headway. (b) In order to avoid collision with the lead vehicle, each driver must maintain a safe distance $(\Delta x)_{safe}$ to the lead vehicle. Therefore, in Pipes models, both the coefficients of the general form (refer to the Equation (2-18), shown as below) are set as $m=l=0$. According to Pipes, $(\Delta x)_{safe}=20ft$ and $\tau = 1.36\ s$.

2.3.4 Forbes' car-following theory

Forbes (1958) approached the car-following behavior by considering the reaction time needed for the following vehicle to perceive the need for decelerating and applying brakes. The final formula proposed, however, is identical to that (Equation (2-12)) in Pipe's model but still with slightly difference, i.e., $(\Delta x)_{safe}=20ft$ and $\tau = 1.5\ s$.

2.3.5 General Motors' (GM) car-following models

The five-generation GM model (1960, also known as GHR model owe to the contribution made by Gazis, Herman and Rothery in late fifties and early sixties, or the *follow-the-leader* model) is perhaps the most well known model. Its general formulation is:

$$\ddot{x}_n \propto sensitivity * stimulus = \frac{\alpha v_n^m(t)}{\Delta x^l(t-T)} * \Delta v(t-T) \qquad (2\text{-}13)$$

where T is the reaction time.

The first prototype car-following model that would eventually lead to general GM formula was put forward in the late *50s* by Chandler, Herman and Montroll (1958) at the General Motors research labs in Detroit, MI. This was based on an intuitive hypothesis that a driver's acceleration was proportional to the relative speed to the front vehicle (Δv), or a deviation from a preset following distance. Also for a more realistic description, the strength of the response of a driver at time t should depend on the stimulus received from the other vehicles at time t-T, where T is a response time lag. Hence, an equation known as the *GM#1* model that similar to Equation (2-12) is derived:

$$\ddot{x}_n(t+T) = \alpha[\dot{x}_{n+1}(t) - \dot{x}_n(t)] \qquad GM\#1\ model\ (m=0,\ l=0) \qquad (2\text{-}14)$$

Where α is the sensitivity coefficient, an experimental constant independent of n, and α varies from *0.17~0.74*.

The second generation *GM* model was proposed later by the same research team in light of the fact there are different driving behaviors for drivers stuck in the platoon. So the sensitivity coefficient α is divided into following two groups:

$$\ddot{x}_n(t+T) = \alpha_i[\dot{x}_{n+1}(t) - \dot{x}_n(t)] \qquad GM\#2\ model\ (m=0,\ l=0) \qquad (2\text{-}15)$$

Where *i=1 or 2*, α_1 is the coefficient for driving in platoon and α_2 is the coefficient for driving not in platoon.

Gazis, Herman and Potts (1959) subsequently attempted to derive a macroscopic relationship describing speed and flow; using the microscopic equation as a starting point. The mismatch between the macroscopic relationship they obtained and the other macroscopic relationships in use at that time led to the hypothesis that the algorithm should be amended further by

introducing a $1/\Delta x$ term into the sensitivity constant (i.e., $\alpha \rightarrow \alpha/\Delta x$), in order to minimize the discrepancy between the two approaches. This led to the third generation GM model:

$$\ddot{x}_n(t+T) = \left[\frac{\alpha_0}{x_{n+1}(t) - x_n(t)}\right][\dot{x}_{n+1}(t) - \dot{x}_n(t)] \quad \textit{GM\#3 model (m=0, l=1)} \qquad (2\text{-}16)$$

Subsequently, Edie (1960) attempted to match the *m=0, l=1* model to new macroscopic data in a similar manner to Gazis, Herman and Potts. However, he concluded that another amendment should be made to the sensitivity constant, namely, the introduction of the velocity dependent term. This produced a new model with *m=1* and *l=1*:

$$\ddot{x}_n(t+T) = \left[\frac{\alpha_0 \dot{x}_n(t+T)}{x_{n+1}(t) - x_n(t)}\right][\dot{x}_{n+1}(t) - \dot{x}_n(t)] \quad \textit{GM\#4 model (m=l, l=1)} \qquad (2\text{-}17)$$

This approach was later used by Gazis, Herman and Rothery (1961) to investigate the sensitivity of their macroscopic relationships to the variations of the speed (Δv) and space headway (Δx). As the consequence, they introduced two general scaling constants *m* and *l* for Δv and Δx terms respectively.

$$\ddot{x}_n(t+T) = \left[\frac{\alpha_{lm}\left(\dot{x}_n(t+T)\right)^m}{\left(x_{n+1}(t) - x_n(t)\right)^l}\right][\dot{x}_{n+1}(t) - \dot{x}_n(t)] \quad \textit{GM\#5 model} \qquad (2\text{-}18)$$

Source	*m*	*l*
Chandler *et al.*	0	0
Herman and Potts	0	1
Greenshields	0	2
Greenberg	0	1
GM#5	1	1
Underwood	1	2
Northwest University	1	3
UC Berkeley	0.8	2.8
Hoefs	1.5/0.2/0.6	0.9/0.9/3.2
Treiterer & Myers	0.7/0.2	2.5/1.6
Ozaki	0.9/-0.2	1/0.2

Table 2-1. Comparison of recommended parameters settings among some famous GM (GHR) models

Thus the generalized formula of GM model was derived. Numerous investigations occurred during the following 15 years, in the attempt to derive

the *"best"* combination of *m* and *l*. However, since the late 70s' the GM model has seen less and less frequently investigated and used, perhaps suffered from the large number of contradictory findings as to the correct values of *m* and *l*. These contradictory findings may be caused by two facts. First, the follower's behavior is likely to vary in accordance with different traffic condition around it; analysis from microscopic perspective has confirmed this argument in part. Second, many of the empirical investigations were taken place at low speeds or in some extreme stop-start conditions, which may not reflect the general car-following behavior. Nevertheless, some famous models in this regard that may be considered to contribute are enclosed in Table 2-1.

2.3.6 Optimal velocity (OV) models

Bando *et al* (1995) assumed that each driver tends to maintain a safe distance to the lead vehicle by choosing a proper speed as his/her desired speed:

$$\ddot{x}_n(t) = \frac{1}{\tau_n}[\dot{x}_n^{desired}(t) - \dot{x}_n(t)] \tag{2-19}$$

where $\dot{x}_n^{desired}$ is the desired speed of the n^{th} driver at time *t*.

Bando *et al* (1998) further assumed that the desired speed depends on the distance headway of the n^{th} vehicle.

$$\dot{x}_n^{desired}(t) = \dot{x}_n^{opt}(\Delta x_n(t)) \tag{2-20}$$

where $\dot{x}_n^{opt}(\Delta x_n(t))$ is the optimal speed, so that

$$\ddot{x}_n(t) = \frac{1}{\tau_n}[\dot{x}_n^{opt}(\Delta x(t)) - \dot{x}_n(t)] \tag{2-21}$$

The performance of OV model depends intensively on the appropriate choice of the optimal velocity function (Equation (2-20)). Through introduction of appropriate optimal velocity, such as Heaviside step function, some important macroscopic characteristics, such as traffic jam and hysteresis effects (refer to Figure 2-8 herein below for description) can be observed.

The main weakness of OV model is that under certain conditions the analytic solution, even for homogenous flow, becomes unstable and thus limits the applicability to mixed flow. The second key impediment is that it is

difficult to specify appropriate optimal velocity function for different traffic condition (e.g., free flow or congested flow).

2.3.7 Safety distance (SD) or collision avoidance models

Also known as *"collision avoidance"* model, the original formulation of *"safety distance"* model can be dated back to Kometani and Sasaki (1959). Their primary methodology does not describe a stimulus-response type function as proposed by the GM model, but seeks to specify a safe following distance through the manipulation of the basic Newtonian equations of motion, in case the vehicle in front were to act *"unpredictably"*. The full original formulation is as follows:

$$\Delta x(t\text{-}T) = \alpha x_{n-1}^{2}(t\text{-}T) + \beta_1 v_n^{2}(t) + \beta v_n(t) + b_0 \qquad (2\text{-}22)$$

The coefficients T, α, β_1, β, b_0 were determined from the calibration data from either a pair of test vehicles on city streets or from a test track. However, it is found that the coefficients vary for different occasions and along that, led to different R^2 values (0.25 and 0.95 respectively).

A major development of this model was made by Gipps (1981), in which he considered several mitigating factors that the earlier formulation neglected. These were that drivers will allow an additional *"safety"* reaction time equal to $T/2$, (it can be shown that this condition is sufficient to avoid a collision under all circumstances), and that the kinetic terms in the above formula are related to braking rates of $1/2b_n$, where b_n is the maximum braking rate that the driver of the n^{th} vehicle wishes to use. Gipps offered no calibration of his parameters, but instead performed simulations showing that his model produced realistic behavior on the propagation of disturbances, both for a vehicle pair and for a platoon of vehicles.

Since the effort of Gipps was published, the SD model continues to be widespread adopted as the simulation model. Part of the attractiveness of this model is that it may be calibrated using common sense assumptions about driver behavior, needing (in the most part) only the maximal braking rates a driver will use and the expected behavior of other drivers, to make it to be fully functional.

Although it produces acceptable results as, for example, comparing the simulated propagation of disturbances against empirical data, there are still some problems that cannot easily be solved. For example, if one examines the *"safe headway"* concept, it would not be a totally valid starting point, as in practice a driver may consider conditions several cars down stream, basing his assumption of how hard the vehicle in front will decelerate on the *"preview information"* obtained.

2.3.8 Linear (Helly) models

The original formulation of this approach dated to Helly (1959). He proposed a model that included additional terms for the adaptation of the acceleration according to whether the vehicle in front (and the vehicle two in front) was braking. The simplified model is shown as the following Helly equation:

$$a_n(t) = C_1\Delta v(t-T) + C_2(\Delta x(t-T) - D_n(t)) \quad (2\text{-}23)$$

where

$D_n(t)=\alpha + \beta v(t-T) + \gamma a_n(t-T)$; $D(t)$ is a desired following distance.

From late fifties to early nineties, there are several researches published in this regard proposing the optimal parameter combination for Helly equation.

A major strength of the Helly model is the specific incorporation of *"error"*, an element of the original formulation that is often overlooked. And some linear models (e.g. the model proposed by Xing, 1995) give an extremely good fit to the observed vehicle trajectories. However, criticism applied to the GM model can also be applied to the linear model, i.e., significantly contradictory findings as to the correct values of coefficients $C_1$and C_2.

2.3.9 Psychophysical or action point (AP) models

The first model of this category was proposed by Michaels (1963), who raised the concept that drivers would initially be able to tell they were approaching a vehicle in front, primarily due to changes in the apparent size of the vehicle, by perceiving relative velocity through changes on the visual angle (θ) subtended by the vehicle ahead. The threshold for this perception is well-known in perception literature and given as $\Delta v/\Delta x^2 \sim 6*10^{-4}$. Once this

threshold is exceeded, drivers will chose to decelerate until they can no longer perceive any relative velocity and the threshold is not re-exceeded. This model in essence is based upon the theory that drivers' actions rely on whether they can perceive any changes in spacing.

The second model in this regard which introduced spacing-based threshold (generically termed an *"action point"*) is particularly relevant at close headways where speed differences are always likely to below threshold. Thus, for any changes to be noticeable, Δx must be replaced by a *"just noticeable distance"* (JND), related to Webers Law. This means that the visual angle must change by a set percentage; typically 10%. It is also noted that this threshold is ~12% for the opening situation, which implies that a driver continually approaches and then moves back from the vehicle in front.

It is important to state that in crossing this last threshold, the driver will set a determined acceleration/deceleration and stay with it until they break another threshold, as the driver perceives no change in conditions, or at very least, no change in the rate of change. It is also likely that in this close-following area the driver is not fully able to control the acceleration/deceleration of his vehicle, due to the very fine adjustments required. Motion is therefore governed by the use of a minimum value.

The next advance of these models came through a series of perception-based experiments conducted in the early seventies, by researchers such as Evans and Rothery (1973) and by the staff at If V Karlsruhe in Germany in the eighties. However, more recent work by Reiter (1994) in which an instrumented vehicle was employed to measure the action points has resulted in the amendment of some of these parameters and led to a totally different functional form, as compared with previous ones.

Besides, although the entire system would seem to simulate behavior acceptably, calibration of the individual elements and thresholds has been less successful. For example, since the sixties, little research work has been undertaken on the concepts involved in these models. It is difficult therefore to either prove or disprove the validity of this model, although the basis upon which it is built is undoubtedly the most coherent, and best able to describe most of the features that we see in everyday driving behavior.

2.3.10 Fuzzy logic-based models

The use of fuzzy logic within car-following models is worthy of mention as it represents the logical step in the attempt to accurately describe driver behaviors. Such models typically divide their inputs into a number of overlapping *"fuzzy sets"* whereas each set describes how adequately a variable fits the description of a *"term"*. For example, a set may be used to describe and quantify what is meant by the term *"too close"*, where for example a separation of less than *0.5s* is definitely *"too close"* and thus has a degree of truth or *"membership"* of 1, while, a separation of *2s* is not close and is given a membership of 0, and intermediate values are said to exhibit *"degrees"* of truth and have differing (fractional) degrees of membership. Once defined, it is possible to relate these sets via logical operators to equivalent fuzzy output sets (e.g., *IF "close" AND "closing" THEN "brake"*), with the actual course of action being assessed from the modal value of the output set, calculated as the sum of all the potential outcomes.

The initial use of this method (Kikuchi & Chakroborty, 1992) attempted to *"fuzzify"* the traditional GM model; using Δx; Δv and acceleration as inputs and grouping them into several natural-language based sets. This model has been used to illustrate how the fuzzy logic system can be used to describe car following, and the outcome was compared with that from the traditional GM models. It is demonstrated that the GM model would produce differing headways according to the rate of deceleration and hence the final speed. This is clearly in contradiction to what would be expected in practice. Additionally, the final following distance was shown to be dependent only on final speed, regardless of the original following distance or original speed.

Although this model generally reflects the changes expected, its formulation is unrealistic for two reasons. The acceleration of a vehicle can be detected (it is highly debatable whether this is possible), and it has been found from the linear (Helly) model that any linear dependence on Δx is exceedingly small.

Other work in this area includes that by Teodorović (1994), Ho *et al* (1996) and work by Yin *et al* (2002). However, none of these approaches have attempted to calibrate the most important part of the model itself—the membership sets.

2.4 Cellular Automaton (CA) Models

CA modeling, also a microscopic approach, is one powerful tool for traffic simulation; owing to its inherent simplicity and the capacity of reproducing important entities prevailed in real traffic, e.g., density-flow relation and the backward movement of traffic jams in congested traffic. As the consequence, it is not surprised that since early nineties it is popularly utilized worldwide to describe the phenomena of real traffic flows characterized with complex dynamic behaviors.

Besides its inherent simplicity and efficiency, CA models also furnish an important advantage as compared with other car-following models—the ability for simulating multi-lane traffic. Most microscopic car-following models endeavored at delineating drivers' reaction to the traffic situation in front whilst few ever tried to take care of the traffic condition aside. As the result, in most car-following models only single lane traffic contexts were considered. Since in real world traffic is usually composed by vehicles with different desired speed (in other word, drivers with heterogeneous attributes), introducing different vehicle attributes in a single lane model will inevitably result in platoon in which slow vehicles are followed by faster ones and the average speed is reduced to the free-flow speed of the slowest vehicle (Nagel *et al*, 1998). It is apparent that such single lane models are not capable of modeling heterogeneous traffic contexts.

Besides, in real world most road systems are comprised of at least two-lanes, thus allow vehicles to change lane, or say, move sideway to overtake a slow vehicle in the front. Consequently, the lane-changing rules that can reflect the driving behaviors must be delineated if one intends to simulate the traffic on multi-lane road contexts. However, as above-mentioned, the car-following models lack the applicability for describing lane change behaviors and hence the multi-lane contexts. In contrast, through the combination of CA models and well-defined lane change rules, simulation of the multi-lane traffic becomes practicable. This might explain its predominance to other car-following models in the past two decades.

Cremer and Ludwig (1986) proposed a simple model which simulated vehicular traffic on the basis of Boolean operations. Several years later, Nagel and Schreckenberg (1992) proposed the renowned NaSch model. Although its

success in reflecting some important traffic features, NaSch model is still deemed as an extreme simplification of the real world conditions. Therefore considerable modified CA models were devised in the following decade (for instance, Nagel *et al*, 1996, 1998; Rickert *et al*, 1996; Chowdhury *et al*, 1997; Barlović *et al*, 1998). Other related works that improved NaSch coarse cells with finer cells have also been found (for instance, Knospe *et al*, 2000; Bham and Benekohal, 2004; Lan and Chang, 2003, 2005; Lárraga *et al*, 2005). In addition, Wolf (1999) employed a modified NaSch model to address metastable states at the jamming transition in detail. Wang *et al* (2000) introduced NaSch model and Fukui-Ishibashi model (1996) to investigate the asymptotic self-organization phenomena of one-dimensional traffic flow. Pottmeier *et al* (2002) studied the impact of localized defect in a CA model for gauging metastable states and the coupled phase separation.

The first attempt for extending the implementation of CA model to multi-lane traffic can be traced back to Rickert *et al* (1996). According to their proposal, drivers will change lane only if both following the criteria are met:

(1) *The incentive criterion*: The gap in front of one vehicle at the current lane should be no greater than its current speed and the gap in front of the adjacent lane should be larger than the current front gap.

(2) *The safety criterion*: Any lateral displacement should not collide or block other vehicles behind. Therefore, the nearest neighbor site must be empty and that the max possible speed of the nearest vehicle behind on the other lane is small than the gap between.

Rickert (1996) also proposed the derivative asymmetric model in which vehicles always try to return to the right lane, independently of their situation on the left lane. This is the real scenario in German freeway where passing should be done on a specified lane (left lane) as a rule. In the following year, a similar model was proposed by Wagner *et al* (1997) which revealed that the passing lane (right lane) will be more crowded than the one for slower vehicles (the right lane) if the traffic flux if high enough.

One year later, Nagel, the pioneer of CA model, with several coworkers (1998) surveyed different lane change rules and concluded that in spite of their differences, all generate similar and realistic results.

Following that, along with development of VDR model, Barlovic (1998) and Knospe (1999) both argued that the anticipation effect should be considered for determining if the lane change should be initiated. Knospe (2002) further suggested that the brake light status of one vehicle (either on or off) may affect the driver's behavior right in its back, if close enough, both for car following and lane change.

Another achievement in this regard is the effort made by Jia *et al* (2005) that evaluated the effect of honking effect of one vehicle if hindering by the preceding slow vehicle. It is shown that the honk has almost no effect in homogenous traffic whereas it enhances the traffic flux in the intermediate density regime for the heterogeneous traffic. In addition, they argued that the honk behavior is not encouraged in asymmetric two-lane models. Some important CA models are outlined as follows.

2.4.1 Cremer and Ludwig's model

In this primitive model, Cremer and Ludwig (1986) proposed a fast numerical model for traffic simulation. They simulated the progression of cars on a street by moving one bit variables through binary positions of bytes. In addition, application of Boolean operations enabled the model to perform diverse movements of vehicles. This model can reflect the basic macroscopic phenomena of traffic flow while at the same time reproduces the main mechanisms of microscopic models.

2.4.2 NaSch model

According to this renowned pioneer model a single lane roadway is divided into squared-cells of length 7.5 meters longitudinally (see Figure 2-3). Each cell can either be empty or occupied by at most one car at a given instant of time-step. The space, speed, acceleration and even the time are all treated as discrete variables. The state of the both road and car at any time-step are derived from one time-step ahead by applying acceleration, braking, randomization and driving rules for all cars that with discrete velocity $v \in \{0,...,v_{\max}\}$ at the same time (i.e., parallel dynamics).

Despite its simplicity by nature, NaSch model is capable of reproducing important entities of real traffic flow, e.g., density-flow relation (see Figure 2-4) and the traffic jam induced by randomized driver behavior (see Figure 2-5). In

NaSch model, car and road condition at time $t+1$ can be obtained from that at time t by applying the following four steps for each car concurrently:

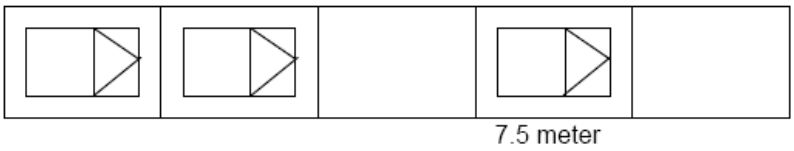

Figure 2-3. Homogeneous cell system utilized in traditional NaSch model.

Step 1 : Acceleration $v_n = \min(v_{n+1}, v_{max})$;

Step 2 : Braking $v_n = \min(v_n, d_n - 1)$;

d_n: the distance to next vehicle ahead.

Step 3 : Randomization with probability p $v_n = \max(v_n - 1, 0)$;

Step 4 : Driving $x_n = x_n + v_n$ x_n : the position of n^{th} vehicle

The NaSch model is a minimal model in the sense that all the four steps are necessary to reproduce the basic features of real traffic (Figures 2-4 and 2-5). However, additional rules need to be formulated if one ever tries to capture more delicate traffic phenomena, such as the hysteresis effect as well as the parallel movement of traffic jams. These phenomena will be illustrated in the following sub-sections.

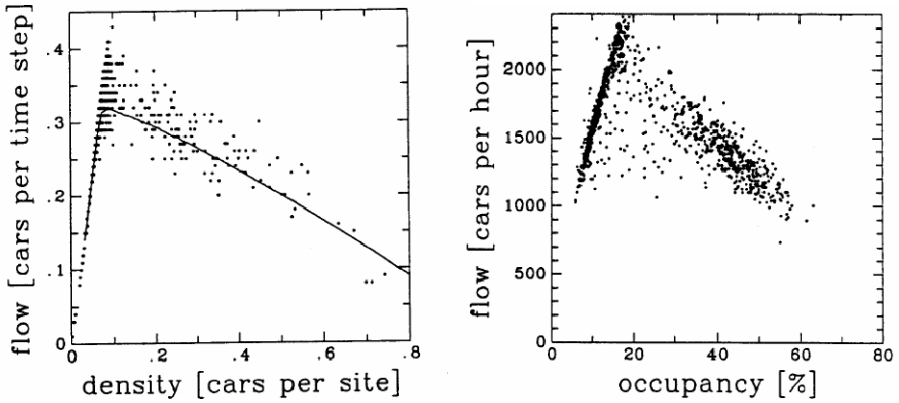

(a) Simulated result (b) Field observation

Figure 2-4. Comparison of simulated fundamental diagram via NaSch model with that from the field observation.

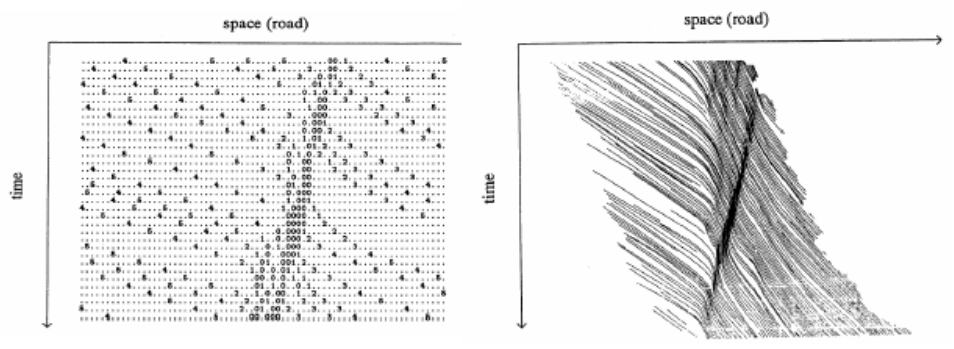

(a) Simulation result (b) Field observation

Figure 2-5. Comparison of simulated *x-t* plot via NaSch model with that from field observation. Note the traffic fluctuation induced by one randomized driver behavior and the its backward movement.

2.4.3 CA models considering slow-to-start phenomena

According to field observations, it is found that for vehicles stuck in traffic jams over a certain period, there is a tendency for postponing acceleration when leave the downstream front of jams. It is so called the "*slow-to-start"* phenomena. This behavior also serves as a crucial factor on the formation of upstream movement of traffic jam fronts (propagate upstream with speed *-15 kph)* and the coupled parallel movement of neighboring traffic jams. (see Figure 2-6 for reference).

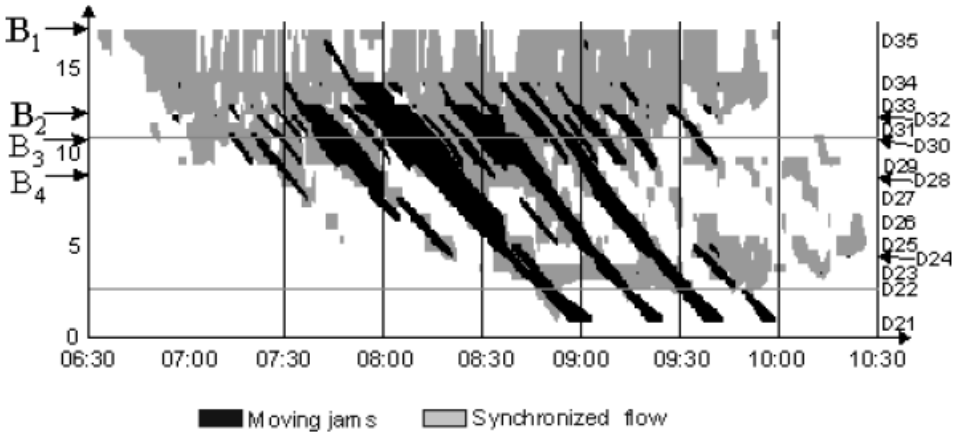

Figure 2-6. Field observed *x-t* diagram of German freeway (A-9, south, dated 2002.04.26). The vertical axis displays the position along freeway (in kilometer) and horizontal axis as the time marched. (note the parallel movement of traffic jams and the coupled backward speed of traffic jams—*15kph* approximately.)

Takayasu and Takayasu (1993) perhaps were the first to suggest a CA model with slow-to-start rule. Next, Benjamin *et al* (1996) modified the updating rule of the NaSch model by introducing an extra step where their *"slow-to-start"* rule was implemented (short as BJH model). According to the BJH rule, the vehicle which has to brake due to the influence of next vehicle ahead will move on the next opportunity with the probability $1 - p_s$ only.

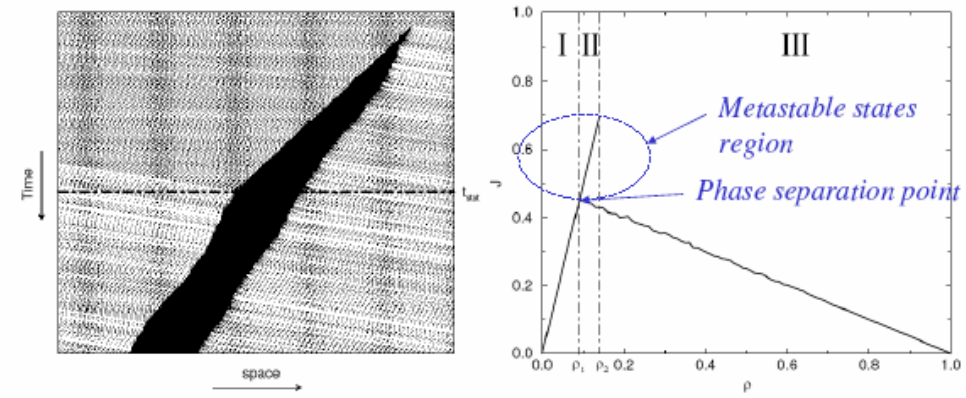

Figure 2-7. Simulated *x-t* diagram (left panel) and fundamental diagram (right panel) of a spontaneously emerging jam through the VDR model.

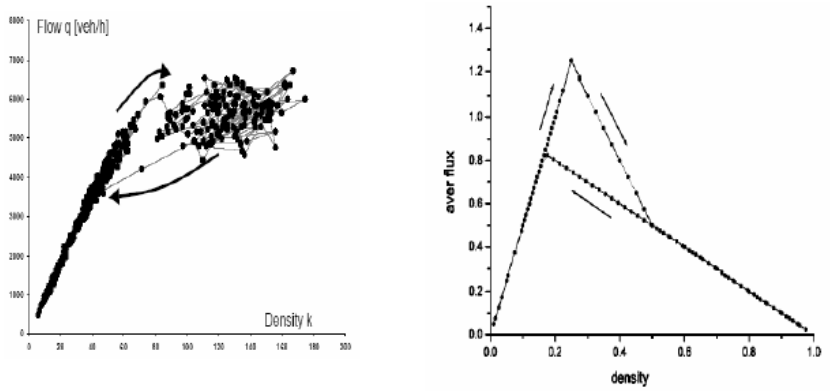

(a) Empirical data (Kerner, 2004) (b) Theoretical hystersis loop

Figure 2-8. Description of hysteresis effect—A local phase transition occurs from one traffic phase (free flow phase) to another phase (synchronized flow phase), and later reverses to the initial phase, transforming the hysteresis loop.

Barlović *et al* (1998) further proposed the velocity dependent randomized (VDR) model which is basically analogous to the BJH model and endeavors to establish proper update rule for randomization (P_n) in accordance with the velocity variation of vehicles. The VDR model did successfully

exhibit the metastable states (a traffic phase in which small perturbation fails to grow if the amplitude of perturbation below some critical threshold; as shown in Figure 2-7) and consequently, the hysteresis effect (refer to Figure 2-8 for details) that was never visible in the previous simulations. Therefore the VDR model has been widely adopted worldwide since then.

In contrast to the original NaSch model, in VDR model the randomization parameter—P_n is determined via the update rule depending on the velocity of vehicles:

$$P_n(v_n)=\begin{cases} P_0 & for \quad v=0, \quad i.e.\ outflow\ from\ jam \\ P_n & for \quad v>0, \quad i.e.\ flow\ in\ metastable\ states \end{cases}$$

Usually $P_0 < P_n$, as to reflect the fact that when driving out from the downstream of jams drivers are more likely to postpone acceleration (the slow-to-start behavior). The update rules of VDR model are summarized as below:

Step 0 : Randomization parameter setting $P_n = P(v_n)$;

Step 1 : Acceleration $v_n = \min(v_n+1, v_{max})$;

Step 2 : Braking $v_n = \min(v_n , d_n -1)$;

Step 3 : Radomization with probability P_n

$$v_n=\begin{cases} \max(v_n-1,0) & with\ probability\ P_n \\ v_n & with\ probability\ 1\text{-}P_n \end{cases}$$

Step 4 : Movement $x_n = x_n + v_n$

v_n:the position of n^{th} vehicle

2.4.4 CA models introducing drivers' anticipation and brake light effect

For single-lane traffic models it is well known that particle disorder leads to platoon formation at low densities. This simulation result still makes sense since a slow vehicle will serve as a moving bottleneck and therefore forces the following vehicle to remain the same speed for sake of collision free. When

considering the two-lane contexts, however, it is found that influence of slow vehicles seems still overestimated—even a small number of slow cars can initiate the formation of platoons at low densities. This result obviously disagrees with real traffic phenomena.

To cope with reality and to weaken the unrealistic effect of slow vehicles, Knospe *et al* (1999) suggested that the anticipation effect for drivers should be considered. They argued that the following driver (follower) will, based on the surrounding situation, consider the anticipated speed of front vehicle (the leader) as part of front headway for next time-step. Therefore the famous effective gap was defined, as shown in Equation (2-24) to replace the geometric gap in the deceleration update rule (i.e., Step 2 in VDR model, as shown above):

$$d_n^{eff} = d_n + \max(v_{anti} - gap_{safety}, 0) \tag{2-24}$$

It has been evidenced that introduction of anticipation effect drastically reduces the influence of slow cars and therefore leads to more reasonable simulation result.

Furthering that, Knospe *et al* (2000 & 2002) suggested that the effect of braking light of front vehicle should also be considered. It is known as the BL model. Their basic methodology is that at large distances the cars move (apart from fluctuations) with their desired velocity v_{max}.; at intermediate distances drivers react to velocity changes of the next vehicle downstream, i.e., to the status of front *"brake lights"*. Last, if at small distances the drivers adjust their velocity to ensure safe driving. Besides, acceleration will be delayed for standing vehicles and for the vehicles directly after braking events.

In BL model, the gap between consecutive cars (where l is the length of the cars) is:

$d_n = x_{n+1} - x_n - l$

b_n is the status of the brake light (on (off)→b_n = 1 (0)).

Randomization parameter P is decided through:

$$P_n(v_n(t), b_{n+1}(t)) = \begin{cases} P_b & \text{if } b_{n+1} = 1 \text{ and } t_h < t_s \\ P_0 & \text{if } v_n = 0 \\ P_d & \text{in all other cases} \end{cases}$$

The values of P_0, P_d and P_b, are determined in accordance with the current velocity v_n and the status of the brake light of preceding vehicle $n+1$, $b_{n+1}(t)$.

where $t_h = d_n / v_n(t)$ is the temporal headway

$t_s = \min(v_n(t), h)$ is the safety time headway required

h determines the range of interaction with brake light

Step 0 : Randomization parameter setting $P_n = P(v_n(t), b_{n+1})$

Step 1 : Acceleration $v_n(t+1) = min(v_n(t)+1, v_{max})$,

if $b_{n+1} = 0$ & $b_n = 0$ or $t_h > t_s$

Step 2 : Braking $v_n(t+1) = (v_n(t), d_n^{eff})$

where $d_n^{eff} = d_n + \max(v_{anti} - gap_{safety}, 0)$

$v_{anti} = \min(v_{n+1}(t+1), d_{n+1}(t+1))$

$b_n = 1$; if $v_n(t+1) < v_n(t)$

Step 3 : Randomization $v_n(t+1) = max(v_n(t+1)-1, 0)$

Step 4 : Movement $x_n(t+1) = x_n(t) + v_n(t+1)$

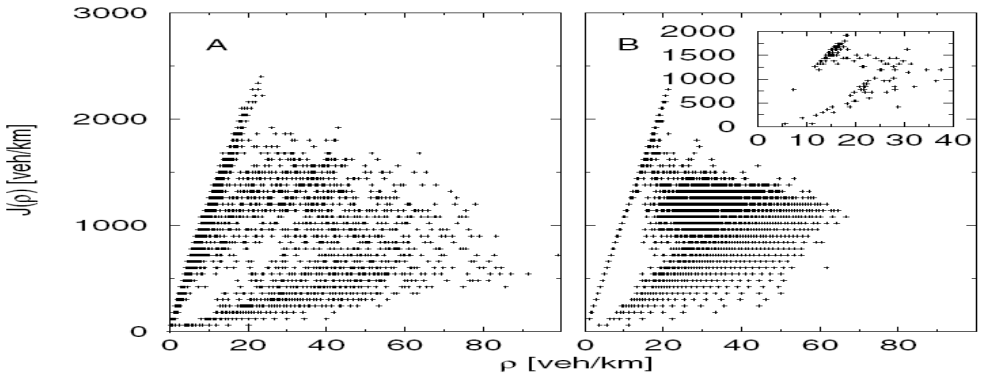

Figure 2-9. Comparison of the Knopse model (2000, left panel) with empirical data (right panel).

The simulations show that the empirical data is reproduced in great detail via the above-mentioned BL model (Figure 2-9).

The original BL model assumes that the drivers of stopped cars are less sensitive than the drivers of moving. Jiang *et al* (2003) based on such philosophy, proposed further amendment. Their revised scheme argues that the driver that has just stopped still remains sensitive; only when the car has stopped for a certain time t_c does the driver become less sensitive.

Therefore, according to Jiang *et al* (2003), the main updates to the original BL model are: First, the acceleration capacity of a stopped car is assumed to be one and that of a moving car is two. Next, the brake light is switched on if the speed decreases; while in the original BL model the brake has nothing to do with the decrease in speed caused by the randomization probability p_d. Finally, after the brake light is on, it will not switch off unless the car begins to accelerate.

Accordingly, the estimation of probability is revised as

$$p_n(v_n(t), b_{n+1}(t)) = \begin{cases} p_b & \text{if } b_{n+1}=1 \text{ and } t_h < t_s \\ p_0 & \text{if } v_n = 0, \text{ and } t_{st} > t_c \\ p_d & \text{in all other cases} \end{cases}$$

Where t_{st} denotes the time that a car stops.

t_c is the threshold time of stopping and choose as *10s.*

The simulated outcome shows that the revised BL model successfully reproduces the light synchronized flow that does not appear in original BL model.

2.5 Other Microscopic Models

Some other microscopic models were also proposed to simulate complicated traffic scenarios, for example, the gap acceptance models. Gap acceptance models have shown success in simulating drivers' reaction when crossing non-signalized intersections and the complex lane changing behaviors in the weaving area of highway on- and off-ramps, e.g., the effort by Mahmassani *et al* (1981), Hamed *et al* (1997), Ahmed *et al* (1997), Lertworawanich *et al* (2001), Cooper *et al* (2002) and Pollatschek *et al* (2002). More recently, Sheu (2008) proposed to introduce the theorem of quantum mechanics in optical flows to explain the motion-related perceptual phenomena

and to model the induced car-following while vehicles approach the incident site in adjacent lanes.

2.6 Three-phase Traffic Theory

Kerner (2004) introduced the three-phase traffic theory which consists of free flow, synchronized flow and wide moving jam phases, as shown in Figure 2-10. The later two phases exist in congested states where downstream front of the synchronized flow phase is often fixed at a bottleneck and the wide moving jam will propagate through the spatial locations of the bottleneck. To explore the emergence of such traffic patterns, Kerner and partners have surveyed complex spatiotemporal behaviors based on the analysis of empirical data from freeway traffic. These efforts include, but not limited to, Kerner and Rehborn, 1996; Kerner, 1996; Kerner and Klenov, 2002; Kerner *et al*, 2002; Kerner and Klenov, 2004.

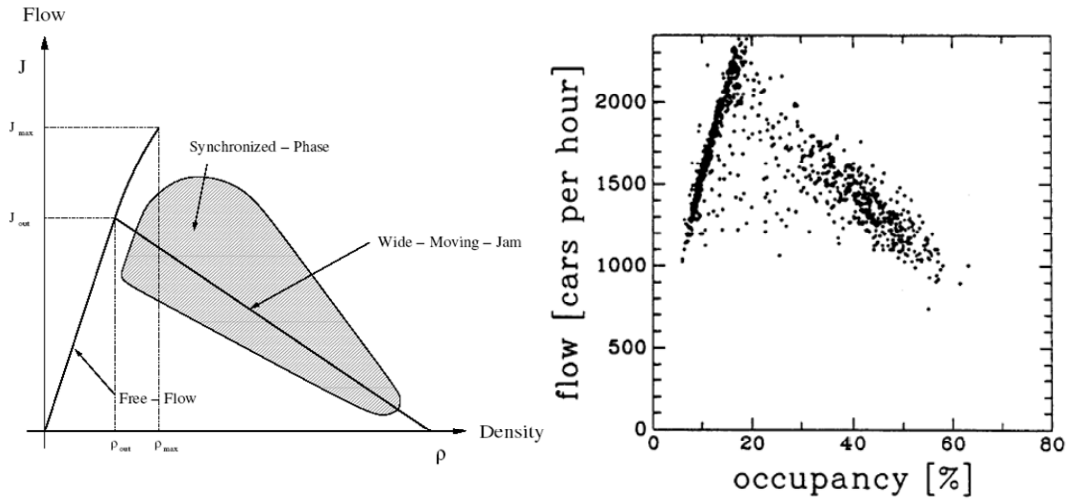

Figure 2-10. Comparison the fundamental diagrams of three-phases interpretation (Kerner, 2004, left panel) and that based on real traffic (right panel).

The concept of three-phase theory was developed based upon the observed field data prevailed on German Highway. According to the local measurements as shown in Figure 2-11, one may find that when traffic density increases beyond some threshold (e.g., *30 veh/km*), the theoretical fundamental diagram (refer to Figure 2-2) will no longer exist, but instead, a dispersedly distributed measurement points on flow-density plane (fundamental diagram) can be identified.

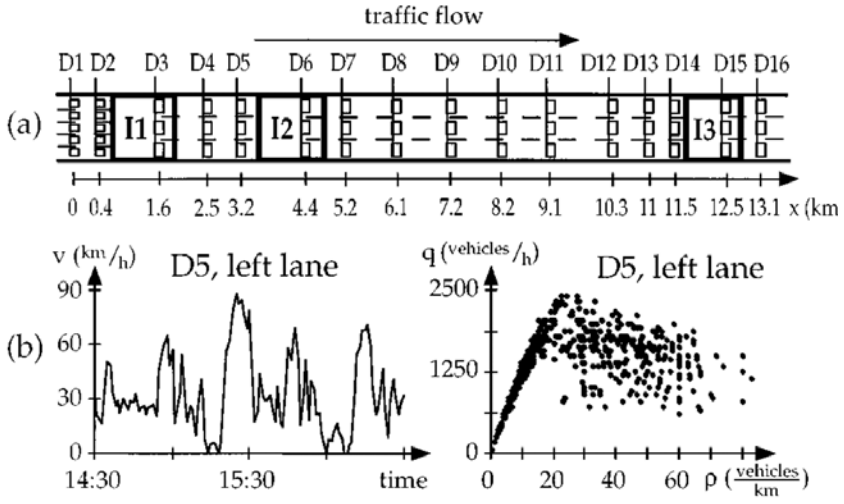

Figure 2-11. Observed flow-density relationships on German highways A-5. (right panel, daily data)

To explore such complex traffic phenomena, Kerner (2004) suggested that in addition to the free and congested traffic flow pattern defined in traditional traffic theory, one new traffic pattern—the synchronized flow phase, should be considered. The core philosophy of three-phase theory can be illustrated as follows.

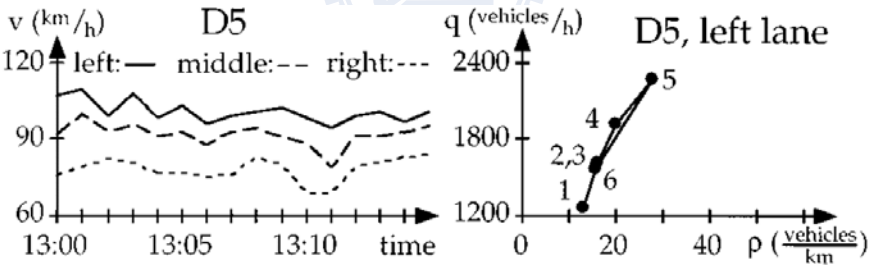

Figure 2-12. Features of free flow phase in three-phase traffic theory.

According to Kerner (2004), when in free flow phase, vehicles move with essentially high but different average speeds in different lanes. An increase in flux will be accompanied by the increase of density, but cut-off at some point q_{max}. This unique feature of free flow phase is illustrated in Figure 2-12.

In contrast, when in synchronized flow phase, vehicles will move with nearly the same average speed in different lanes. But the average speed of vehicles is noticeably lower and density is higher than the corresponding values in free traffic flow. Besides, an increase in flux could be accompanied by an

increase or decrease in density. Generally speaking, the measurement points will cover a region on flux-density plane, as shown in Figure 2-13.

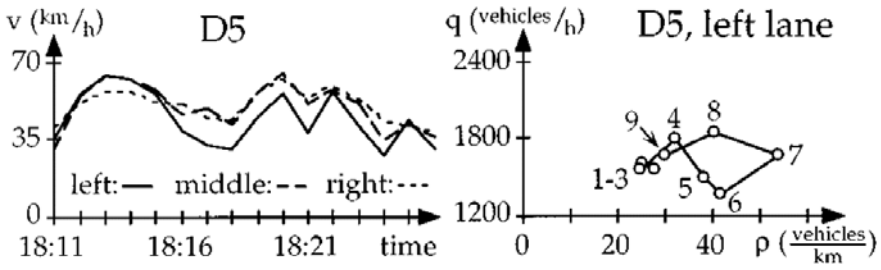

Figure 2-13. Features of synchronized flow phase in three-phase traffic theory.

The third traffic phase in three-phase theory is that wide moving jam phase. In this traffic phase, an upstream moving compact cluster is restricted by two jam fronts, one upstream and other downstream. Inside the jam the velocity of vehicles and hence the flow is negligibly small. The jam fronts are decoupled due to the sharp decline of flow, as shown in Figure 2-14.

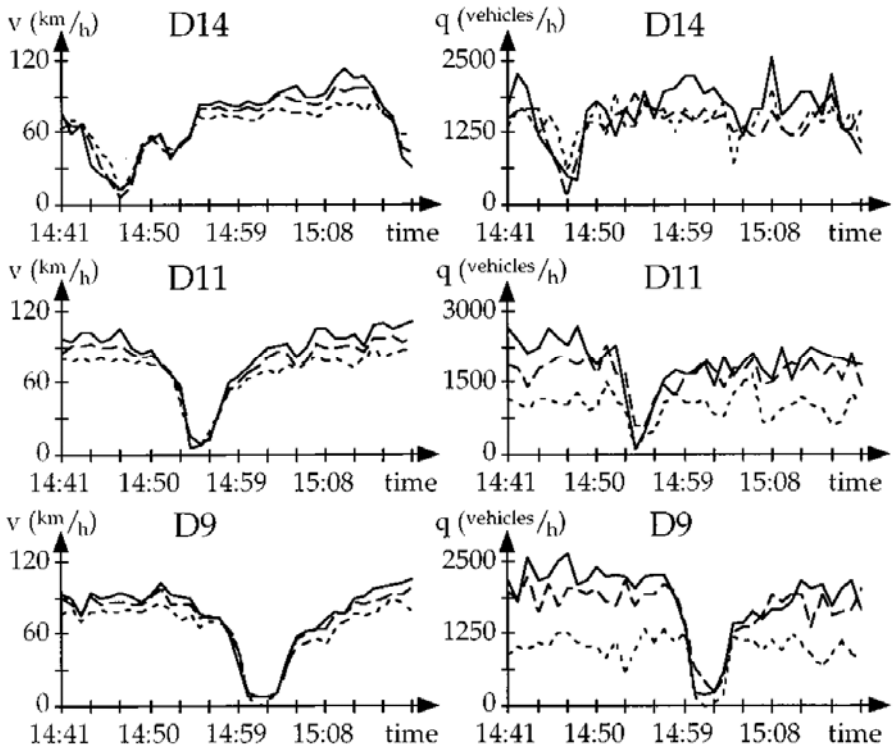

Figure 2-14. Upstream propagation of wide-moving jams in three-phase traffic theory.

One important feature of traffic jams is their propagation upstream unhindered with speed approximately *15 kph* through either free flow or synchronized flow. This means sometimes coexistence and parallel movement of multiple traffic jams will be observed, as supported by the *x-t* plot of measured traffic data in German highway (Figure 2-15). Besides, most of time traffic jams emerge out of synchronized traffic.

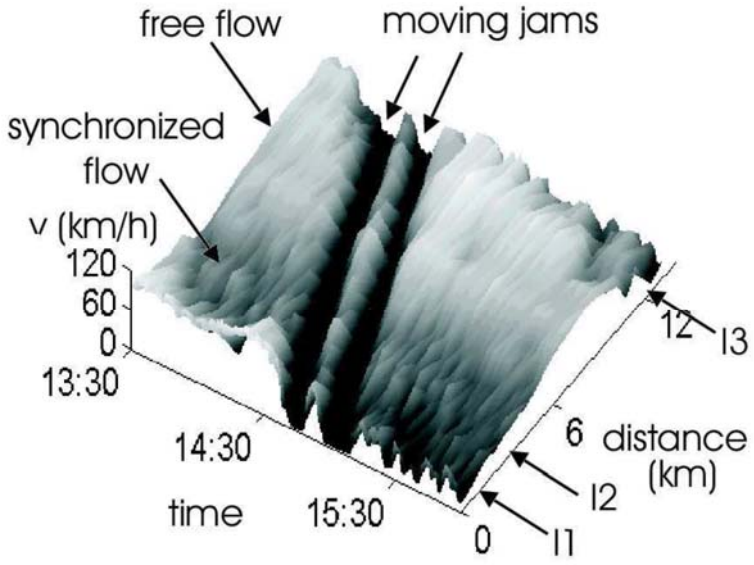

Figure 2-15. Coexistence of moving jams and their parallel propagation to the upstream.

2.7 Discussion

Owing to their few and directly measurable parameters, macroscopic and mesoscopic models are easier to calibrate than microscopic models. Nevertheless, their application is limited to cases where the interaction of vehicles is not crucial to the results of the simulation. For instance, analysis of merging areas usually requires the explicit simulation of gap acceptance behavior of the vehicles, as well as a precise reproduction of the geometrical features of the ramp and freeway. Due to the high level aggregate representation of traffic and road geometry in macroscopic (and to a lesser degree mesoscopic) models, these facilities cannot be accurately replicated and analyzed. Accurate modeling of signal control is also difficult in both macroscopic models and mesoscopic models. In macroscopic models, the vehicles are not modeled individually and in mesoscopic models the positions and behavior of vehicles are approximated. When these vehicle positions are

not known, or are inaccurate, it is difficult to simulate the activations of detectors that are used in the traffic control system. This brings us to a general problem of comparing results from macroscopic/mesoscopic models with real life detector data. While it is possible to obtain measures such as flows and speeds from these models, exact location of the measurements can be difficult to determine. Normally they are averages over a whole link or segment, while in real life the location of a detector can make a difference on the measured flows, speeds and occupancies. These types of models are most successfully applied to large scale networks and long time periods, where the shortcomings due to the limited detail of these models may not be important. For applications where these shortcomings can have a larger effect on the results, including modeling of intelligent transport systems (ITS) and the examples mentioned above, one should consider applying microscopic models instead.

As regard to microscopic models, there are several obvious advantages for selecting CA model into traffic simulations. First, the rule set that describes the update of each vehicle is small. Next, the update schedule, being completely parallel, is simple, too. The most important and subtle reason is the computation explicitness. It means that data is directly updated and iterations for converging to some predefined residue are never required. The beneficial aspect of using explicit computation is obvious—it minimizes the simulation time and thereby increases likelihood for real-time simulation and henceforth the traffic control for complex scenarios, especially for the urban network road system.

CHAPTER 3 DEVELOPMENT OF REFINED CA MODELS

3.1 Shortcomings of Existing CA Models

Despite the inherent simplicity and its supremacy in simulation expedition, one might find that most existing CA models dealt with pure traffic (only one type of vehicle such as cars) on freeways. Incorporation of more realistic CA rules into the simulation of mixed traffic (various types of vehicles such as cars, motorcycles, buses) on urban streets or surface roads are comparatively much less addressed. It is most likely that this bias mainly suffers from the restraint circumvented by the coarse cell systems utilized by existing CA models.

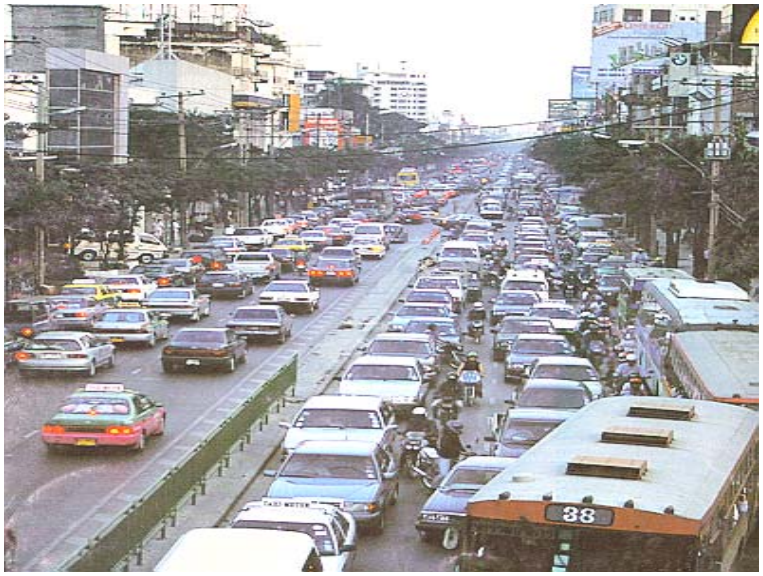

Figure 3-1. Erratic motorcyclists' behaviors in congested urban traffic, such as sneaking into traffic jam and transverse crossing between two adjacent still vehicles.

As mentioned, most existing CA models utilized comparatively coarse cell system proposed in the primitive NaSch model (refer to Figure 2-3) in which each lane only allowed to be occupied by a single vehicle laterally. One crucial defect aroused from such coarse cell system is that it would be difficult to implement mixed traffic simulations where vehicles have different sizes (length and width) and/or possess distinct behavior. For example, it is

ubiquitous in many Asian urban streets that motorcycles oftentimes move concurrently with the cars by sharing the *"same lane"* (see Figure 3-1). According to Figure 3-1, one may find that some erratic motorcyclists do not even follow the lane disciplines at all. They may make lateral drifts breaking into two moving cars. Once blocked by the front vehicles, they even make wide transverse crossings through the gap between two stationary cars in the same lane, in order to keep moving forward. In this circumstance, obviously, conventional coarse cell system is deficient to describe various vehicle sizes with their coupled interactions. However, though the mixed traffic contexts hitherto are seldom studied through CA modeling, an in-depth understanding of mixed traffic behaviors can be imperatively important in many Asian cities where motorcycles are prevailing.

Another shortcoming of the coarse cell system is the derived low resolution which stands as the crucial barrier for implementing CA models into urban traffic simulation. In urban streets, the speed limits are usually low. For instance, if the speed limit is *60kph*, there would be only three speed options available for any vehicle—*0, 28kph* and *56kph* provided that the cell system in NaSch model *(7.5m)* is used for CA simulation. This is apparently not so practical if one wishes to scrutinize in detail the microscopic traffic features or to trace the realistic behavior of an individual vehicle. Furthermore, most existing CA works only considered basic heterogeneity among vehicles, including various speed limits and/or different vehicle lengths. For instance, Chowdhury *et al* (1997), Nagel *et al* (1998), Ebersbach *et al* (2000) and Wang *et al* (2007) analyzed the impact of partial vehicles equipped with lower or higher maximum speed in the traffic flow. Ez-Zahraouy *et al* (2004) evaluated the effect of mixture lengths of vehicles on the traffic flow in a single-lane context. In Knospe's *et al* (2000) paper, a two-lane system with smaller cell sizes and different types of vehicles were studied. Kerner *et al* (2004) further evaluated both the effects of different vehicle lengths and various maximum speeds. In these CA models, except that by Knospe *et al* (2000), Wang *et al* (2007) and Kerner *et al* (2004), the small vehicles occupy one cell, while the big ones take two cells, but none ever take the impact of vehicular widths into consideration. The only existing effort taking vehicular width into account is perhaps that by Meng *et al* (2007). They tried to divide a single-lane into three sub-lanes and thus allowed the introduction of motorcycles into simulation.

As for urban traffic simulations, the existing CA studies in this regard can be categorized into two approaches. The first approach considers an abstract network which assumes a two-dimensional lattice and focuses on the investigation of phase transitions, e.g., Simon *et al* (1998), Chowdhury *et al* (1999) and Watanabe (2003). The second approach tries to describe the real-world traffic prevailing on the surface roadways in populated cities, e.g., Jiang *et al* (2006) and Spyropoulou (2007). Since these models basically followed the NaSch's coarse cell system, inevitably the vehicular speeds had merely three theoretical options *(0, 1, 2)* to cope with the prevailing urban speed limits.

Moreover, for CA simulation there is one common defect yet rectified—abrupt deceleration when vehicles encounter stationary obstacles or traffic jams. In fact, deceleration limitation was seldom been considered in the past; perhaps suffered from the utilized coarse cell system. Most CA models just considered a collision-free criterion explicitly by imposing arbitrarily large deceleration rates, which can be far beyond the practical braking capability under prevailing pavement and tire conditions. Consequently, most previous CA simulations have revealed that, for sake of collision prevention, a vehicle can take as short as 1 second to come to a complete stop, even from a full speed (e.g., *100kph*), apparently exceeding the vehicular deceleration capabilities. Such unrealistic abrupt deceleration can be easily identified via checking the vehicular speed profiles in the front of traffic jams or stationary obstacles.

When scrutinizing the existing efforts, one may agree that simulation through CA model has led to satisfactory outcome if only long-term average traffic features are concerned or only macroscopic traffic phenomena or global traffic parameters are examined; because the effects of locally realistic deceleration have been smoothed out. However, if we want to scrutinize in detail the microscopic traffic parameters around signalized intersections or the neighborhood of some unexceptional scenarios, such as an accident vehicle or a work zone blocking the partial highway lanes, it is evident that the deceleration rule in CA model requires further revisions.

To overcome the above-mentioned impediments for implementing CA into urban traffic simulation, we will propose three major modifications that

differ from the traditional CA models. First we propose to establish a refined CA cell system. For this, the concept *"cell"*, *"site"*, *"common unit"* (short for CU hereinafter) and the relationships among them will be defined. Next, Daganzo's (1997) two-dimensional generalized traffic variables—density *k(A)* and flow *q(A)*—are further extended to three-dimensional ones to account for the distinct vehicle widths and lane widths. As such, the generalized spatiotemporal occupancy *ρ(S)* and flow rates *q(S)* are defined. Finally, upon these two amendments, we further suggest the piecewise-linear variation of vehicular speed within each time-step. The methodology thereof is illustrated in detail in the following Sections.

3.2 Common Unit, Cells and Sites

Basically numerical method for traffic simulation is twin-object oriented, i.e., we have to consider roadway condition and the vehicular movement concurrently. So as the beginning the basic unit for vehicles and for roadway must be defined separately. Here *"cell"* is defined as the basic unit for representing vehicular size whereas a *"site"* is defined as the basic unit for representing the roadway space. Figure 3-2 illustrates this concept, in which the comparison between the proposed refined CA grid (i.e., cell/site) system and the cell system of the traditional CA model for a 2-lane roadway is also depicted. For the cell system utilized by most traditional CA models, as shown in Figure 3-2(a), usually a single cell can be occupied by a single vehicle, both longitudinally and laterally. A long vehicle (for example a bus or a truck) can be represented by multi-cells and occupy multi-sites longitudinally, e.g., Ez-Zahraouy *et al* (2004). However, it is clear that neither roadway nor vehicular width can be addressed if equips with such coarse cell system.

On the other hand, when utilizing refined CA grid system, the size of site and cell can be selected in accordance with the scenarios simulated as well as the resolution of simulation required. Here the *"resolution"* represents the degree of detail or the acceptable approximation of traffic phenomena one expects to analyze. For instance, a standard freeway lane with width of 3.75 meters (12 feet), as shown in Figure 3-2(b), can be arranged with 3 sites laterally with site width of 1.25 meter or 5 sites laterally with site width of 0.75 meter. Similarly, for other case such as a narrow street lane with width close to

3 meters, it can be set with 3 sites laterally with site width of 1 meter, etc. Also the cell size can be selected in light of the various lengths and widths of different vehicle types. The sole restriction is that the size of both basic site and basic cell should be identical, i.e., to be the common unit (CU). The concept of CU is evolved to serve as the joint basis for both vehicle and/or roadway; so as to describe different vehicle types and their required clearances for safe movement in the contexts of various widths of lanes and roadways.

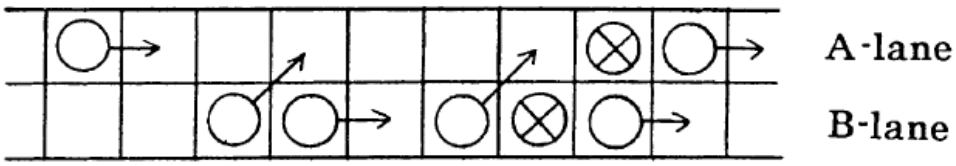

(a) The cell system utilized by most existing CA models. Note that neither roadway nor vehicular width can be addressed.

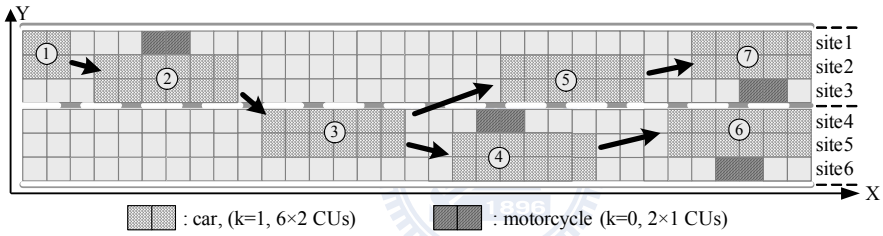

(b) The cell/site system utilized in the refined CA model.

Figure 3-2. Comparison between the proposed refined CA grid (i.e., cell/site) system and that of the traditional CA model for a two-lane roadway context.

According to Figure 3-2(b), it is obvious the refined grid system would be much easier to represent heterogeneous vehicle sizes and to measure the relative distances of any specific vehicle to its nearby vehicles on different roadway contexts.

The philosophy thereof is straight-forward and is analogous to the grid system that is popular in computational fluid dynamics (CFD) or the discrete mesh system that is commonly used in finite element method, a typical technique in structure strength and fatigue analysis. Figure 3-3 shows a typical example of CFD simulation in which first the grid system around the airfoil is

constructed (refer to Figure 3-3(a)). One can be easily aware of the philosophy for such grid system development—the area where higher local variation of Mach number (a proxy of speed) is anticipated, the denser grid density is constructed. Figure 3-3(b) represents the simulated Mach number contours that in fact is the iterated solution of renowned Navier-Stokes equation via the finite difference method. Based on the similar philosophy, here for traffic simulation we introduce the refined cell/site system so as to attain the required resolution of simulation.

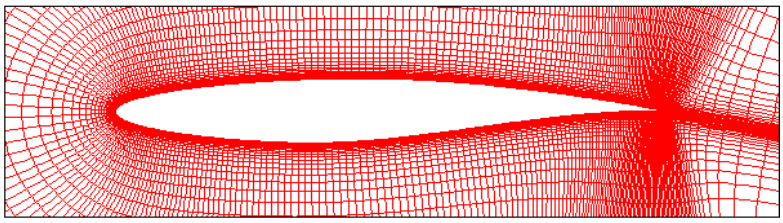

(a) The grid generated around the 2-D airfoil

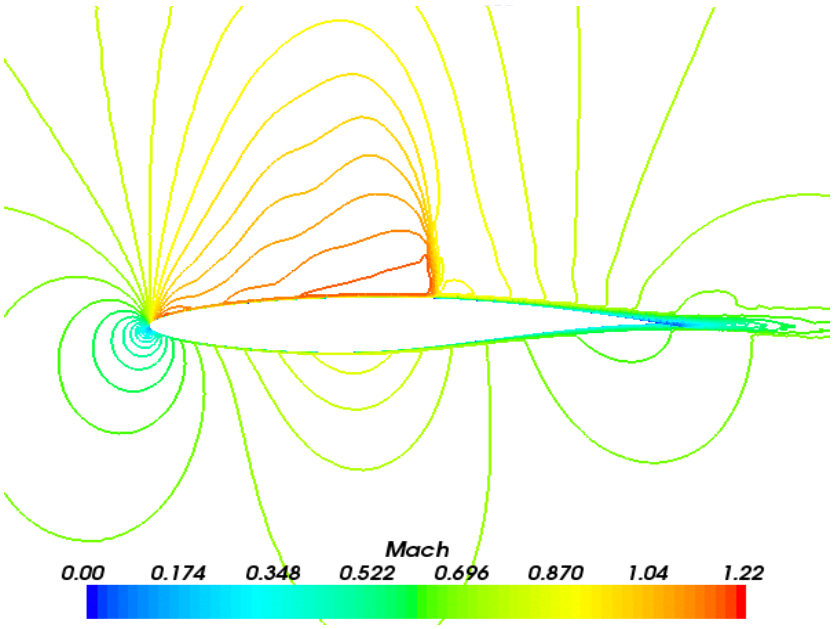

(b) The simulated Mach number contours.

Figure 3-3. Typical grid generation prevalent in computational fluid dynamics (CFD) analysis. In this case, 2-D flow field around an airfoil is analyzed.

A short recap, a refined grid system will bring about required resolution and is more efficient to describe the real traffic condition, such as mixed traffic contexts.

In this study, usually 3.75-meter freeway lanes are considered. Therefore a rectangular grid of 1×1.25 meters as the CU for cells and sites can be defined. Setting the length of CU to be 1 meter can effectively simulate the vehicular speed variation to a minimum accuracy of 1 meter per second, provided that the time-step of simulation is set as 1 second. This would largely improve the resolution of simulation results, which is particularly crucial for simulating the traffic via CA modeling where low speed limit is regulated (e.g., highway work zone, urban street) and wherein vehicles move with slight speed variations. For safe movement with acceptable clearances, in this study a light vehicle (car) is represented by a particle of 6×2 cells, always taking up 12 sites of road space; whereas a motorcycle is represented by 2×1 CUs, always taking up 2 CUs of the roadway space (refer to Figure 3-2).

3.3 Definition of 3-D Generalized Traffic Variables

To cope with the 3-D grid system that considers time and both vehicular length and width, we additionally extend the 2-D traffic parameters that proposed by Daganzo (1997) to be three dimensional. The philosophy is demonstrated as follows.

In conventional traffic flow theory, there are three important traffic parameters—traffic flow *(q)*, traffic density *(k)* and vehicle velocity *(v)*. For a single-lane roadway with length *L*, the local traffic parameters can be defined as:

$$k(t) = \frac{nubmer\ of\ vehicles\ observed\ over\ a\ road\ of\ given\ lentgh\ L\ at\ time\ t}{length\ of\ observed\ \ roadaway\ L}$$

$$q(x) = \frac{nubmer\ of\ vehicles(m)\ observed\ during\ given\ time\ period\ T\ at\ loc.\ x}{length\ of\ observed\ time\ period\ T}$$

So that

$$k(t) = \frac{n(t)}{L} \tag{3-1}$$

$$q(x) = \frac{m(x)}{T} \tag{3-2}$$

The vehicular speed *(v)* can be measured via local detector or through the formula:

$$q=kv \tag{2-4}$$

Equation (2-4) was originally developed by scholars in the field of fluid mechanics upon the assumption that fluid flow is continuous. This formula later was commonly utilized into traffic analysis since then for estimating vehicular average speed. However, a newcomer may be confused about the validity of such applicability since that traffic flow is no longer continuous but in essence discrete by nature. Besides, by definition, the 1-D local traffic flow-*q(x)* is a time-based parameter measured at fixed point whereas the local traffic density-*k(t)* is a space-based traffic parameter for an certain instant. So although Equation (2-4) seems reasonable from dimensional analysis perspective, it is criticized that this formula is strictly correct only under some very restricted conditions, i.e., homogeneous state in which each vehicle equips with identical features (e.g., same headway and identical speed, etc), or in the limit as both the space and time measurement intervals approach zero. If neither of those situations holds, then use of the formula to calculate speed can give misleading results, which would not agree with empirical measurements. These issues are important, because this formula has often been uncritically applied to situations that exceed its validity.

To overcome this restriction, Daganzo (1997) proposed to extend the 1-D local traffic parameters to be 2 dimensional to cover both time and distance and hence defined the 2-D general traffic parameters, shown as follows.

According to Daganzo (1997), for a finite *x-t* region, for example, the rectangular region *A* in Figure 3-4 with length *L* and width *T*, the 2-D generalized density *k(A)* can be defined as:

$$k(A) = \frac{\sum_{\Delta t} n(t)\Delta t}{\sum_{\Delta t} L\Delta t} = \frac{t(A)}{|A|} \tag{3-3}$$

where *t(A)* is the total time of all vehicles spent in *A* and $|A|$ denotes the area of *A*.

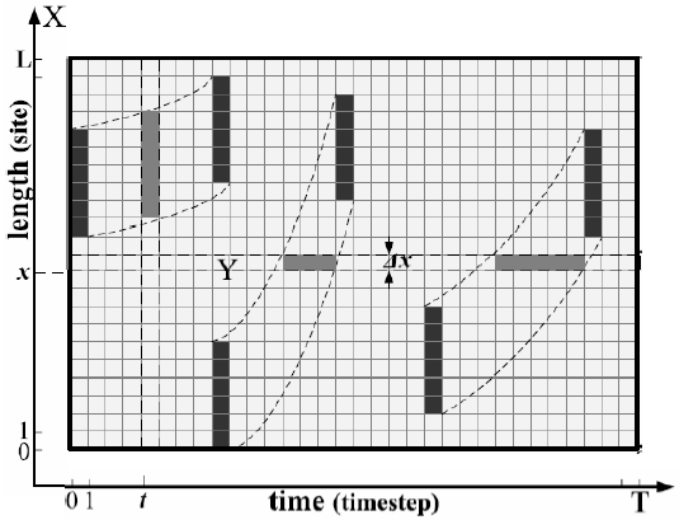

Figure 3-4. Definition of 2-D traffic parameters, proposed by Daganzo (1997).

Similarly, the flow over the same larger region *A*, the 2-D generalized traffic flow, *q(A)*, can be defined as:

$$q(A) = \frac{\sum_{\Delta x} m(x)\Delta x}{\sum_{\Delta x} T\Delta x} = \frac{d(A)}{|A|} \tag{3-4}$$

where *d(A)* represents the total distance traveled by all vehicles in *A*.

The ratio of Equation (3-3) to (3-4) leads to the space-and-time mean speed in *A*, which can be further reduced to "*the ratio of the total distance*

traveled to the total time spent by all vehicles in A " as expressed in equation (3-5):

$$v(A) = \frac{q(A)}{k(A)} = \frac{d(A)}{t(A)} \tag{3-5}$$

Thus the 2-D generalized density, flow and speed on vehicle basis over a 2-D time-distance region (including 1-D for the longitudinal roadway and 1-D for the time) can be defined respectively. However, such definitions may not exactly depict the collective behaviors of traffic movement over a 3-D domain, including 2-D for the roadway (longitudinal and transverse) and 1-D for the time. Therefore, to further enhance the resolution of CA simulations, we propose to expand the definition of these traffic parameters and define the traffic variables on site or cell basis over a spatiotemporal domain *S*, as shown in Figure 3-5.

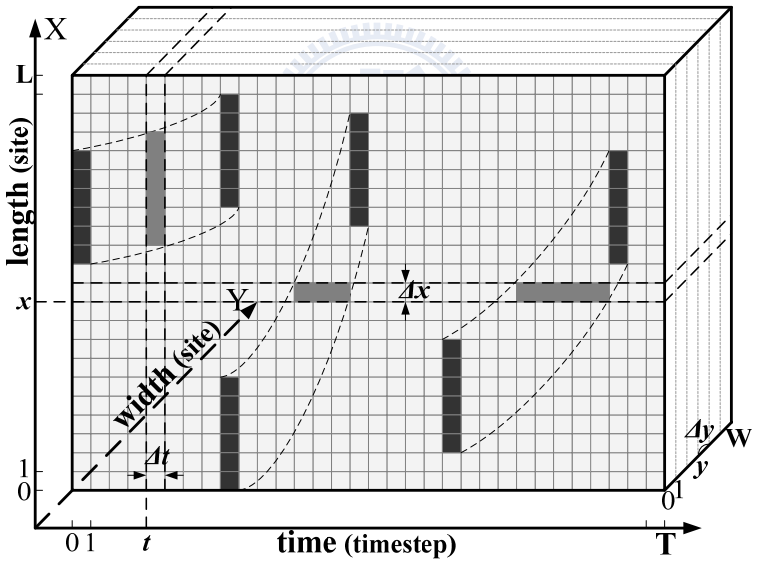

Figure 3-5. Vehicular trajectories over a specific transverse slice in a spatiotemporal domain S enclosed by $L \times W \times T$.

According to Figure 3-5, for the 3-D domain *S* expressed by $L \times W \times T$ where *L* denotes the longitudinal length and *W* denotes the transverse width of roadway, and *T* is the observed period of time, a generalized definition of density over this spatiotemporal domain *S*, *ρ(S)*, can be defined as:

$$\rho(S) = \frac{\sum N_0(t)\Delta t}{\sum N \Delta t} = \frac{t(S)}{|S|} \tag{3-6}$$

where. $|S|$ represents the *"volume"* of this spatiotemporal domain *S*. $N_0(t)$ represents the total number of sites occupied by cells (vehicles) at the instantaneous time *t* and *t(S)* is its accumulated value for all times simulated; $t(S) = \sum N_0(t)\Delta t$. Likewise, a 3-D generalized definition of traffic flow in the spatiotemporal domain *S* can be defined as:

$$q(S) = \frac{\sum M_0(x)\Delta x}{\sum T \Delta x} = \frac{d(S)}{|S|} \tag{3-7}$$

where $M_0(x)$ is the total number of squared sites occupied by cells (representing vehicles) at a specific location *x* in road. *d(S)* is the total distance traveled by all cells in *S*; $d(S) = \sum M_0(x)\Delta x$. The ratio of Equation (3-7) to Equation (3-6) defines the generalized space-mean speed in *S*, which can be further reduced to the ratio of the total distance traveled to the total time spent by all cells in *S*, expressed in Equation (3-8):

$$v(S) = \frac{q(S)}{\rho(S)} = \frac{d(S)}{t(S)} \tag{3-8}$$

The above generalized spatiotemporal density, traffic flow and speed of *"cells"* moving over 2-D sites and over the time marched, as expressed in Equation (3-6), (3-7) and (3-8) are used in this study to depict the collective behaviors of traffic flow patterns in the following CA simulations.

3.4 Primitive Update Rules for Refined CA Model

Corresponding to refined grid system, we first contrive the primitive forward and lane-change update rules, based upon the existing CA models, to govern the vehicle movements over a spatiotemporal domain. This study sets the time-step as one second, thus the positions and speeds for all vehicles will be updated in parallel per second.

3.4.1 Forward rules

As discussed, the mixed flow condition leads to the demand for transferring vehicles into cell units. In previous 1-D CA models, the forward rules depend on the gap, which is simply defined as the number of sites between the head of a vehicle to the rear of its preceding vehicle. The forward rules in our CA model are based on 2-D mixed traffic prerequisites; thus, a gap in this study is defined as the *"minimum number of sites"* between the head cells of a vehicle and the tail cells of all its preceding vehicles. For instance, if two motorcycles (2×1 CUs) moving in parallel (one is a little behind the other) in front of a car (6×2 CUs), the gap should be measured from the tail of the behind motorcycle to the head of that car. In addition, since all vehicles may move at different speeds, the closest preceding vehicle of a vehicle may vary over time-steps. Consequently, the calculation of a gap is a dynamical process.

Since car and motorcycle are both considered in the present study, we will check the distances (in terms of number of sites) from each cell head of a vehicle to its preceding occupied sites and choose the minimum one as the gap.

Basically the renowned NaSch model is utilized. However, some modifications are introduced, in accordance with the scheme proposed by Jiang *et al* (2003), into our CA models to reflect the real driver behavior the extent as possible. These include the anticipation effect, the VDR concept, and the delay-to-start phenomena, as mentioned in Chapter 2. The primitive forward rules can be described as the following seven steps.

Step 1: *Determination of the randomization probability.* Three possibility values are introduced, P_b-which considers the impact of decelerating vehicle in close front, P_0 - which reflects the delay-to-start behaviors of some vehicles located on downstream front of traffic jam, and P_d -the probability for all the other situations.

$$p(v_n(t), t_h, t_s, S_{n+1}(t) = \begin{cases} p_b: & \text{if } S_{n+1} = 1 \quad \text{and} \quad t_h < t_s \\ p_0: & \text{if } v_n = 0 \quad \text{and} \quad t_{st} \geq t_{k,c} \\ p_d: & \text{in all other cases} \end{cases} \tag{3-9}$$

where

$$t_h = d_n / v_n(t) \quad , \quad t_s = \min(v_n(t), h_k)$$

t_{st} denotes the time the vehicle stops. Only when the car has stopped for a certain time $t_{k,c}$ does the driver become less sensitive.

Step 2: *Acceleration.* Determine the speed of vehicles in next time-step. Here the status identifier, $S_n(t)$, is also taken into consideration. The value of $S_n(t)$ is determined in Step 5.

$$\text{if } (S_{n+1}(t) \geq 0 \text{ and } S_n(t) \geq 0) \text{ or } (t_h \geq t_s)$$

$$\text{then } v_n(t+1) = \min(v_n(t) + a_k,\ v_{k,max}) \tag{3-10}$$

$$\text{else } v_n(t+1) = v_n(t)$$

Where $v_{k,max}$ and a_k are the maximum speed and acceleration capacity of vehicle, respectively.

Step 3: *Deceleration.* Set velocity restriction when the vehicle in front is too close, thus locates within the effective distance (d_n^{eff}), as defined by Knospe *et al* (1999, enclosed as Equation (2-24) hereinabove).

$$v_n(t+1) = \min(d_n^{eff}, v_n(t+1)) \tag{3-11}$$

Step 4: *Randomization.* In real situations, not all drivers or vehicles of the same type have identical behaviors. Therefore, in stochastic CA simulations, we assume with probability p (determined in step 1) a vehicle will not accelerate or with smaller acceleration at the next time-step.

$$\text{if } (rand() < p), \text{ then } v_n(t+1) = \max(v_n(t+1) - 1,\ 0) \tag{3-12}$$

Step 5: *Determination of vehicle status identifier $S_n(t)$ in next time-step.*

$$S_n(t+1) = \begin{cases} 0 & \text{if } v_n(t+1) > v_n(t) \\ S_n(t) & \text{if } v_n(t+1) = v_n(t) \\ 1 & \text{if } v_n(t+1) < v_n(t) \end{cases} \tag{3-13}$$

Step 6: *Determination of time (t_{st}) stuck inside the jam.*

$$t_{st} = \begin{cases} t_{st} = t_{st} + 1 & \text{if } v_n(t+1) = 0 \\ t_{st} = 0 & \text{if } v_n(t+1) > 0 \end{cases} \tag{3-14}$$

Step 7: *Update position.* Move vehicle in accordance with the calculated velocity.

$$x_n(t+1) = x_n(t) + v_n(t+1) \tag{3-15}$$

In sum, the forward rules in our primitive CA model are the revised versions of NaSch model in several aspects. First, due to different definitions of the cell size with time-step 1 second, the minimum acceleration rate in our model is 1 m/s^2, but in the NaSch model is 7.5 m/s^2. Second, our model anticipates the preceding vehicles action in the next time-step, but the NaSch model does not. Thirdly, our model takes the minimum clearance of all front sites into consideration but NaSch model and the following works do not. Thus, our model can simulate the shoulder-to-shoulder forward movements (without lane discipline) in mixed traffic contexts but NaSch model cannot.

3.4.2 Lane change rules

The lane-change rules utilized in this study are defined as follows. These lane-change rules can be applied to all vehicles (car, bus, truck, etc) except the small ones (such as motorcycle, bike) since that oftentimes small vehicles do not obey the lane change disciplines.

Step 1: *Vehicle orientation.* For example, if a vehicle is on the left lane of a two-lane road, the possible lane-changing scenarios are 1→2→3, 2→3, 3→4, and vice versa, depending on its original and final locations, as demonstrated in Figure 3-6.

Step 2: *Check incentive criterion.* Determine whether the vehicle in front on the other lane moves with higher speed than that of the vehicle in right front. If yes, the vehicle has incentive to change lane.

Step 3: *Check gap ahead.* Estimate the front gap at the next time-step. If the front gap is too small, then check the gap between the vehicle and its downstream vehicle on the other lane to determine if it allows for a not-decreasing movement when performing a lane-change in the next time-step.

Step 4: *Check safety criterion.* Estimate the gap between the vehicle and its upstream vehicle on the other lane at the next time-step. If the gap on the other lane is larger than its upstream vehicle's velocity, it means that a safe lane-change can be performed without cutting in someone else's way.

Step 5: *Randomization.* In real situations, not all drivers will make the lane changes even if the above lane-change rules are satisfied. Thus, in stochastic CA simulations, this paper assumes that with probability *p=0.5* the drivers will remain in-lane provided all lane-change rules are met.

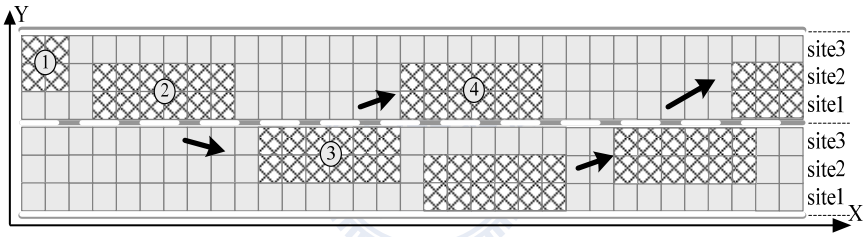

Figure 3-6. Lane changes for a car on a two-lane roadway

Taking a vehicle on the left lane in Figure 3-6 as an example, the lane change rule can be recapped as:

$$\begin{aligned} &LC^{l\to r}: \text{If } \ v_{l,n}(t) > v_{l,n}(t) \ \text{ and } \ v_n(t) > v_{l,n}(t) \\ &\text{and } \ g^r_{l,n}(t) > \min(d^{eff}_n, v_n(t+1)) \\ &\text{and } \ g^r_{b,n}(t) > \min(d^{eff}_{b,n}, v^r_{b,n}(t+1)) \end{aligned} \tag{3-16}$$

where,

g means the gap and the suffix b means the vehicle in nearby upstream.

3.5 Proposed Revision to CA Update Rules

3.5.1 Forward rules with limited deceleration

Simulation through the above-mentioned CA updated rules has shown its success in capturing essential features of traffic flows that were also found in previous works. However, it is found that although the idea of limited acceleration is implemented, (refer to Equation 3-10) deceleration limitation has seldom been considered in the past. In fact, most prevailing CA models have considered a collision-free condition explicitly by imposing arbitrary deceleration rates (refer to Equation 3-11). Thus, unrealistic traffic behaviors would be found if one had investigated the speed profiles of vehicles, especially in the vicinity of the upstream front of a traffic jam or a stationary obstacle, as shown in Figure 3-7.

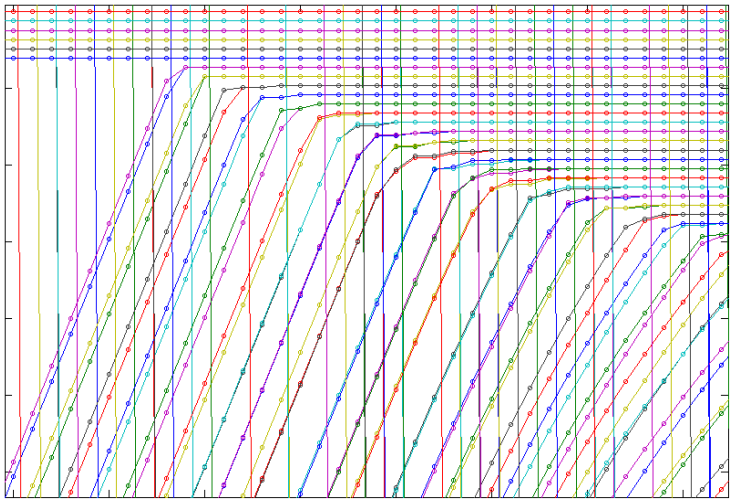

Figure 3-7. Unrealistic simulated *x-t* diagram of primitive CA model—unlimited deceleration behaviors of vehicles when approaching upstream front of traffic jams. The horizontal axis represents time marched from left to right whereas the vertical axis represents the upward displacement of vehicles.

In fact, for traditional CA models, the collision-free flow is just the natural consequence of preset infinite vehicle braking capabilities. However, notwithstanding the success of prevailing CA models in simulating the global traffic parameters, it is our opinion it is imperative to incorporate limited deceleration capability into CA models if more realistic and concise simulation of microscopic/local traffic is intended.

As mentioned by Lee *et al* (2004), however, when setting limited deceleration into simulations, the bounded braking capability changes the

collision-free mechanism entirely. In addition, discrete variations of traffic parameters that are essentially the nature of CA model exaggerate the consequence further. When vehicles characterize with finite deceleration capacity, the simulations by prevailing CA models reveal that with high probability vehicles will collide with the front vehicle that is stationary or abruptly decelerated.

In the past, some relevant efforts can be located for rectifying this defect. For example, Krauss *et al* (1997) introduced the limited deceleration capacity into CA modeling. Accordingly, the *"safe speed"* was defined. Lee *et al* (2004) further introduced the limited capability of acceleration *(a)* and deceleration *(D)* in their model and proposed the following safety criteria for vehicle movement; which is theoretically similar to that proposed by Krauss *et al*, as cited above. Recently, Yamg *et al* (2007) proposed that the vehicular speed can be deemed as the function of front gap for ensuring complete stop and defined the abrupt deceleration threshold V_d for initiating the deceleration mechanism.

All three above-mentioned modifications are established under the assumption that drivers will always be aware of speed of preceding vehicles and hence will continuously maintain adequate distances for collision prevention, in case the preceding vehicle in next time-step starts to decelerate to a complete stop. However, it is argued that the following vehicle always takes caution to consider the required stop distance to the lead vehicle is over-conservative. It is our opinion that drivers can easily sense the relative speeds to the front vehicles rather the absolute speeds of the front vehicles. In other words, drivers would be able to tell they are approaching vehicles in front, primarily due to the changes in apparent size of the vehicles, by perceiving relative speed changes. Besides, only with positive relative speeds to the front vehicles would the following drivers take caution for collision prevention. Upon this, we propose the following modifications:

3.5.2 Piecewise-linear speed variation

To evaluate the proper speed update, the Newton's kinematics will be implemented. For this, we first suggest that the CA discrete speed variations adopted in most conventional CA models to be revised as piecewise-linear in

each time-step, as shown in Figure 3-8, thus to simulate more realistically the accelerating/decelerating behaviors of vehicles. It is our opinion that the particle-hopping manner, as shown in Figure 3-8(a), adopted by most existing CA models, is over-simplified. Therefore, we alternatively suggest that vehicles will smoothly vary their speeds from the original ones at the beginning to the desired speed by the end of each time-step, as shown in Figure 3-8(b). Thus more realistic accelerating/decelerating behaviors of vehicles can be generated. Besides, only upon this revision and coupled with the refiner cell/site system can the Newton's kinematics be introduced to determine the appropriate deceleration.

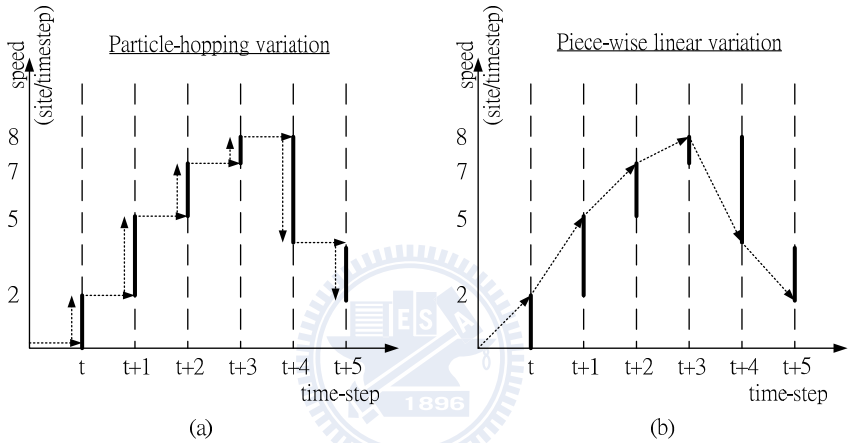

Figure 3-8. Different definitions of vehicular speed update: (a) particle-hopping variation; (b) piecewise-linear variation.

One point worthy mentioned here is that this simple amendment, however, has altered the nature of the proposed model. Generally speaking, as mentioned by Sprott (2003), spatiotemporal models can be categorized according to whether space, time and the state of variables are quantized, as summarized in Table 3-1. The simplest model is a CA model in which everything is discrete and the most complicated models are described by PDEs in which everything is continuous and lead to, if possible, analytic solution. Therefore, our proposed model that coupled with piecewise-linear speed variation may no longer be a CA model but instead, be categorized as one *"coupled mapped lattice model"*. Nevertheless, for sake of facilitating readability, the terminology *"refined CA model"* will be maintained throughout this thesis when refer to our proposed model.

Space	Time	State	Model
Discrete	Discrete	Discrete	Cellular automata
Discrete	Discrete	Continuous	Coupled map lattices
Discrete	Continuous	Discrete	
Discrete	Continuous	Continuous	Coupled flow lattices
Continuous	Discrete	Discrete	
Continuous	Discrete	Discrete	
Continuous	Discrete	Continuous	
Continuous	Continuous	Continuous	Partial differential equations

Table 3-1. Summary of spatiotemporal models (source: Sprott (2003))

3.5.3 Revised deceleration mechanism

Next, we propose to revise vehicular deceleration mechanism as follows. When with positive relative speeds to the front vehicles, the following drivers will first estimate the relative speeds to the front vehicles at next time-step. Then with known limited acceleration and deceleration capability, drivers will determine the adequate relative speeds they should take at next time-step; so as not to collide with the front vehicles. In other words, the following drivers would maintain speeds in such a way that they can decelerate to sustain some certain distance gaps to the front vehicles, assuming that the front vehicles move with the estimated speeds in the future.

The rationale for this assumption is that drivers can anticipate straightforwardly the relative speeds to the front vehicles for the next time-step but they may have difficulty to identify those speed variations for further time-steps. As a result, drivers are likely to presume that the front vehicles will maintain the anticipated speeds and henceforth evaluate appropriate reaction as required. In any case, however, drivers will keep checking the nearby traffic conditions and react repeatedly in each time-step.

This revised speed update mechanism in essence the extension of classic car-following concepts proposed by Pipes (1953) and/or Forbes (1958), as mentioned in Section 2.3 and the coupled car following formula (Equation (2-12)). The main deviation is that appropriate deceleration rate is determined through Newton's kinematics rather based on given time headway (τ).

$$\ddot{x}_n(t) = \frac{1}{\tau}[\dot{x}_{n+1}(t) - \dot{x}_n(t)] \quad (2\text{-}12)$$

3.5.4 Implementation of Newton's kinematics

Our final suggestion is to implement Newton's kinematics for position update and adequate speed evaluation. The philosophy is described in short as follows.

For n^{th} vehicle with speed V_0 at instant t, if the updated speed (V_1) at next time-step t+1 is larger than the anticipated speed (V_f) of front vehicle also at time-step t+1, then the effective gap (S_1) to the front at t+1 will be evaluated and check if it allows for n^{th} vehicle to decelerate to V_f with no risk of collision. If not, then re-evaluate the proper speed n^{th} vehicle should be selected at time-step t+1.

As mentioned, thanks to the piecewise linear variation of vehicles within each time-step and the refined grid system utilized, the Newton kinematics can be implemented for gap evaluation. The coupled algorithm is demonstrated as below.

First, after the acceleration update rule (Equation 3-10) is implemented, check the relative speed to the front. If with negative relative speed to the front, then there is no risk for collision, at least for instant *t+1*, so no further evaluation need to be performed.

On the other hand, if with positive outcome, this implies a decreased gap in the further, then additional attention must be taken to ensure that no collision will occur in case the front vehicle start to decelerate at next time-step. For this, the following supplemental steps will be performed.

(1) Evaluate the front effective gap for n^{th} vehicle at next time-step *t+1*

Since one time-step is set as *1s*

$S_1 = S_0 - (V_0 + a/2) + V_f$

$= S_0 - [V_0 + 1/2(V_1 - V_0)] + V_f$

$$= S_0 - 1/2(V_1 - V_0) + V_f \quad (3\text{-}17)$$

where:

S_0: the original front gap at instant t

S_1: the front gap at instant $t+1$

V_0: the original speed at instant t

V_1: the update speed at instant $t+1$ per Equation (3-10)

$a = V_1 - V_0$ is the evaluated acceleration or deceleration of n^{th} vehicle at $t+1$ per Equation (3-10)

V_f: the anticipated speed of front vehicle at instant $t+1$

(2) Check front gap at $t+1$ for n^{th} vehicle if it allows for decelerating from V_1 to V_f with known deceleration capacity d_m

Since the initial speed V_1, he target speed V_f and the deceleration capacity d_m are all known, time-steps required for deceleration can be obtained through the following equation

$$t_{req} = \frac{V_1 - V_f}{d_m} \quad (3\text{-}18)$$

Accordingly, the Newton's kinematics formula can be adopted to check if positive gap still exists after t_{req} time-steps upon the assumption V_f remains unchanged in the further.

$$S_{final} = S_1 - (V_1 t_{req} - \frac{1}{2} d_m t_{req}^2) + V_f t_{req}$$

$$= S_1 - [V_1 \frac{V_1 - V_f}{d_m} - \frac{1}{2} d_m (\frac{V_1 - V_f}{d_m})^2] + V_f (\frac{V_1 - V_f}{d_m})$$

$$= S_1 - \frac{1}{2d_m}(V_1 - V_f)^2 \quad (3\text{-}19)$$

where

S_{final}: the evaluated final front gap after time-steps t_{req}

d_m: the known deceleration capacity

On the occasion that $S_{final} \geq 0$, it means that a safety margin still remains to prevent collision to the front, no further action will be required. Otherwise the speed at time $t+1$ must be revised (reduced).

(3) If $S_{final}<0$, find the proper deceleration and speed for at time $t+1$

The proper deceleration for collision prevention can be found through the following calculation. Be aware that here we use S_0 as the initial gap and V_0 as the initial speed to supersede the originally estimated V_1 and derived S_1, since both values have been identified as unacceptable.

$$t_{req} = \frac{V_0 - V_f}{d_m} \tag{3-20}$$

$$S_{final} = 0 = S_0 - (V_0 t_{req} - \frac{1}{2} d t_{req}^2) + V_f t_{req}$$

$$0 = S_0 - [V_0 \frac{V_0 - V_f}{d} - \frac{1}{2} d (\frac{V_0 - V_f}{d}^2] + V_f (\frac{V_0 - V_f}{d})$$

where

d: the appropriate deceleration for n^{th} vehicle at time $t+1$

So the proper deceleration should be:

$$d = \frac{1}{2S_0}(V_0 - V_f)^2 \tag{3-21}$$

Also the speed of n^{th} vehicle when by end of time-step $t+1$ can be found as:

$$V=V_0-d \tag{3-22}$$

3.5.5 Amendment to vehicular movement

Through the above-mentioned revised steps, the realistic deceleration behaviors can be successfully gauged. Coupled with this, vehicular movement can also be derived. Through basic integral calculation, as shown below, one

may find that the movement of vehicle is simply the average of the existing speed and the desired speed by the end of each time-step. (also see Figure 3-9 for reference)

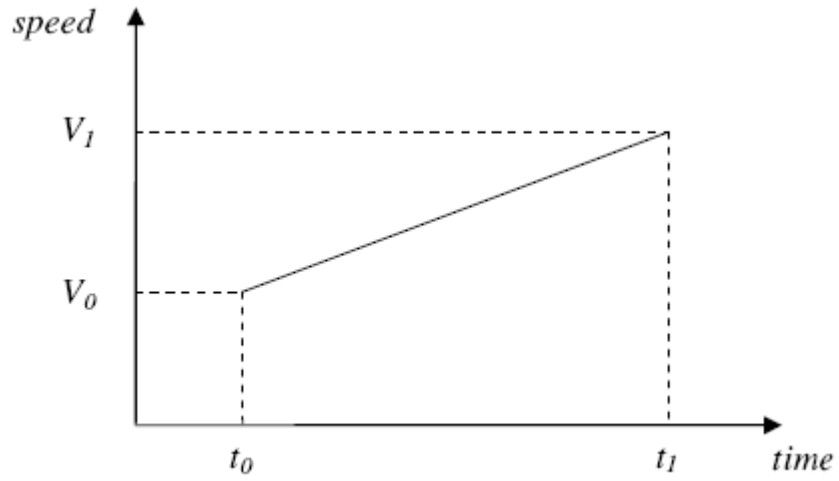

Figure 3-9. Piecewise-linear variation of speed during time interval (t_0~t_1).

Since $V=V_0+(t-t_0)(V_1-V_0)$

Displacement in the interval (t_0, t_1) can be found as:

$$\Delta S = \int_{t_0}^{t_1} V dt = \int_{t_0}^{t_1} V_0 + (t - t_0)(V_1 - V_0)\, dt$$

$$= V_0 + \frac{t^2}{2}(V_1 - V_0)\Big|_{t_0}^{t_1} - t_0(V_1 - V_0)\Big|_{t_0}^{t_1}$$

$$\text{if } timestep = 1s, (t_1 = t_0 + 1), \text{ then}$$

$$\Delta S = V_0 + \frac{2t_0 + 1}{2}(V_1 - V_0) - t_0(V_1 - V_0)$$

$$= V_0 + \frac{1}{2}(V_1 - V_0)$$

Therefore $\Delta S = \frac{1}{2}(V_1 + V_0)$ (3-23)

However, the derived average requires rounding off to the nearest integer since, by nature of CA modeling, vehicles still move on cell/sites basis. This

approximation is deemed acceptable when the refined cell/site system is implemented. In this study we deliberately choose the truncated integers to ensure that no collision with the front vehicles would be incurred.

3.5.6 Revised primitive forward rules

To recap the above demonstration, step 3 (Equation 3-11) and step 7 (Equation 3-15) of the primitive CA forward updated rules are respectively revised as follows:

Revised Step 3: *Deceleration.* If $v_{n+1}(t+1)<v_n(t+1)$, check the following safety criteria to determine speed at the next time-step

$$x_n(t+1)+\Delta+\sum_{i=1}^{\tau_n(c_n(t+1))}(c_n(t+1)-\frac{Di}{2}) \le x_{n+1}(t+1)+\sum_{i=1}^{\tau_n(c_n(t+1))}v_{n+1}(t+1) \quad (3\text{-}24)$$

where:

$n(n+1)$: denotes the follower (leader)

$x_n(t)$, $v_n(t)$: the location (speed) of the follower at time t

$x_n(t+1)$: the location of follower by end of time $t+1$

$c_n(t+1)$: the safe speed at time $t+1$ of follower

$x_{n+1}(t+1)$, $v_{n+1}(t+1)$: the anticipated location (anticipated speed) of leader at time $t+1$

τ_n : the time-steps required for follower at time $t+1$ with $c_n(t+1)$ decelerating to $v_{n+1}(t+1)$

D : maximum braking capacity; based on field observation, it is set as *6* m/s^2 for light vehicles (cars)

$\triangle$: minimum clearance of the follower

Revised Step 7: *Update position.*

$$x_n(t+1)=x_n(t)+roundoff(\frac{v_n(t)+v_n(t+1)}{2}) \quad (3\text{-}25)$$

3.6 Description of Numerical Simulation

3.6.1 Simulation codes

The simulation code is programming via the C# (C sharp) language that is developed by Microsoft and is incorporated into the Visual Studio integrated development environment (IDE) interface, as shown in Figure 3-10. The MS Visual Studio IDE is one popular software development tools available to software engineers in computer science industry owing to its excellent capacity of integrating and communicating computer programs that are written in various computer languages (such as C#, C++, JAVA, Visual Basic, etc). On the other hand, the C# language, the improved version of the original C++ language, is OOP (Object Oriented Programming) by nature. It possesses the powerful functionality and flexibility of original C++. This merit is so crucial since in traffic simulation various vehicular sizes and driver behaviors need to be precisely depicted. Besides, C# also benefits from the important advantage of Visual Basic and JAVA language—conciseness; thus facilitates the simulation pace. The concept of OOP and some important features of the developed C# codes are illustrated as follows.

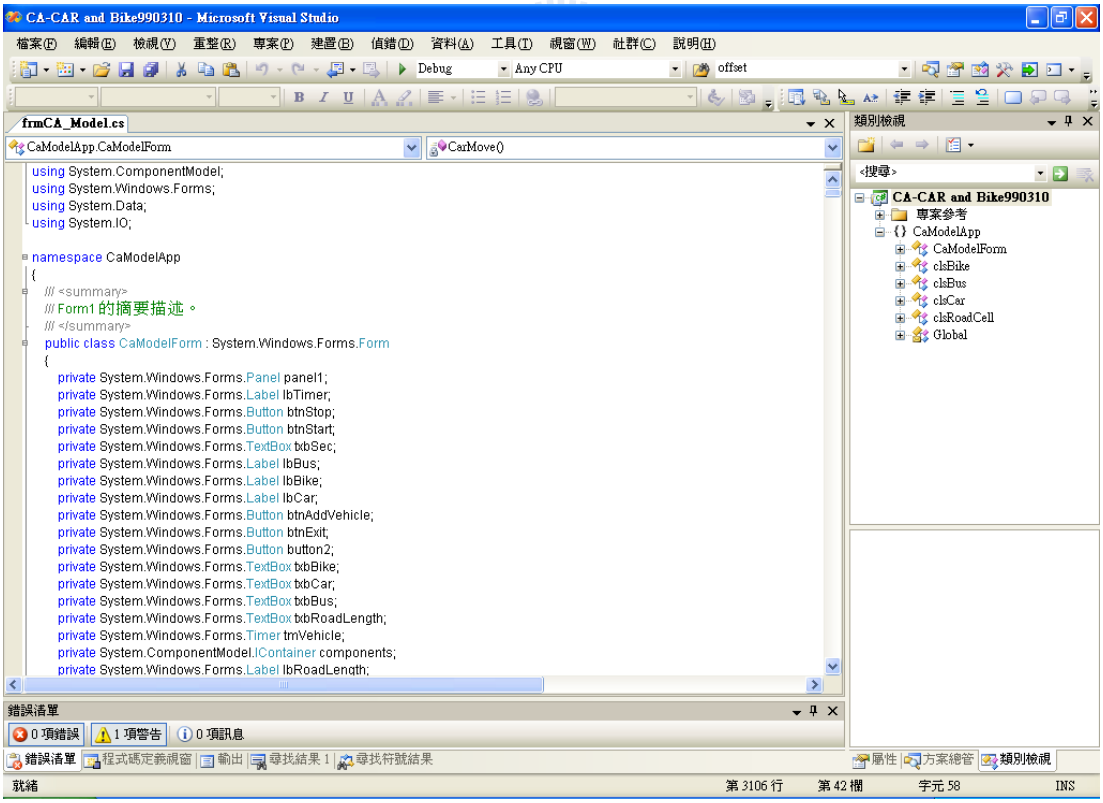

Figure 3-10. Demonstration of developed C# code; it is constructed upon MS Visual Studio IDE environment.

3.6.2 Concept of OOP

Commercial traffic simulation software such as VISSIM, PARAMICS, CORSIM and INTELSIM have been successful in simulating pure traffic (consider one kind of vehicle only). Nevertheless, these software are not believed to be appropriate for studying heterogeneous (consider more kinds of vehicle) traffic, due to wide variations in flow characteristics of heterogeneous traffic. For example, VISSIM is very difficult to perform non-lane-based simulation. In fact, most heterogeneous traffic simulation models have been developed using procedural languages, such as FORTRAN. FORTRAN is an important tool for development of scientific and engineering computational codes. However, it has own limitations: maintenance of programming is time consuming and difficult due to coupling among the procedures. Moreover, from the previous studies it is revealed that existing models are mostly developed for some specific traffic analysis and it is difficult to extend for newer applications and even if they are extended, it would involve considerable time, effort and rewriting and debugging code.

OOP, in contrast, is a major shift from traditional method of software construction. The benefits of OOP are easy maintenance, enhanced modification and reusability of the program. In OOP, a system can be viewed as a collection of entities that interact together to accomplish certain objectives. This is in contrast to the existing modular programming that focused on the function of a module and, rather than specifically the data, tends to consider data and behavior separately and enable collaboration through the use of linked modules (subroutines). OOP focuses on data rather than processes, with programs composed of self-sufficient modules (*"classes"*), each instant of which (*"objects"*) contains all the information needed to manipulate its own data structure (*"members"*).

For a computer programmer, the developed OOP program may be viewed as a collection of interacting objects, as opposed to the conventional model in which a program is seen as a list of tasks (subroutines) to perform. Each object is capable of receiving messages, processing data, and sending messages to other objects and can be viewed as an independent *"machine"* with a distinct role or responsibility. Hence, the OOP technique offers a highly sophisticated versatile programming environment for the development of large

scale and/or complex software system because of its inherent features of encapsulation, inheritance and polymorphism.

In one program written in C#, a class defines the abstract characteristics of object (an object is defined as the actual instant of a class), including its characteristics (its attributes, fields or properties) and the thing's behaviors (the things it can do, or methods, operations or features).

3.6.3 Description of classes

In the developed C# code, three important classes are defined, including the *CaModelForm* class, vehicular classes (*clsCar*, *clsMotor*, etc) and the *clsRoadCell* class. The purpose and function thereof are explained as follows.

(1) CaModelForm class

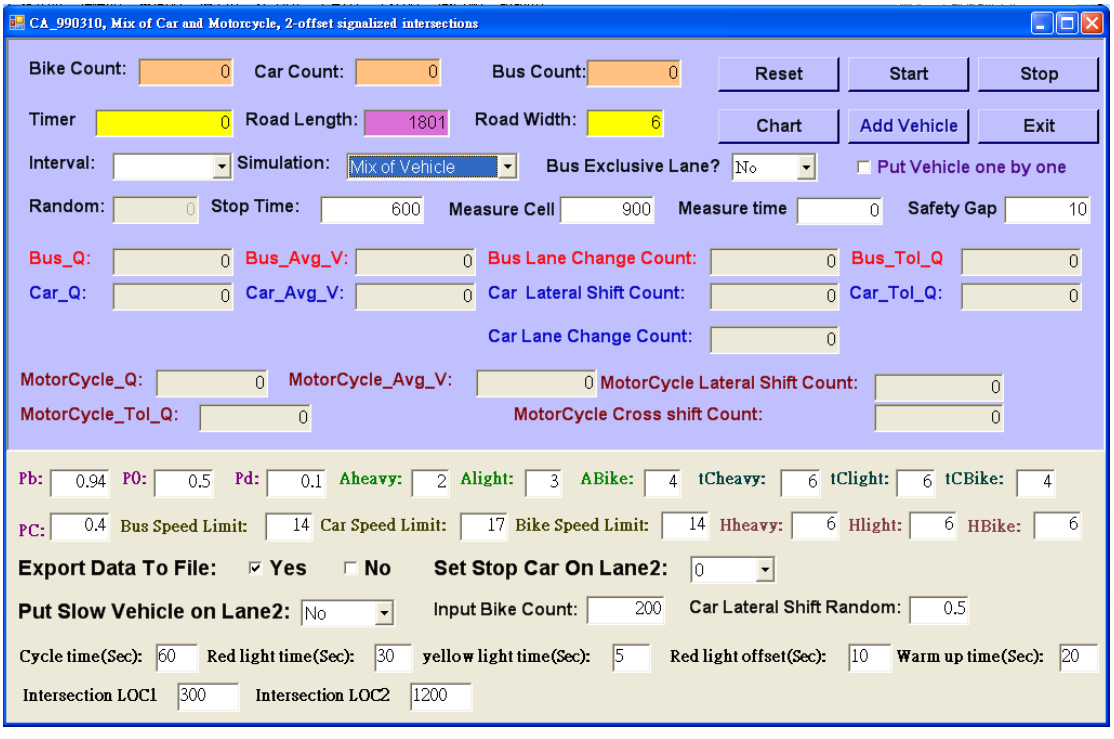

Figure 3-11. User interface of the developed C# simulation code

The *CaModelForm* class is the main and most important class in which the initial vehicle density, vehicle positions and speeds are defined. This class also defines the numerical algorithms; monitors time marched and determines the occasions different vehicular update rules should be implemented. Besides,

a friendly user interface is also developed in this class, as shown in Figure 3-11. This well-defined user interface has significantly expedited the pace of our study. Some important methods related to *CaModelForm* class are outlined in Table 3-2.

Method defined	Purpose
tmVehicle_Tick	Count the time simulated
btnStart_Click	Initialize simulation
Initial_All_Vehicles	Set the vehicles' positions when simulation starts
btnStop_Click	To interrupt the simulation as required
CarMove	Determine the cars' movement i.a.w preset update rules
BikeMove	Determine the motorcycles' movement i.a.w preset update rules
Check_All_Vehicle	Update vehicles' position and speed by end of each times step
OutPutCellData	Output simulation data when simulation complete

Table 3-2. Summary of important methods defined for Class *CaModelForm*

(2) Vehicular classes

Various vehicular classes can be defined in accordance with the simulated scenarios. Therefore *clsCar*, *clsBus* and *clsMotor* class are defined to describe the light vehicle (car), heavy vehicle (bus or truck) and motorcycle respectively. Additional class may be introduced as simulated situation requires. Each vehicle class equips with its own unique attributes, such as vehicular sizes, vehicular performance and driving behaviors as well. For example, the *clsCar* class is assigned with the movement attributes (methods), both forward and laterally. Some important methods related to *clsCar* class are cited in Table 3-3 for reference. As for more active vehicle such as motorcycle, more complicated movement option (e.g., transverse crossing) can also be incorporated. Chapter 5 will illustrate the details.

(3) clsRoadCell class

Since we have to consider roadway condition and the vehicular movement concurrently, the *clsRoadCell* class is also defined to describe the roadway conditions. This class monitors the condition of each roadway site—whether it is occupied, the occupied vehicle type, the designated vehicular number and the speed thereof. The *clsRoadCell* class communicates

with vehicular class during each simulated time-step to ensure the simulated traffic phenomena can be precisely reflected.

Method defined	Purpose
Can_Accel	Define the forward movement disciplines
Car_Accel	Update the car forward position
Can_LC	Define if lane change (LC) discipline
Car_LC	Update the car position if LC is taken
Can_LS	Define if Lateral shift (LS) discipline within the same lane
Car_LS	Update the car position if LC is taken.
Check_Rowcell_Space	Check the front gap
Check_BackCell_Space	Check the backward gap
GetMinFrontSpace	Check the minimum gap in front
Getpeerroadstate	Check if the sites aside are empty
DecisionRandom	Determine the randomized probability value

Table 3-3. Summary of important methods defined for Class *clsCar*

3.6.4 Simulation flowchart

The simulation flowchart is essentially a simple and straightforward. When the simulation code is executed, the user interface will first pop out then the user can defined the simulation scenarios, decide the simulation times and set the simulation parameters. Next, simulation starts when the *btnStart_Click* is selected and proceeds until reaching the preset simulation time. The simulation sequence is shown in Figure 3-12. However, as mentioned, the mechanism of lateral movement varies, depending on the simulated contexts. This will be illustrated in the in following chapters of this thesis.

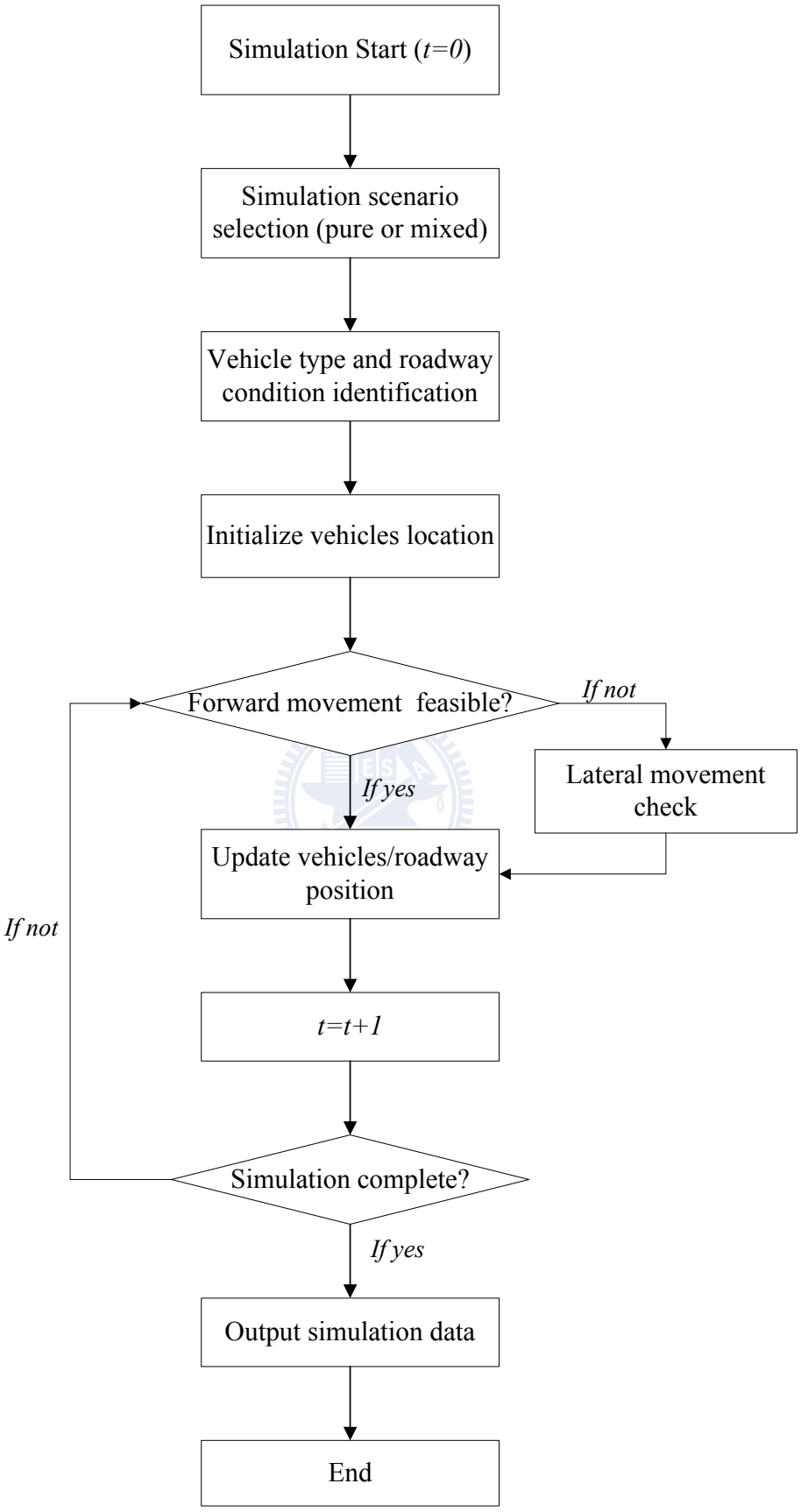

Figure 3-12. Primary hierarchy of simulation program

3.7 Simulation Results and Validation

The validation simulations are performed for pure traffic context (i.e., consider light vehicle only) on a closed track containing *1,800×6* site CUs, which represents a two-lane freeway mainline stretch of width 7.5 meters and length *1,800* meters. Initially, all the vehicles are set equally spaced or line up from end of road section on the circular track, with speed *0* at time-step *0.* We simulate for *600* time-steps. The maximum speeds are defined in accordance with the prevailing speed limits *(110 kph)* on Taiwan's freeways, that is, v_{max}*=31cells/sec (111.6kph)*. Based on field observation, maximum acceleration is set as $a=3m/s^2$ whereas maximum deceleration as $-6m/s^2$. The values of other parameters are set as $p_b=0.94$, $p_o=0.5$, $p_d=0.1$, $t_c=10$ *s*, $h=6$.

Three criteria are selected for validating the revised CA model: (a) According to the field observation, the backward speed of downstream front of traffic jam should be around *15 kph.* (b) The speed drop near upstream front of stationary bottleneck should cope with limited deceleration capability. (c) The transition among global traffic patterns, as shown in distance-time *(x-t)* diagram, should be reasonable.

Figure 3-13 depicts the simulated *x-t* diagrams of scenarios with different preset densities, in which vehicles line up from the end of road section when the simulation initiates. According to the simulations, the backward speed of downstream front of traffic jam is *14.7 kph,* very close to the field observation, *15kph*.

Figure 3-14 displays the zoom-out plot of vehicle trajectories when they approach upstream front of traffic jam. One could easily tell that the revised CA model has successfully fixed the above mentioned unrealistic deceleration behaviors (see Figure 3-7 for reference). Vehicles decelerate in timely manner thus can reflect the genuine driver behaviors in real world.

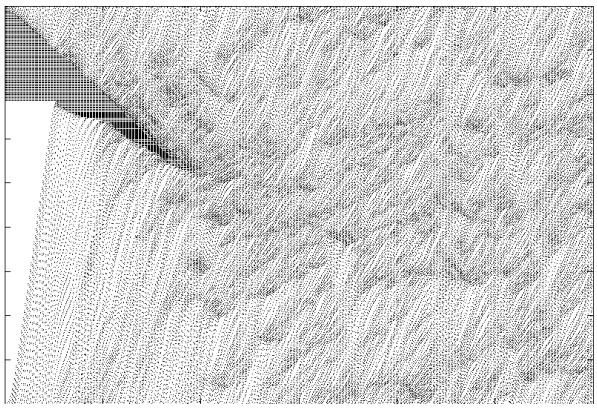

(a) *ρ=40 veh/km/lane*

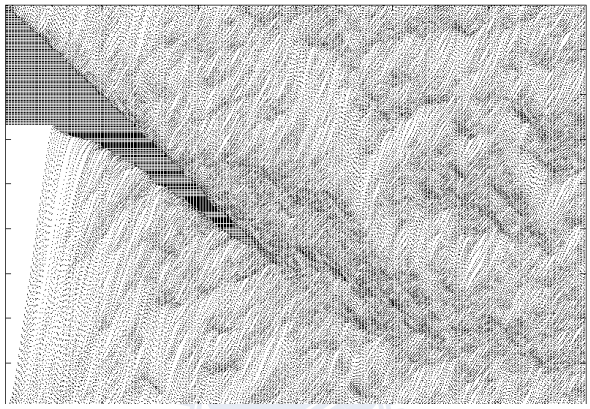

(b) *ρ=50 veh/km/lane*

Figure 3-13. Simulated *x-t* diagram via the revised model, the horizontal axis represents the time (seconds) passed whereas the vertical axis represents the locations of vehicles.

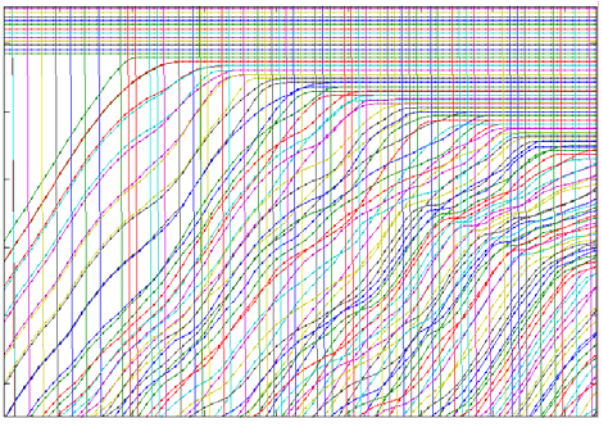

Figure 3-14. Zoom-out vehicular trajectories via the revised model when approaching upstream front of traffic jam.

As the ending of our validation, we check the maximum flow rate available through revised model. We compare the simulated results between the original model and the revised model, as shown in Figure 3-15. Figure 3-15(a) presents the global flow-density relations (fundamental diagrams). For clearer description, the flow rate *q(S)* is converted from cells into number of vehicles and occupancy *ρ(S)* is converted into vehicle per kilometer, as the flow-density relations shown in Figure 3-15(b). It is noticed that due to randomization effect, slight difference always exists but would disperse within a certain area for each separate CA simulation run, even with completely identical parameters settings. Therefore, Figure 3-15 can be deemed as just the typical representative of simulated results.

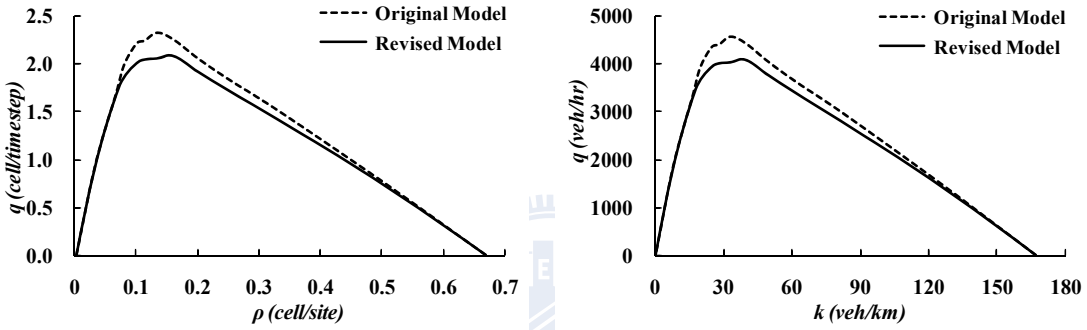

(a) Counted in cells/time-step (b) Counted in vehicles/hour

Figure 3-15. Comparison of simulated global flow fundamental diagrams of original and that of the revised model.

From global point of view, the shapes of simulated flow-density results are principally similar, though the revised model demonstrates lower maximum traffic flow rate-around *2,000 veh/hr/ln*. As mentioned above, due to randomization effect, slight difference always exists for each separate CA simulation. It is interesting, nevertheless, to find that occasionally a higher traffic flow rate can still be sustained at the traffic density around *32 veh/km*. This can be interpreted through the derived *x-t* diagram, as shown in Figure 3-16. Figure 3-16(a) is the ideal, but seldom derived, case in which vehicles move smoothly and basically no complicated interference among them. In this special case, the simulated traffic flow will approach the ideal value—*2,350 veh/hr/ln*. In contrast, Figure 3-16(b) represents the typical, and the frequently derived, case. In this typical case vehicles also move with no fluctuation first but later start to alter speeds in accordance with the preset deceleration rule

when a small perturbation is introduced. This also triggers dramatic traffic pattern change and thus outcomes with less traffic flow rate. This phenomenon is consistent with field observations, for example, those provided by Kerner (2004), as shown in Figure 3-17, that the maximum traffic flow (*2,400 veh/hr/ln*, as proposed by 2000HCM) is rarely found since it is based upon an ideal condition that there are minimum interactions among vehicles. Accordingly, in most cases maximum traffic rates around *2,000~2,200 veh/hr/ln* are usually identified.

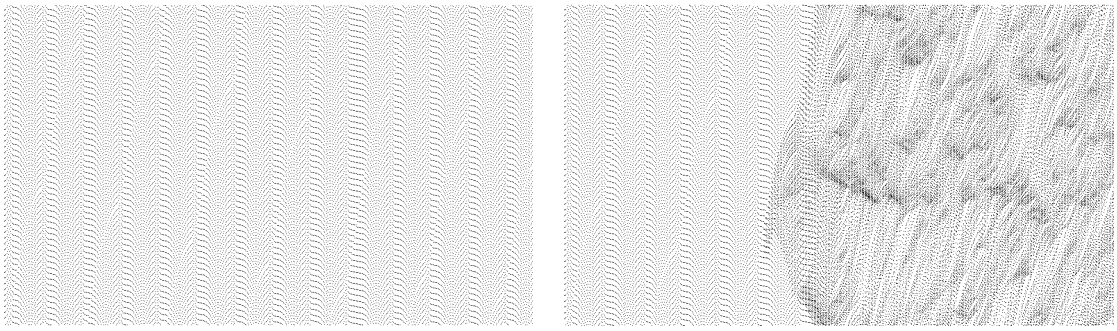

(a) The ideal case (b) The typical case

Figure 3-16. The simulated *x-t* diagrams of same parameters setting (traffic density *32 veh/km/ln*) but with different outcomes. (a) The ideal case, interference among vehicles can hardly be observed. (b) The typical case, a small perturbation incurs dramatic traffic pattern change.

Figure 3-18 further demonstrates the influence of limited deceleration to the *x-t* diagram. In the beginning of each simulation, vehicles are equally spaced in accordance with different preset traffic density values. One may find that, the revised model can precisely reproduce the synchronized flow region, as prevailed in real world. One may also find that, due to the limited deceleration, in the revised model, vehicles operate with moderate speed variation and consequently, some wide-dispersed synchronized flow regions can be identified, which are more in line with the field observation.

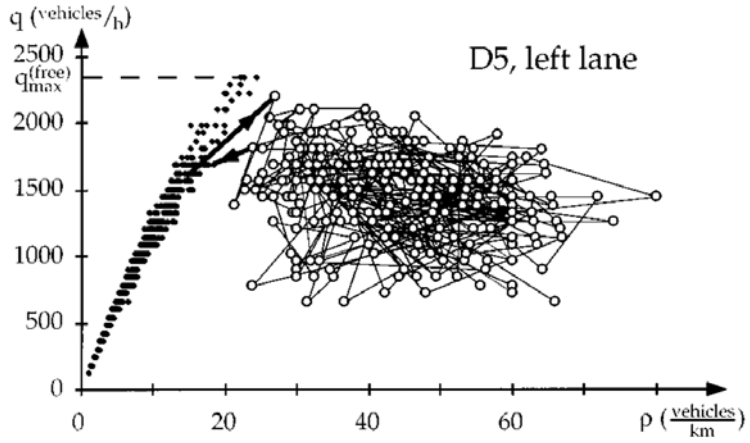

Figure 3-17. Field observed fundamental diagram (Kerner, 2004), German highways A-5, daily data 7:00-22:00). Note that the theoretical optimum traffic flow *2,400 veh/hr/ln* is seldom found. In most occasions, lower traffic flow prevails and disperses within a certain area in the fundamental diagram.

In addition, one surprising bonus of the revised CA model is that, the spontaneously-induced traffic moving jams can be located as the traffic density increases and exceeds *70 veh/km/ln*. It is, however, very difficult to appear such moving jams when implementing original CA model, no matter whatsoever the traffic density is. Besides, the retro-transitions between traffic patterns, even the parallel moving of traffic jams (refer to Figure 2-6 and/or Figure 2-15 for details) can also be effectively simulated through the revised CA model.

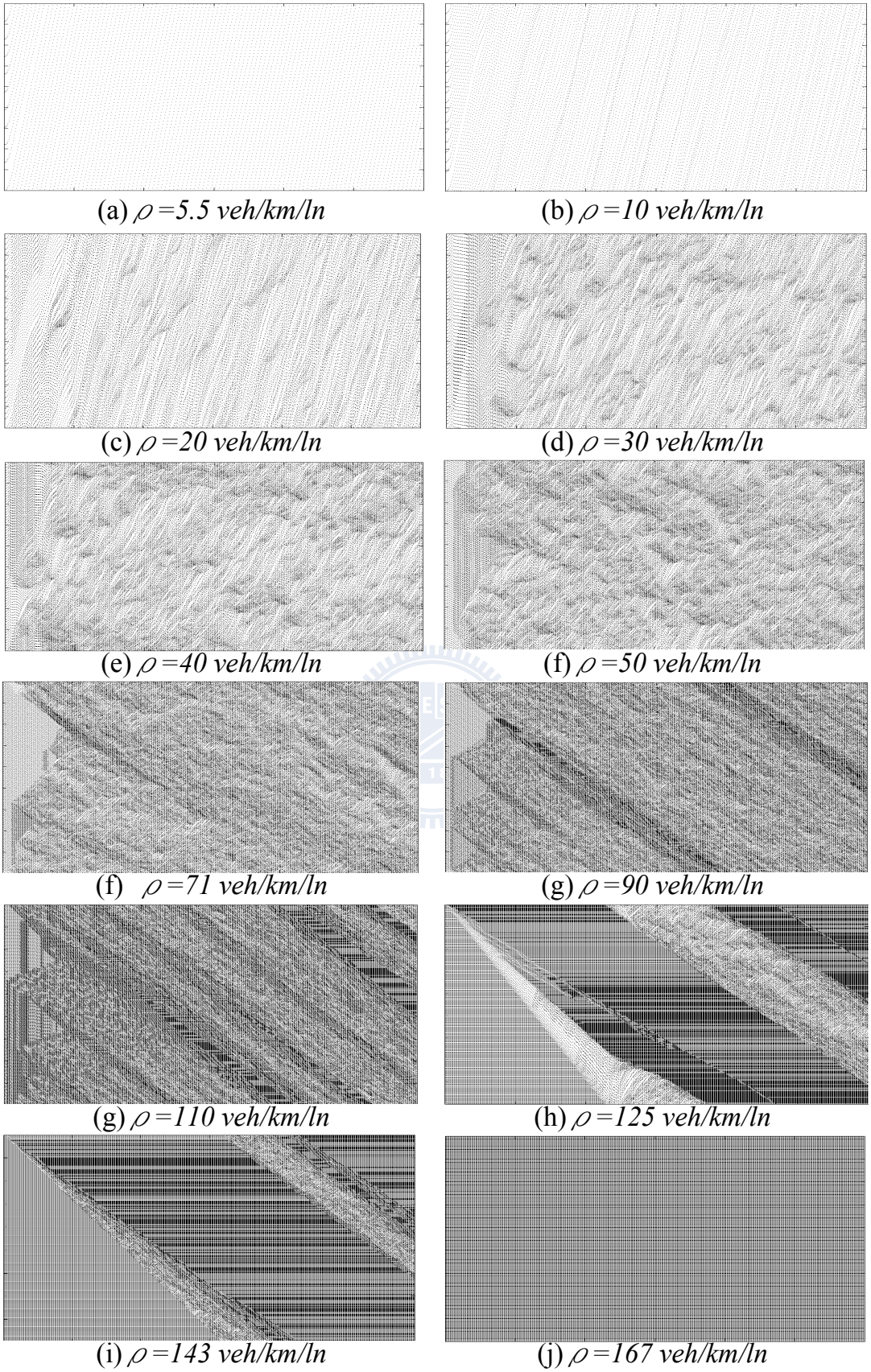

(a) ρ =5.5 veh/km/ln (b) ρ =10 veh/km/ln

(c) ρ =20 veh/km/ln (d) ρ =30 veh/km/ln

(e) ρ =40 veh/km/ln (f) ρ =50 veh/km/ln

(f) ρ =71 veh/km/ln (g) ρ =90 veh/km/ln

(g) ρ =110 veh/km/ln (h) ρ =125 veh/km/ln

(i) ρ =143 veh/km/ln (j) ρ =167 veh/km/ln

Figure 3-18. Simulated traffic patterns and their transitions (*x-t* diagrams) for various traffic densities via the revised CA model.

CHAPTER 4 LOCAL TRAFFIC DETECTION

In real world usually traffic parameters are measured locally via preset detectors rather in a global manner; since measurement for traffic condition covering a long roadway section would be difficult and expensive even it is deemed feasible. Despite this, methodology for deriving the local traffic parameters, especially for the refined grid system, remains seldom addressed until recently (e.g., Mallikarjuna & Ramachandra, 2006, 2008). Besides, some difficulties can even be identified if one intends to adopt the methods suggested in these existing studies into the refined CA model. Therefore in this study we will demonstrate in detail the algorithm utilized in the revised CA model as to capture the local traffic parameters and local traffic patterns.

4.1 Local Traffic Parameters

As mentioned, in conventional traffic flow theory, there are three important traffic parameters—traffic flow rate *(q)*, traffic density *(k)* and vehicle velocity *(v)*. In this chapter we will define the method for deriving local traffic flow and occupancy (a proxy of density) so as to establish the fundamental diagram to illustrate the traffic patterns and the coupled transitions of some complex traffic scenarios.

First, the measurement of local traffic flow rate is conceptually simple and straightforward since; according to its definition (refer to Equation (3-2)), traffic flow rate is collected directly through point measurements, and then takes average over the measured time span. This feature coincides with the nature of local traffic condition—focus on the stationary location only.

In contrast, it would be tricky when one intends to obtain the local density at a fix spot. As mentioned before, density is defined as the number of vehicles occupying a certain length of roadway at a given instant (Equation (3-1)). So basically it is a measure over space. On the other hand, it would not be practical to take constant snapshot of fixed length of road for density measurement. As the natural instead, usually the occupancy is measured. Occupancy is defined as the percent of time a point or short section of roadway

is occupied (May, 1990). It can be measured only over a short section (shorter than the minimum vehicle length) with the preset detectors, and therefore does not applicable if we intend to cover a long section.

One got to agree that the majority opinion at present remains in favor of density, perhaps because the concept of density has been a part of long history of traffic measurement since at least 1930's. But a minority view is that occupancy should begin to enter theoretical work instead of density. There are three principal reasons put forward for adopting occupancy as the surrogate of density for local traffic measurement. The first is that there should be improved consistency between theoretical and practical approach. The second reason is that density, as vehicles per length of road, ignores the effects of vehicle length and traffic composition. Therefore it would be difficult for implementing into mixed traffic analysis. Occupancy, on the other hand, is directly affected by both of these variables and therefore gives a more reliable indicator of the amount of a road being used by vehicles. The last merit and maybe the most important one, is the easiness for occupancy measurement.

Notwithstanding with this, for pure traffic context in case the averaged vehicular length is known, local density can still be estimated from the derived occupancy by the formula:

$$k = \frac{52.8}{l(A) + L_d} O(t) \tag{4-1}$$

where L_d is the detection zone length,

$l(A)$ is the averaged vehicular length

$O(t)$ represents the local occupancy at instant t

Normally occupancy considers single lane only and can vary from 1 percent to 100 percent. However, since our refined CA model is constructed mainly on 2-lane roadway contexts, we will develop the methodology of deriving occupancy and traffic flow rate on 2-lane basis. Compared with the traditional definition of occupancy that only taking vehicular length into consideration, the proposed algorithm will take both the vehicular length and width into consideration yet basically remains the merit of simplicity. The

proposed occupancy *O(t)* and the local traffic flow rate *q(t)* are derived via the virtual detectors arranged into the simulated road section. Both local traffic flow rate and local occupancy are counted by cells. However, they can be transferred into vehicular basis through simple manipulations.

It is worthy noting here that since in our refined CA model one car occupies only two sites laterally, for a two-lane roadway with 6 sites in width, the maximum occupancy available for pure car traffic would be 0.667 only if counted on the cell/site basis. The left 2 sites in lateral direction can be occupied by vehicle of smaller sizes such as motorcycle or bike when simulating the mixed traffic. Only in these cases can the theoretical maximum occupancy (*100* percent) be achieved, which implies that the lateral 6 sites where the detector located are all occupied. The study of mixed traffic via the proposed refined grid system will be presented in Chapter 5.

4.2 Measurement Method

For a local virtual detector with length *1 site* located at position *ms* on the roadway of width *W*, there are four possibilities can be identified for one vehicle with width *VW* and length *VL* to pass through it within each time-step (denoted as time *t* hereinafter). All the possibilities are shown in Figure 4-1. The first possibility is that when at time *t* the vehicle does not arrive the detector yet but pass through it when at time *t+1* (Figure 4-1(a)). The second possibility is that at time *t* the vehicle does not arrive the detector yet, but *"sit"* on the detector at time *t+1* (Figure 4-1(b)). In the third case, the vehicle remains on the detector for both time-steps (Figure 4-1(c)), this usually happens in congested traffic. The final case is that the vehicle reaches the detector at time-step *t* and has left it behind at time *t+1* (Figure 4-1(d)).

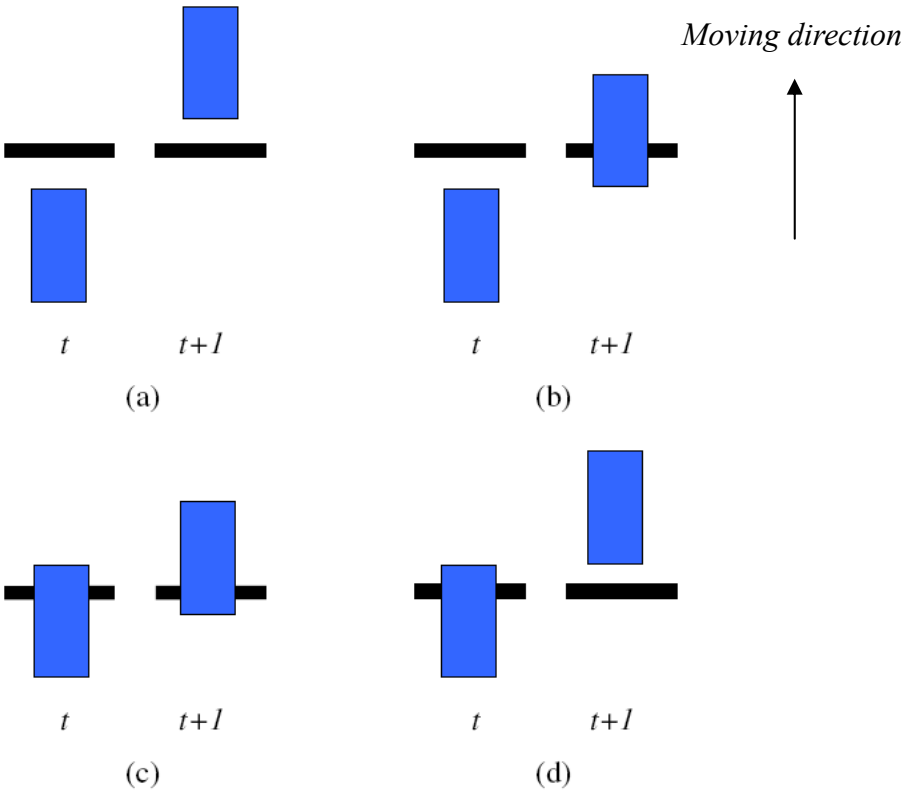

Figure 4-1. Four possibilities for a vehicle passing through one stationary detector for a certain time-step *t*.

Upon above, for a virtual detector arranged at the middle of the simulated road section, the local flow rate and occupancy can therefore be extracted respectively for the 4 above-mentioned possibilities through the following Equation (4-2) and (4-3). Note that both flow rate and occupancy are counted by cells.

$$O(t) = O(t-1) + \begin{cases} \dfrac{VL \times VW}{W \times v_i(t)} & \text{if } T_i(t) > ms \text{ and } H_i(t-1) < ms \\ \dfrac{H_i(t) - ms}{v_i(t)} \times \dfrac{VW}{W} & \text{if } H_i(t) \geq ms \text{ and } T_i(t) \leq ms \\ & \text{and } H_i(t-1) < ms \\ \dfrac{VW}{W} & \text{if } H_i(t) \geq ms \text{ and } \mathrm{T_i}(t) \leq ms \\ & \text{and } H_i(t-1) \geq ms \text{ and } T_i(t-1) \leq ms \\ \dfrac{(ms - T_i(t) + 1)}{v_i(t)} \times \dfrac{VW}{W} & \text{if } (T_i(t) > ms) \\ & \text{and } H_i(t-1) \geq ms \text{ and } T_i(t-1) \leq ms \\ 0 & \text{otherwise} \end{cases} \quad (4\text{-}2)$$

$$q(t) = q(t-1) + \begin{cases} VL \times VW & \text{if } T_i(t) > ms \text{ and } H_i(t-1) < ms \\ (H_i(t) - ms) \times VW & \text{if } H_i(t) \geq ms \text{ and } T_i(t) \leq ms \\ & \text{and } H_i(t-1) < ms \\ v_i(t) \times VW & \text{if } H_i(t) \geq ms \text{ and } \mathrm{T_i}(t) \leq ms \\ & \text{and } H_i(t-1) \geq ms \text{ and } T_i(t-1) \leq ms \\ (ms - T_i(t) + 1) \times VW & \text{if } (T_i(t) > ms) \\ & \text{and } H_i(t-1) \geq ms \text{ and } T_i(t-1) \leq ms \\ 0 & \text{otherwise} \end{cases} \quad (4\text{-}3)$$

where

O(t): the cumulate occupancy at time-step *t*

q(t): the cumulate flow (cells) at time-step *t*

ms: location of virtual detector

VL: vehicle length, counted in cells

VW: vehicle width, counted in cells

$H_i(t)$: head location of vehicle *i* at time-step *t*

$T_i(t)$: tail location of vehicle *i* at time-step *t*

W: road width, counted in sites

4.3 Arithmetic Averaged versus Un-weighted Moving Averaged Traffic Parameters

Traditionally the derived traffic parameters are averaged over a fixed time interval to alleviate the oscillation raised by local noise. It is the arithmetic-averaged (short for AA hereinafter) traffic data. For further illustration, we also introduce the un-weighted moving average (short for UMA hereinafter) for analyzing the local traffic parameters.

The moving average technique is commonly used with time series data to smooth out short-term fluctuations and highlight longer-term trends or cycles. For example, given a series of traffic data and a fixed time interval (for example, *30s*), the moving average data can be obtained. As the start, the average of the first time interval is calculated. Then the fixed time interval is moved forward to form a new time interval but with same duration, and the second average is also calculated. The process is repeated over the entire traffic data. Thus, a moving average traffic data is not a single value but a group of numbers, each of which is the average of the corresponding time interval of a larger set of traffic data points.

The simplest moving average may be the UMA which is simply the mean of the previous n data points, which can be calculated via the following formula:

$$V_{ma}(t) = \frac{1}{n}\sum_{i=1}^{n} V_{t-i+1} \tag{4-4}$$

$$V_{ma}(t+1) = V_{ma}(t) - \frac{V_{t-n+1}}{n} + \frac{V_{t+1}}{n} \tag{4-5}$$

where V_t is the local parameters ($O(t)$ and $q(t)$) detected by Equations (4-4) and (4-5) at time-step t, whereas $V_{ma}(t)$ is their UMA values.

4.4 Simulation Scenarios

The scenarios simulated are identical to that for validating the refined CA model (refer to Section 3.7 for details) i.e., pure traffic context that considering passenger car only on a closed track containing *1,800×6* site CUs, which

represents a two-lane freeway mainline stretch of width 7.5 meters and length *1,800* meters. Initially, all the vehicles line up from end of road section on the circular track. Maximum speeds are set as v_{max}*=31cells/sec (111.6kph)*. Maximum acceleration is set as $a=3m/s^2$ whereas maximum deceleration as $-6m/s^2$. All the other parameters remain unchanged.

4.5 Local Traffic Features

The local traffic flow and occupancy derived from the CA simulations are analyzed as below. Here we simulate pure car traffic with three different generalized densities (*ρ(S)=0.05, 0.11* and *0.28*) that reflect the traffic phenomena of free flow, synchronized flow and jam traffic (i.e., *12.5, 27.5* and *70 veh/km/ln*) rspectively. When simulations initiate, all the vehicles line up by end of roadway. For description, we first express our results as distance-time *(x-t)* relationship in Figures 4-2(a) to 2(c). Following that, the local fundamental diagram is shown in Figure 4-2(d) in order to compare with the global fundamental diagram.

(a) *ρ(S)=0.05* (b) *ρ(S)=0.11* (c) *ρ(S)=0.28*

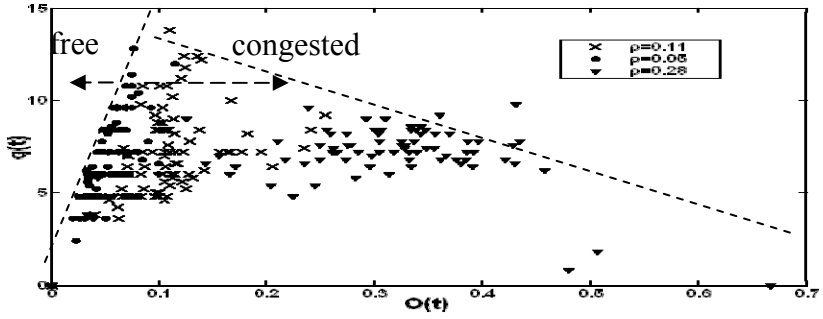

(d) The derived fundamental diagram

Figure 4-2. The traffic patterns and flow rate-occupancy relationship. *(30s* AA data)

We notice that traffic pattern in Figure 4-2(a), *ρ(S)=0.05*, represents the free flow traffic since few interactions occurred among vehicles and most vehicles operate with maximum speed. As density increases (*ρ(S)=0.11*), both

free flow and synchronized patterns can be identified. Finally, when density increases further ($\rho(S)=0.28$), all possible traffic phases (free, synchronized flow and moving jam) can be clearly observed (Figure 4-2(c)).

The thirty-second AA local flow rate and occupancy of above-mentioned three simulations, as derived through Equations (4-2) and (4-3), are gathered and shown in Figure 4-2(d). It is interesting to find that the derived data spreads in the pattern reflects the fundamental diagram profile recommended by Kerner (2004). An inverse-λ profile appears, in which free flow data mainly locates near the left boundary which represents the free flow phase. In contrast, data for congested flow (including synchronized flow and moving jam) sparely locates but most of them below the upper envelope. This validates our methodology for local traffic parameter detection.

4.6 Traffic Patterns

4.6.1 AA traffic data

To further explore diversified traffic patterns, we simulate a more complicated scenario—congested flow with high density ($\rho(S)=0.28$) and arrange a bottleneck in the middle of the right lane. Two local virtual detectors are introduced—one upstream and one downstream of this bottleneck as shown in Figure 4-3. According to the simulated *x-t* diagram, there are sequential traffic patterns transiting around the downstream virtual detector, i.e., F, F→J, J→S, S→F (denoted by Ⅰ through Ⅳ respectively); while in the upstream, traffic patterns around the detector transits from *F,* F→S, S→J, J→S (denoted by Ⅴ through Ⅷ respectively). For description, one should be aware that here the free flow phase is denoted as F phase, synchronized flow phase as S phase and traffic jam as J phase respectively.

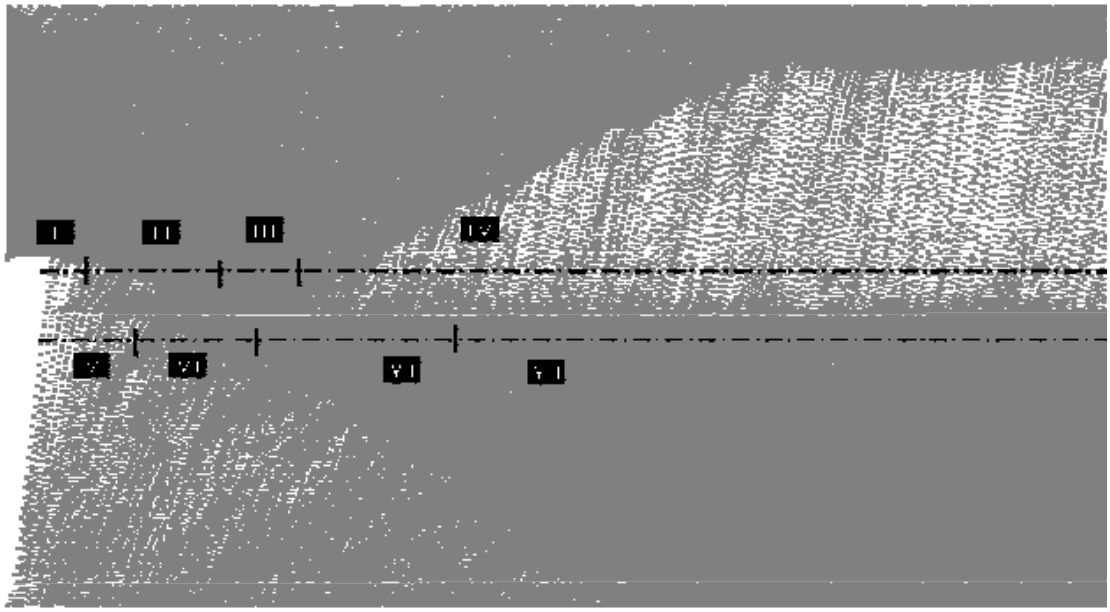

Figure 4-3. The *x-t* diagram of traffic flow with one bottleneck introduced in mid-roadway.

These complex traffic pattern transitions can be elucidated in more detail when introducing a *30s* AA *q-O* diagram. It can be found from Figure 4-3 that due to the reduced capacity at the bottleneck and thus the reduced flow rate, vehicles that pass the virtual detector downstream of bottleneck have enjoyed the long headways, except for the first *200* seconds. Therefore in the fundamental diagram (Figure 4-4(a)), the *q-O* pairs mainly spread in the free flow region. On the other hand, Figure 4-4(b) provides the *q-O* information around the upstream detector. Owing to the impact of bottleneck to the upstream, complicated traffic patterns and transitions can be observed (F, F→S, S→J, J→S.) As the consequence, *q-O* pairs sparely spread in the congested area (Figure 4-4(b)). It is worthy mentioned that for the last *300s*, synchronized flow prevails, so the *q-O* pairs reflect this phenomenon in a consistent manner, i.e., they randomly spread in the congested region. Furthermore, once combining the upstream and downstream data together, the aggregated *q-O* profile (Figure 4-4(c)) that agrees with three-phase traffic theory proposed by Kerner (2004) can be clearly identified.

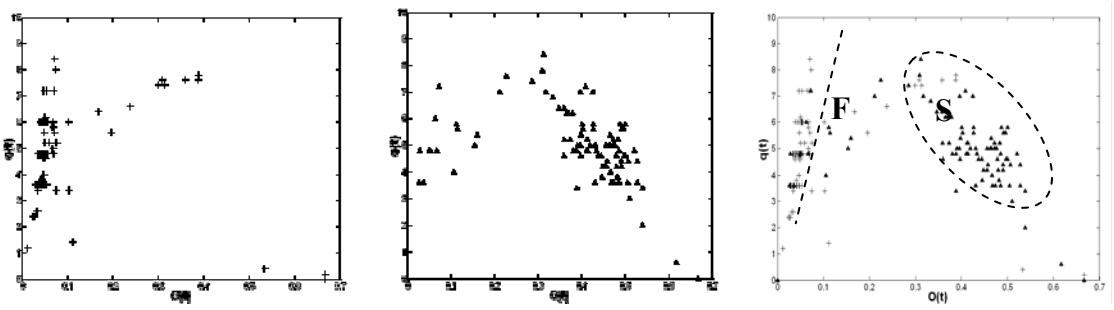

(a) downstream (b) upstream (c) combination

Figure 4-4. Simulation results for light vehicles with bottleneck. (*30s* AA data)

4.6.2 UMA traffic data

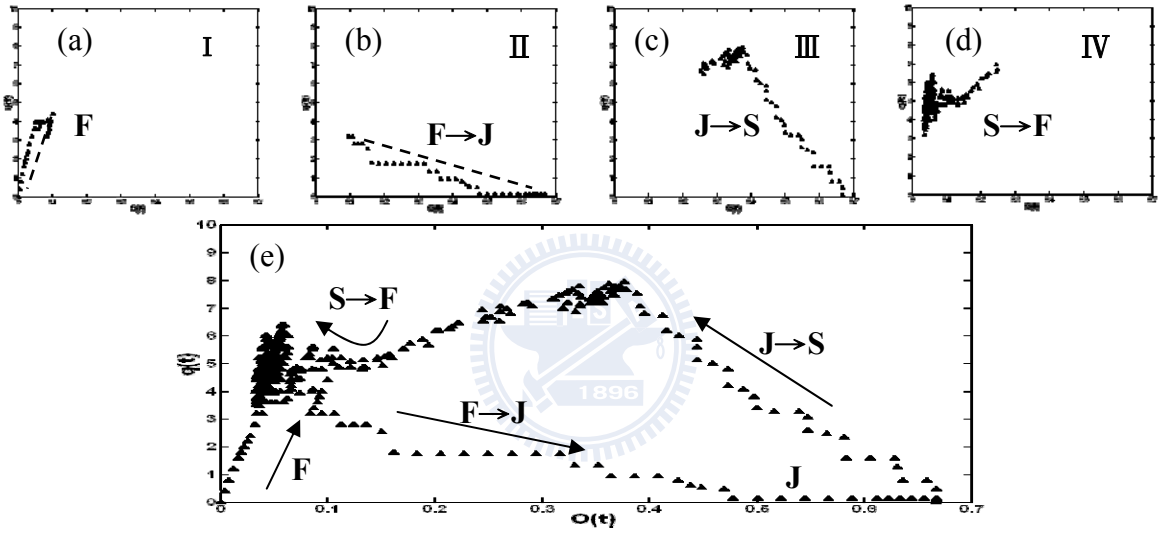

Figure 4-5. Traffic patterns and transitions in the downstream of bottleneck. (*30s* UMA data)

In this sub-section we utilize the un-weighted moving-averaged (UMA) traffic data, as derived by Equation (4-4) and (4-5), to elucidate the same scenario. First, we focus on the downstream of bottleneck. Again per *x-t* diagram (Figure 4-3), traffic pattern around downstream detector will be free flow in the beginning (region I, F phase, also refer to Figure 4-5(a)) and then pass through the bottleneck to reach upstream of jam. Vehicles joining the jam will keep stationary (region II, J phase, also refer to Figure 4-5(b)) till all the vehicles in front have left and then start to move (region III, J→S phase transition, also refer to Figure 4-5(c)). Later on as the flow rate reduces due to the impact of bottleneck, the traffic transits into free flow (region IV, S→F phase transition, also refer to Figure 4-5(d)). A clearer picture of these flow

patterns and the relative transitions can be obtained by aggregating all data into one plot, shown in Figure 4-5(e).

Similarly, we can describe the upstream flow patterns of bottleneck through the same algorithm, as shown in Figure 4-6. Also per *x-t* diagram (Figure 4-3), traffic patterns around upstream detector will be free flow in the beginning (region V, F phase). Owing to the effect of downstream bottleneck, when approaching the bottleneck the flow patterns will transfer to synchronized flow (region VI, F→S phase, also refer to Figure 4-6(a)) till reaching the upstream front of jam (region VII, S→J phase, also refer to Figure 4-6(b)). Vehicles stay still and wait for the front condition for movement (region VIII, J→S phase transition, also refer to Figure 4-6(c)). For the rest of time, because the bottleneck shrinks the road capacity and thus influences the upstream traffic significantly, the flow patterns will keep as synchronized flow (region VIII, S phase, also refer to Figure 4-6(d)). When aggregating all data into one plot, as shown in Figure 4-6(e), the flow patterns and the phase transitions can be seized exactly.

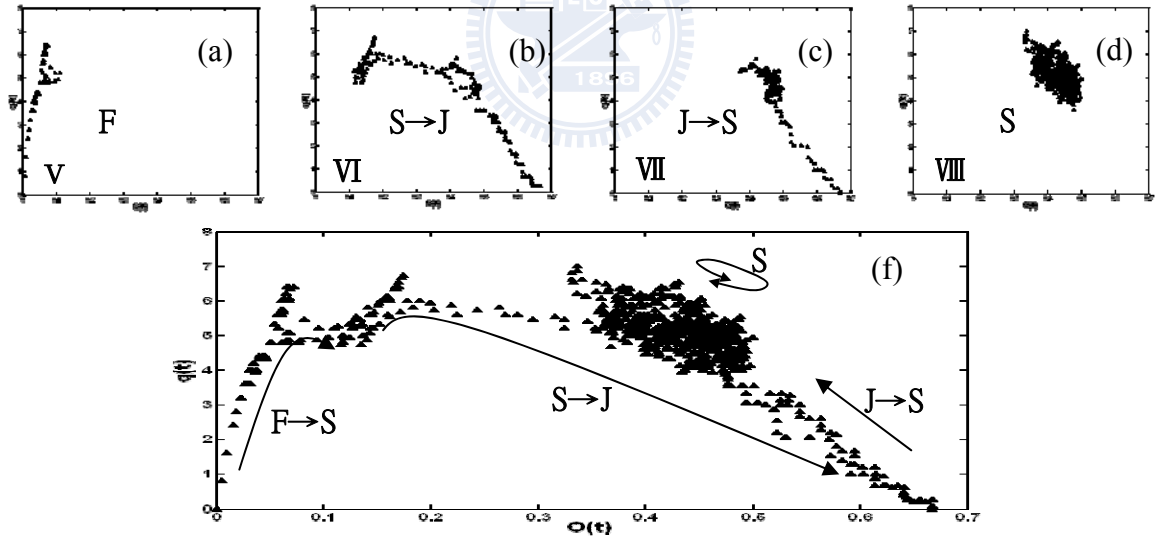

Figure 4-6. Traffic patterns and transitions in the upstream of bottleneck. (*30s* UMA data)

4.7 Comparison

As mentioned, conventionally traffic flow are derived via the accumulated data that derived by local detectors for a preset finite interval and

then take the arithmetic averaged (AA) values as final outcome; since it is very difficult to make long-term spatiotemporal measurement over a broad distance. One criticism arisen since is that whether the local traffic data (*O(t)* and *q(t)*) could serve as the appropriate proxies for their global counterparts (*ρ(S)* and *q(S))*? On the other hand, one important merit of numerical simulation is the excellent capability for monitoring vehicles' behaviors throughout the whole simulated domain, both in space and time frame. Therefore, trajectories of all vehicles during the simulated period can be précised gauged. In other words, the simulated global traffic flow is in essence an aggregation of all local, even the tiny ones, traffic fluctuations and hence can be deemed as a paradigm for evaluating the effectiveness of locally derived traffic information. As such, it is our recommendation that the *q(S)* rather *q(t)* be selected as the reference index for evaluating traffic performance. Upon this, we are interested in uncovering the relationships or linkage between global and local traffic parameters, including the following:

A. Whether locally derived traffic data can reflect the trends shown in global perspective? If yes, what is the precision might achieve?

B. What is the difference between the outcome of AA and UMA local data? Which would be better proxy for global data?

C. What is the proper time interval selected for taking AA or UMA on the local traffic data?

To answer these questions, we simulate pure car traffic again with four different generalized densities (*ρ(S)=0.06, 0.12, 0.25* and *0.5*) that reflect the traffic phenomena of free flow, synchronized flow and jam traffic (i.e., *15, 30, 62.5 and 125 veh/km/ln*) respectively. When simulations initiate, all the vehicles are equally spaced on the circular track of *1,800* meters in length. A detector is settled in the middle of roadway and the derived local traffic data (*O(t)* and *q(t)*) are taking AA and UMA average for different time intervals*(1s, 30s* and *60s*). Finally, outcome of four simulations is collected and compared with their global counterparts (*ρ(S)* and *q(S)*) in the fundamental diagram shown in Figure 4-7 to 4-9.

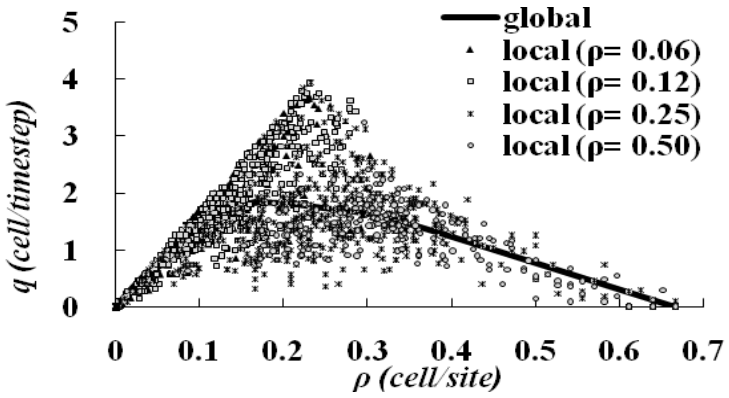

Figure 4-7. Comparison of global fundamental diagram with local *1s* data for four different scenarios. (*ρ(S)*= 0.16, 012, 0.25, 0.50)

As shown in Figure 4-7, as expected, the *1s* local flow rate *q(t)* significantly deviates from its global counterpart *q(S),* especially around the region *ρ(S)=0.1~0.4.* The maximum flow rate is also overestimated. This is deemed reasonable since that the *1s* data aims only at the local traffic information for one certain instant; thus the effect of some extreme situations occurred locally will be exaggeratedly amplified. Therefore, although in the fundamental diagram the aggregated local data transforms into some traffic patterns that perfectly match the three-phase traffic theory, it is concluded that the *1s* local data is not sufficient to reflect the traffic conditions in global perspective.

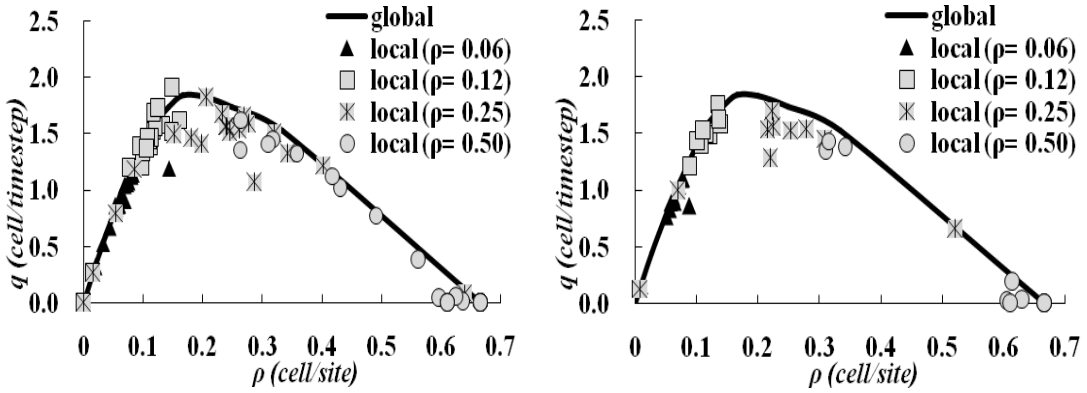

(a) *30s* AA (b) *60s* AA

Figure 4-8. Comparison of global fundamental diagram with local AA data for four different scenarios. (*ρ(S)*= 0.16, 012, 0.25, 0.5)

Figure 4-8 provides the comparison of *30s* and *60s* AA local data with the global data. One may find that there is no considerable difference can be identified between them. Basically both data groups spread in the neighborhood of global *ρ(S)-q(S)* curve though most of times the local traffic flow rate is lower. However, one may find that the *60s* AA data presents better ability for gauging the global situation since that in general the *60s* data scatters within a comparatively smaller region beside the global *ρ(S)-q(S)* curve.

Figure 4-9 provides the comparison of *30s* and *60s* UMA averaged local data with the global curve. Our first finding is that the *60s* UMA data also presents better performance for reflecting the global situation because the *60s* data group tends to approach closer to the global *ρ(S)-q(S)* curve. However, when compared with the outcome of the AA data that provided in Figure 4-8, we can find that UMA data provides comparatively poorer simulation quality, no matter when *30s* or *60s* average is chosen. The cause for this defect is that a local fluctuation (noise) in traffic flow will influence multiple data points when taking UMA average, but usually affect one traffic data only when taking the AA average. In other words, the AA average local traffic data is excellent in smoothing out the local oscillations and henceforth can cope better with the global traffic data, as revealed in Figure 4-8.

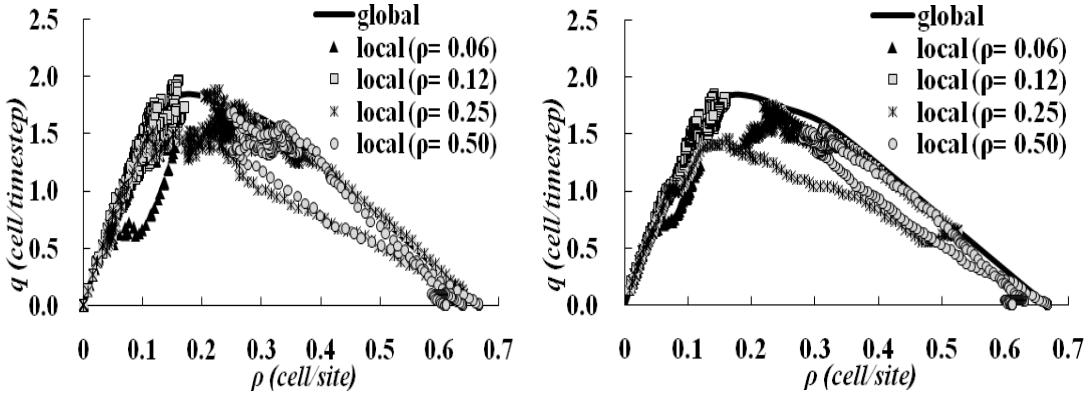

(c) *30s* UMA (d) *60s* UMA

Figure 4-9. Comparison of global fundamental diagram with local UMA data for four different scenarios. (*ρ(S)*= 0.16, 012, 0.25, 0.50)

However, one must agree that, as discussed in Section 4-7, the UMA traffic parameters are efficient in reflecting the complicated traffic phase transitions. Besides, for each individual simulation, implementation of the

UMA average provides notably more precious data points than that via AA averaged technique.

4.8 Summary

The proposed methodology for extracting local traffic flow rate and occupancy from the refined grid system has been successfully validated through the simulations performed for several complex scenarios in this chapter, Besides, the results also show that the UMA traffic parameters are efficient in reflecting the complicated traffic phase transitions whereas the AA traffic data is consistent with the three-phase traffic theory. In addition, the AA traffic data is more excellent to reflect the global traffic features. This evidences the speculation that three-phase flow theory is developed in accordance with the AA field data. Finally it is recommended that the time interval selected for taking average, either AA or UMA values, would be *30s* at least.

It is concluded that the UMA traffic data grasps more precisely the traffic characteristics than the AA traffic data, though only local rather global information is gathered. As a consequence, the UMA traffic parameters are recommended for further research from microscopic viewpoint. The AA traffic data, on the other hand, reveals the potential for evaluating global traffic features based upon the local measured traffic data.

CHAPTER 5 DEVELOPMENT OF SOPHISTICATED CA MODELS

Based on the refined CA models proposed, in this chapter we further develop one sophisticated CA model to elucidate the mixed traffic comprising cars and motorcycles. This is a challenging task since that, as mentioned in Section 3.1 (also refer to Figure 3-1), motorcycles oftentimes move concurrently with the cars by sharing the *"same lane"*. In addition, some erratic motorcyclists do not even follow the lane disciplines at all. They may make lateral drifts breaking into two moving cars. Once blocked by the front vehicles, they even make wide transverse crossings through the gap between two stationary cars in the same lane, in order to keep moving forward. In this circumstance, obviously, conventional coarse cell system is deficient to describe various vehicle sizes with their coupled interactions. Consequently, there is few CA effort can be located to date that dedicate to simulation of mixed traffic comprised by cars and motorcycles, for example that by Meng *et al* (2007). Notwithstanding with this, even in this pioneer work only single lane is considered. The main improvement thereof is to divide the lane under analysis into three sub-lanes thus allowed the motorcycles to be introduced into simulation. However, even in this primitive work it is assumed the motorcycles' behaviors are analogous to that of cars and neither motorcycles' lateral shift nor transverse crossing was ever considered.

Taking the advantages of enhanced resolution of the refined grid system, more realistic traffic speeds prevailing in urban streets with various vehicular sizes (both in width and length) can be simulated. Therefore, for sake of more precise reflecting motorcycles' behaviors, in this chapter we propose one delicate CA model which is essentially developed upon the refined CA model illustrated in Chapter 3. In this novel CA model, in addition to the conventional moving forward and lane-change rules, also the lateral drift behaviors for cars moving in the same lane, the lateral drift behaviors for motorcycles breaking into two moving cars, and the transverse crossing behaviors for motorcycles through the gap between two stationary cars in the same lane will be explicated. The simulations on such mixed traffic are thoroughly examined under various scenarios.

The rest of this chapter is organized as follows. The proposed sophisticated CA rules are narrated first, wherein lateral drift update rules for cars and motorcycles, the transverse drift update rules for motorcycles will be carefully elucidated. Next, simulations for mixed traffic contexts are reported and compared with existing effort. The relationship between global and local derived traffic parameters in mixed traffic are also compared. Finally, a preliminary simulation on two signalized intersections is also presented.

5.1 Sophisticated CA Rules

5.1.1 Forward rules for cars and motorcycles

All the update rules, both for forward movement of the refined CA model, remain effective for both cars and motorcycles in the mixed traffic, including the amendments considering limited deceleration and piecewise-linear movement. Accordingly, Equation (3-9)-(3-15) applies except that the deceleration update step Equation (3-11) and the position update step Equation (3-15) are superseded by Equation (3-24) and Equation (3-25) respectively.

5.1.2 Lateral movement rules for cars

According to Nagel *et al* (1998), despite the difference among different lane-change rules, basically all generated similar and realistic results. This conclusion may be valid only for pure traffic scenarios wherein all vehicles have identical size. In mixed traffic comprising cars and motorcycles, the lane-change behaviors will be notably different due to the complex interaction triggered by various maximum vehicular speeds as well as by different vehicular sizes.

Based upon the proposed refined grid system, this study tries to divide the lateral movements for cars into two types: lane-change and lateral drift. The former refers to as a car (with 2CUs in width) changing from one lane (with 3 CUs in width) to the neighbor lane (also with 3 CUs in width), for instance, from position 2 to 3 or from position 3 to 5 (see Figure 5-1); whereas the later refers to as a car moving forward in the same lane but drifting from rightmost two sub-lanes to leftmost two sub-lanes (e.g., 4→6 or 5→7 in Figure 5-1) or from leftmost two sub-lanes to rightmost two sub-lanes (e.g., 1→ 2 or 3→4 in

Figure 5-1). Both lane-change and lateral drift rules for cars are explained as follows.

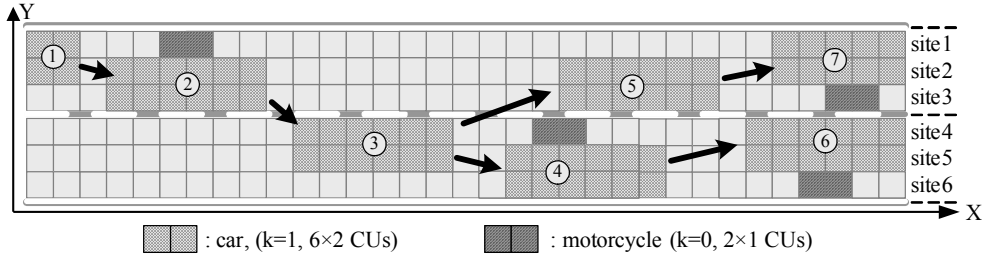

Figure 5-1. Lateral movements for cars in mixed traffic: lane-change and lateral drift.

The lane change update rules defined in Chapter 3 will be applied to cars only since basically motorcycles move on non-lane basis. Furthermore, it is assumed that lane-change is only allowed when cars locate along the lane markings, such as positions 2, 3, 5, and 6 in Figure 5-1. For cars located away from the lane markings, such as positions 1, 4, and 7 therein, it would take a little longer time to complete a lane-change.

According to the proposed fine cell system shown in Figure 5-1, a car (2 CUs in width) can locate either on the leftmost or rightmost 2 CUs (sub-lanes) within the lane (3CUs in width) before making a lane-change. For example, cars locating on the leftmost side of the left lane (e.g., position 1) would take slightly longer time to make a lane-change than those on the rightmost side of the same lane (e.g., position 2). A car may require even longer time to make a lane-change provided that the adjacent sites are occupied by motorcycles (e.g., position 4). There are two possibilities for a car to make a lane-change: the movements of 2→3 and 3→5 therein. After the lane-change, it is assumed that in next time-step the car will remain aligned with, but on the opposite side to, the lane markings. In a two-lane roadway, for example, if a car on the left lane wishes to change to the right lane, provided that no vehicles locate aside on the right lane, the lane-change CA rule is defined as Equation (3-16), i.e.,

$$\begin{aligned} &LC^{l\to r}: \text{If} \quad v_{l,n}(t) > v_{l,n}(t) \quad \text{and} \quad v_n(t) > v_{l,n}(t) \\ &\text{and} \quad g^r_{l,n}(t) > \min(d^{eff}_n, v_n(t+1)) \\ &\text{and} \quad g^r_{b,n}(t) > \min(d^{eff}_{b,n}, v^r_{b,n}(t+1)) \end{aligned} \tag{3-16}$$

In addition to the above lane-change behavior, this study introduces another lateral movement *"lateral drift"* to further replicate the movement behavior for cars in a fine cell system. The lateral drift behavior happens when a car locating away from the lane markings intends to make a lane-change (e.g., 1→2→ 3 in Figure 5-1) or when the car remains moving in the same lane but trying to overtake a slower motorcycle in front (e.g., 3→4→6). In this study, when lateral drifts take place, cars remain within the same lane in next time-step, as the movements of 1→2, 3→4, 4→6 and 5→7 in Figure 5-1.

Upon above, we define the cars' lateral movements (lane-change or lateral drift) update rules as follows:

Step 1: *Incentive criteria.* When cars move with positive speed and enjoy sizeable time headway to the front vehicle (say, 10 seconds), they will move forward with no lateral drift, since there is no incentive to do so. However, if there are vehicle(s) in near front, then different lateral movements may be triggered, depending on the sites they situate at present time. It is explained in Step 2.

Step 2: *Safety criteria.* Check if situations around allow for lateral movements. Likely options for cars' lateral movements will depend on the original position.

Step2A: When cars move aside the lane markings (e.g., the car marked in black in Figure 5-2), both lane-change and lateral drift are likely to take place depending on the traffic situation around. The following sub-steps for lateral movements are applied (see Fig. 5-2):

Step 2A-1: Check the gaps backward on both sides (d^{lb1}, d^{lb2} and d^{rb}) to determine if a lateral movement is allowed. The rationale for considering both $d^{lb1}$and d^{lb2} is that in mixed traffic context the next two sites behind (for instance, site 2 and site 3 in Figure 5-2) in the target lane may be occupied by different vehicles with different speeds. Hence, both sites

must be evaluated to find out the exact backward gap.

Step 2A-2: When with allowable gaps backward, check the front gaps if a lane-change or a lateral drift is taken so as not to be hindered by a slow vehicle in front. For example, for the designated car in Figure 5-2, five gaps (d^{lf1}, d^{lf2}, d^{rf1}, d^{rf2} and d^{f}) must be evaluated to determine the best option to be taken. In case that both options are allowed, the one with longer gap, i.e., more advantageous, will be selected. Also aware that the front gaps are the effective gaps in next time-step, as defined by Knospe (2002) to catch more precisely the real traffic condition.

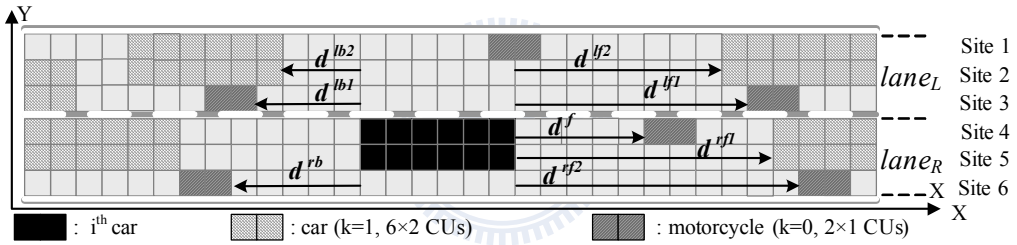

Figure 5-2. Gaps evaluated by a car to perform either lane-change or lateral drift.

Step 2B: When cars move along the side lane away from the lane markings (e.g., the car marked in black in Figure 5-3), only the lateral drift is considered because lane-change could be taken only after the car drifting to the right side of the lane it locates. Consequently, the following sub-steps apply for a car's lateral drift (see Figure 5-3):

Step 2B-1: Check the space backward on the inner side (d^{rb}) to determine if a car lateral drift is allowed.

Step 2B-2: When with allowable gap backward, check the minimum front gap if a lateral drift is to be taken for not being hindered by a slow motorcycle in

front. For example, d^{lf1}, d^{lf2} and d^{lf} require being evaluated.

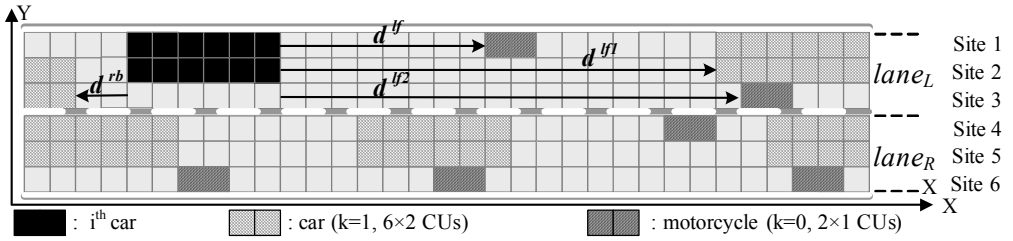

Figure 5-3. Gaps evaluated by a car to perform lateral drift.

5.1.3 Lateral drift rules for motorcycles

Unlike most cars which will move within the lane, motorcycles in practice do not follow the lane disciplines. From the field observation one can easily find that motorcycles in effect move in a rather erratic manner without obeying the lane disciplines. Sometimes the motorcycles follow the lead vehicles; but more than often, they share the "*same lane*" with the moving cars or break into two moving cars in the same lane. During traffic jams, some motorcycles, once blocked ahead, even cross the gap between two queued cars with a wide transverse displacement to keep moving (see Figure 3-1). This evidence justifies the non-lane based movements for motorcycles. Based upon field observation by Lan and Chang (2005), possible motorcycle movements can be categorized into 5 classes, as shown in Figure 5-4.

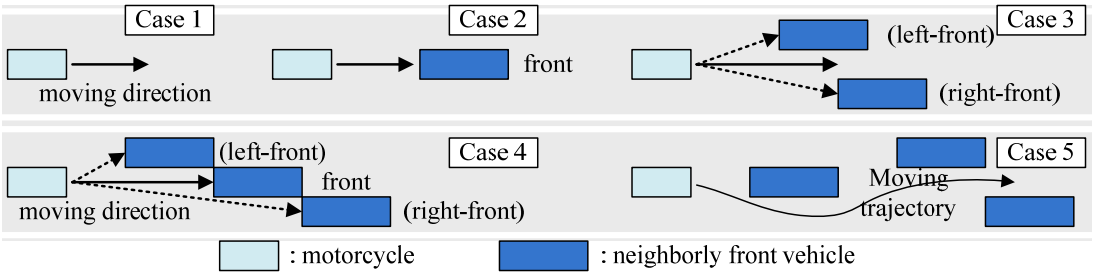

Figure 5-4. Field observed motorcycles' possible movements (Lan and Chang, 2005).

In a moving traffic condition, although different movements of motorcycles can be identified, basically the lateral displacement can be characterized as a motorcycle's lateral drift—displace one site laterally in next time-step. In this case, the lateral movement update rule for motorcycles is a

simplified version of the counterpart for cars, which can be described as follows:

Step 1: *Incentive criterion*. It is identical to that for cars. When a motorcycle enjoys sizeable time headway to the front vehicle, no lateral displacement will be activated. Next, if there is a vehicle in near front on the same sub-lane, either drifting to the left sub-lane or the right sub-lane could be chosen, depending on the position it situates at present time. It is explained in Step 2.

Step 2: *Safety criterion*. Check if situation around allows a lateral drift. However, available options for a motorcycle's lateral drift will depend on the original position.

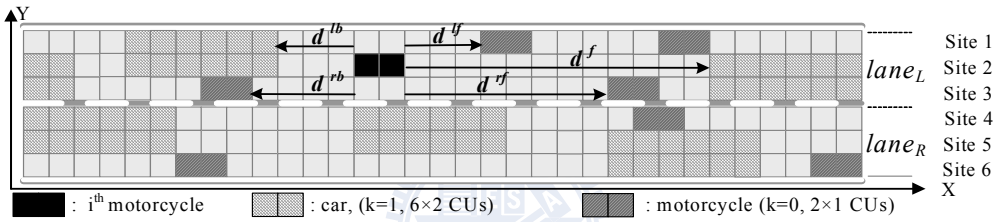

Figure 5-5. Gaps evaluated by a motorcycle to perform lateral drift from the middle site.

Step2A: When a motorcycle locates in the middle sub-lane (e.g., site 2, 3, 4, or 5 in Figure 5-5), lateral drifts to both outer and inner sites are feasible. Therefore, the following sub-steps require further examination.

Step 2A-1: Check the gaps backward on both sides. For instance, for the designated motorcycle marked in black in Figure 5-5, backward gaps d^{lb} and d^{rb} require being evaluated to determine if a lateral drift is allowed.

Step 2A-2: When with allowable gaps in the back, check the front gaps if a motorcycle's lateral drift is to be taken. For example, for the designated motorcycle in Figure 5-5, three gaps (d^{lf}, d^{rf} and d^{f}) are evaluated to determine the best drift option. Similar

to cars, in case that both options are allowed, the lateral drift option with larger gap is chosen.

Step 2B: When a motorcycle locates on the innermost or outermost sub-lane (i.e., site 1 or 6 in Figure 5-6), only drifting inboard is available. Taking the motorcycle marked in black in Figure 5-6 as an example, the only lateral drift option is from site 1 to site 2. The following two sub-steps apply:

Step 2B-1: Check the gaps backward on inner side (d^{rb}) to determine if a motorcycle's lateral drift is allowed.

Step 2B-2: When with an allowable gap in back, check the minimum front gap should a motorcycle's lateral drift be taken. d^{lf}, and d^{f} must be evaluated.

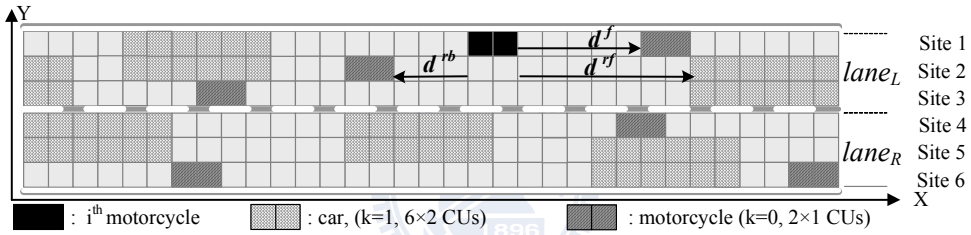

Figure 5-6. Gaps evaluated by a motorcycle to perform lateral drift from the outermost site.

5.1.4 Transverse crossing rules for motorcycles

Another unique feature for motorcycles is the *"transverse crossing"* which is frequently observed when motorcycles are stuck in traffic or forced to halt in front of signalized intersections. The transverse crossing is defined as motorcycles' lateral movement of one or two sites, as long as situation allowed, e.g., between two still-standing vehicles; even with slight or no forward displacement at all. The possible options for transverse crossing behavior are demonstrated in Figure 5-7 with update CA rules described as follows:

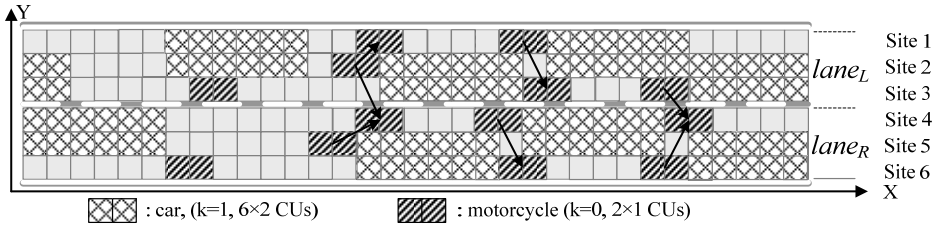

Figure 5-7. Transverse crossing behavior for motorcycles when stuck in traffic.

Step 1: *Incentive criterion.* When a motorcycle is stuck in traffic jam and remains stationary for a certain period (say, *3s*), there is an incentive for the motorcycle to take a transverse crossing through the gap between two queued vehicles, either to the left or to the right sub-lane, in order to keep moving as forward as possible.

Step 2: *Safety criterion.* Check if situations around allow for a transverse crossing. First, check if the next left or right sub-lane in front is occupied. If no, then evaluate the forward and backward condition on the target sub-lane whether a transverse crossing is allowed. In case the next sub-lane in front is also occupied then check the next second sub-lane whether the backward and forward condition allows for taking a transverse crossing. In the case both left and right sub-lanes allow for a transverse crossing maneuver, select the option that is most advantageous.

5.2 Simulation Results

The simulations are performed on a closed track containing *6×1,800* site CUs, which represents a two-lane roadway section of width *7.5* meters and length *1,800* meters. Both pure traffic and mixed traffic scenarios are simulated. The pure traffic scenario (cars only) simulates the freeway context; whereas the mixed traffic scenario (cars and motorcycles) simulates the urban surface road context. We simulate for *600* time-steps. Initially, all the vehicles are set equally spaced or lined up from the end of the road section on the circular track, with speed *0* at time-step *0*. For pure traffic simulation in freeway, the maximum speed for cars is set according to the speed limits *(110 kph)* prevailing in Taiwan, that is, *31cells/sec*. For mixed traffic simulation in

surface road, the maximum speed is set as *17cells/sec (60 kph)* for cars and *14cells/sec (50 kph)* for motorcycles, respectively.

5.2.1 Pure car simulation

In order to analyze the effect of car lateral drift behaviors on traffic flow, we first compare simulated pure car traffic, with and without car drifts, on a periodic boundary 2-lane freeway roadway with maximum speed of *31 cell/sec*. All the parameter settings are identical except that the probability of cars' lateral drifts (P_{ld}) is set as *0* and *0.5* respectively. When simulations begin (*t=0*), cars are equally spaced but randomly locate on outer or inner side of both lanes. The derived simulation results, with and without introducing cars' lateral drifts, are both shown as flow-density relations (fundamental diagrams) in Figure 5-8.

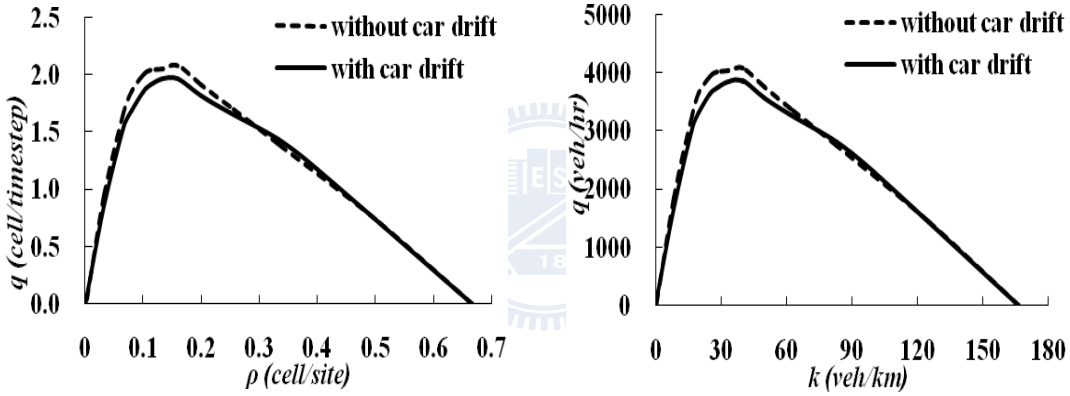

(a) Counted in cells/time-step (b) Counted in vehicles/hour

Figure 5-8. Fundamental diagrams for cars in pure traffic with and without introducing lateral drift.

As shown in Figure 5-8, both fundamental diagrams, with and without car drifts, are similar. Introducing the car lateral drift behavior will slightly lower the maximum flow. This is due to the rule that cars locating away from the lane markings need to take a little longer time (2 time-steps) to make a lane-change. However, there is less incentive for cars to take a lateral drift within the lane because there are no aside motorcycles sharing (disturbing) the same lane, the deviation in traffic flow is not so significant. Our results concur with Nagel *et al* (1998) that in spite of different lane-change rules being introduced, similar and realistic results are generated.

5.2.2 Mixed traffic simulation

For mixed traffic scenario with prevalence of cars and motorcycles, the effects of cars' lateral drifts should be more significant due to the complicated interactions between cars and motorcycles triggered. We examine the mixed traffic CA simulations under different car-motorcycle ratios (hereinafter, C:M). Owing to the complex nature of mixed traffic, one should be aware that even for a given general density *ρ(S)*, the mixed traffic may be composed of different C:M ratios. Given that one car always occupies *6×2* CUs, 6 times as large as one motorcycle which occupies *2×1* CUs, and that our simulations are performed on a closed track containing *6×1,800* CUs, for a given density, the relationship between number of cars (NC) and number of motorcycles (NM) can be expressed as a linear relationship, illustrated in Figure 5-9 and in Equation (5-1).

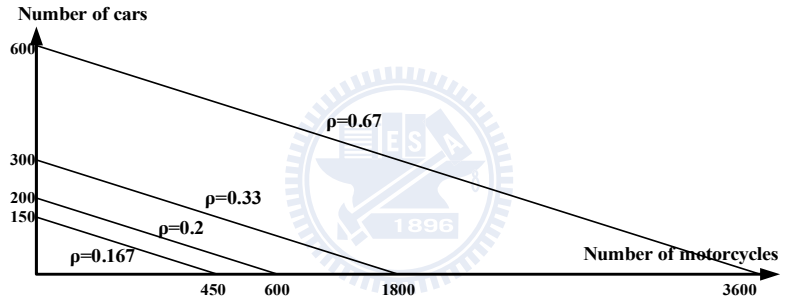

Figure 5-9. Linear relationship between numbers of cars and motorcycles under given general densities *(ρ(S))*.

$$6NC+NM=5400*\rho(S) \tag{5-1}$$

In order to analyze the impact of motorcycles' lateral drifts and transverse crossing behavior on the traffic, we deliberately fix the number of cars in each simulation and choose three C:M ratios (1:3, 1:1 and 3:1) for the following experiments. When initiating the simulations, cars line up from the end of road section in the left two sub-lanes of both lanes, while motorcycles line up aside in the right sub-lane of both lanes. Figure 5-10 is the derived fundamental diagrams wherein the vertical axis represents the car traffic flow and the horizontal axis shows the car density. One may find that as the number of motorcycles increases, larger deterioration of car flow can be identified. This

phenomenon indicates that introduction of more slow motorcycles will inevitably impair the cars' movement and thus results in a lower traffic flow.

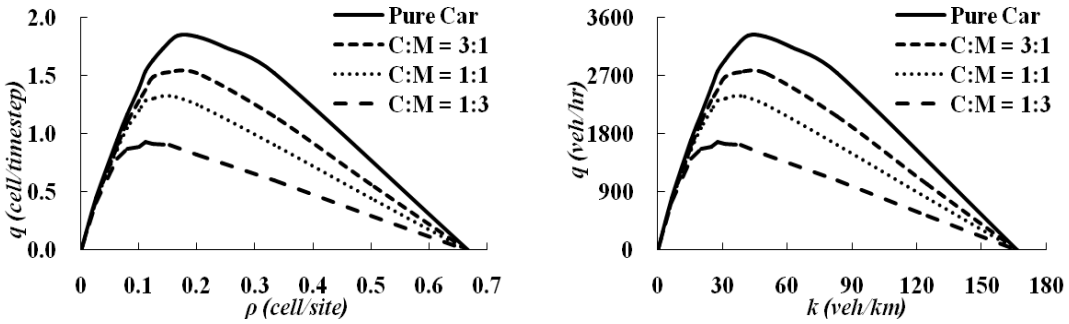

(a) Counted in cells/time-step (b) Counted in vehicles/hour

Figurr 5-10. Fundamental diagrams for cars in mixed traffic under various C:M ratios.

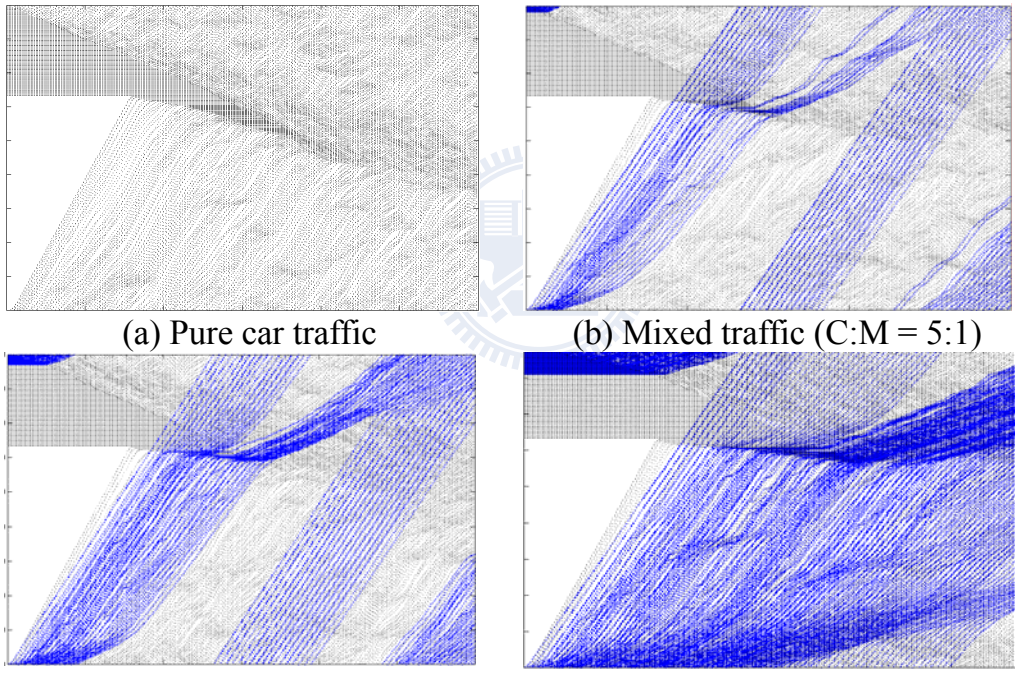

(a) Pure car traffic (b) Mixed traffic (C:M = 5:1)

(c) Mixed traffic (C:M = 3:1) (d) Mixed traffic (C:M = 1:1)

Figure 5-11. *x-t* plots in mixed traffic with different C:M ratios under car density *ρc =50 veh/km/ln*.

This phenomenon can be further illustrated through the simulated *x-t* plots, as shown in Figure 5-11, with fixed car density (*ρc=50 veh/km/ln*) in various C:M ratios. Both the trajectories of cars and motorcycles are displayed in Figure 5-11 where x-axis represents the time, advancing from left to right, and y-axis represents positions of vehicles, moving from bottom to top. For ease of distinguishing, the head positions of motorcycles are shown in blue dots

and cars in black dots therein. As shown in Figure 5-11(b)-(d), it is clear that even for low C:M ratios, the car platoons preset at *t=0* will disperse quickly as time marches. This phenomenon significantly differs from that in the *x-t* plot for pure car traffic, as shown in Figure 5-11(a). It is clear that when motorcycles in front with lower average speed will seriously impair the cars embarking from the downstream front of the initial platoon and, henceforth, on average, cars have to take longer time to arrive at the upstream front of the initial platoon. Consequently, the car platoon shrinks quickly and disperses in shorter time, implying a lower traffic flow for cars.

We further simulate similar scenarios proposed by Meng *et al* (2007), in which car density varies but with fixed motorcycle density. For comparison, we select identical motorcycle densities to those set by Meng *et al*. According to Figure 5-12, it is found that the derived car flow profiles are similar. Car flow constantly decreases as more motorcycles are introduced because of more interference to cars.

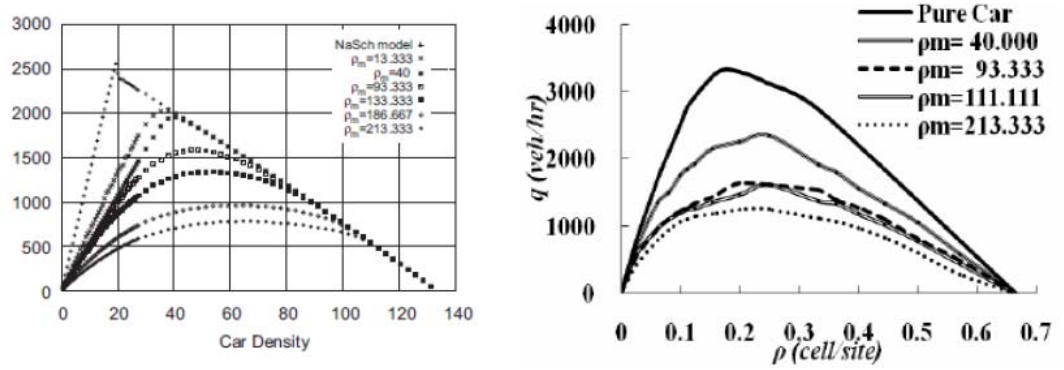

(a) Meng *et al* (2007) (b) This study

Figure 5-12. Comparison with existing of fundamental diagrams for cars under various motorcycle densities (ρm). The horizontal axis represents the preset car density ρc, vertical axis shows the simulated car flow.

In contrast, our simulation (Figure 5-13(b)) reveals that on each motorcycle curve (with fixed motorcycle density) shown in Figure 5-13, motorcycle flow also decreases as more cars are introduced. This phenomenon agrees with that by Meng *et al* (Figure 5-13(a)) and is consistent with the general rule that more congested traffic would couple with a lower flow.

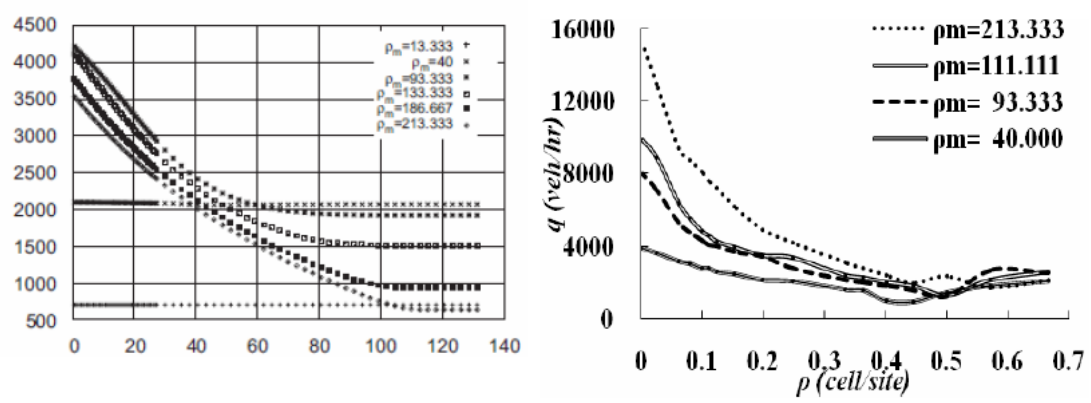

(a) Meng *et al* (2007) (b) This study

Figure 5-13. Comparison of fundamental diagrams for motorcycles under various motorcycle densities (ρm) with existing study. The horizontal axis represents the preset car density ρc, vertical axis shows the simulated motorcycle flow.

Nevertheless, we note that there is still some difference can be observed between regarding the simulated motorcycle flow. Our simulation reveals that for pure motorcycle traffic ($\rho c=0$), motorcycle flow stably increases as motorcycle density rises (see Figure 5-13(b)). This phenomenon differs from that in existing effort (Figure 5-13(a)). The reason for this deviation is that in the existing study only one lane with 3 sub-lanes is simulated whereas in the scenario we simulated there are 6 sites available in lateral in the roadway, therefore in our simulation motorcycle traffic pattern remains free flow even if motorcycle density (ρm) has reached *213 veh/km/ln* (or *35.5 veh/km/site*). Besides, our simulation also shows that with high car densities, motorcycle flow will converge to a certain margin, regardless of the preset motorcycle density, as shown in Figure 5-13(b). This phenomenon again significantly differs from that provided by Meng *et al* (Figure 5-13(a)). The cause of this deviation could be induced as the coupled effect of cars' lateral drifts and motorcycles' lateral drifts as well as transverse crossings, interpreted as follows.

In our simulation and in high car densities where road section is almost occupied by cars (e.g., $\rho > 0.6$, or $\rho c > 150$ *veh/km/ln*), owing to the cars' lateral drift behaviors, cars locate randomly on either left or right two sub-lanes of each lane, which stands as obstacles to the motorcycles. Nevertheless, owing

to the unique features of motorcycles' lateral drift and transverse crossing behaviors, motorcycles can always move further if situations allow. Since a slow car in right front will serve as a fixed or moving bottleneck for motorcycles, a converged trend for motorcycle flow is eventually observed. This also coincides with our previous work (Lan *et al*, 2009) and that by other researchers (Zhu *et al*, 2009) that when bottleneck is introduced, a plateau regime may be identified in the mid-density range, as shown in Figure 5-14.

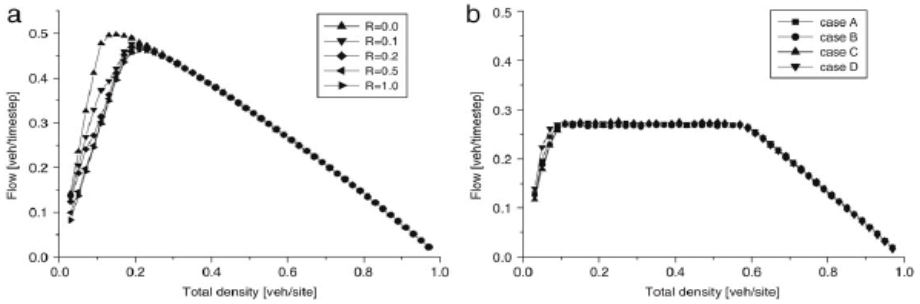

(a) Zhu *et al* (2009)-45% capacity loss. Left panel shows the simulation in which no bottleneck is presented; the right one represents the result when one bottleneck is introduced in the middle of roadway.

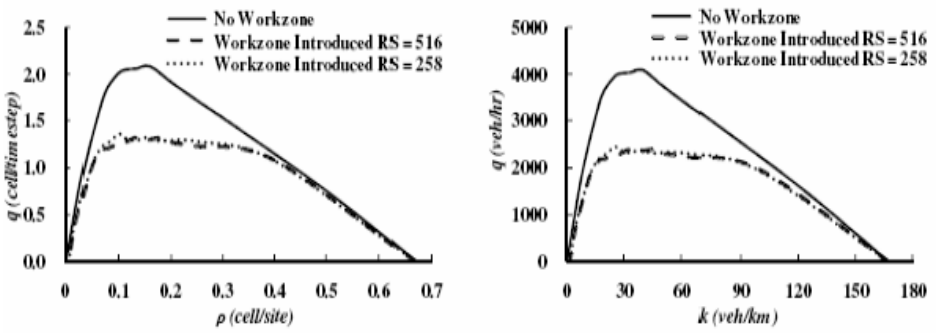

(b) Lan *et al* (2009)-43 % capacity loss

Figure 5-14. Simulated capacity loss suffered from introduction of one bottleneck in the middle of right lane. Note that a plateau regime may be identified in the mid-density range.

The lateral drift and transverse crossing behaviors of motorcycles can be further demonstrated through the simulated *x-t* plots, as shown in Figure 5-15. The scenario simulated is under *ρc=100 veh/km/ln* (congested traffic). As the simulation starts, cars line up from the end of road section on the left side of both lanes so as to form the initial car platoons. To clearly demonstrate the

motorcycle trajectories in such congested traffic conditions, only few motorcycles (say, *10 veh/km/ln*) are introduced, which also line up next to the car platoons on the right empty sub-lane of each lane.

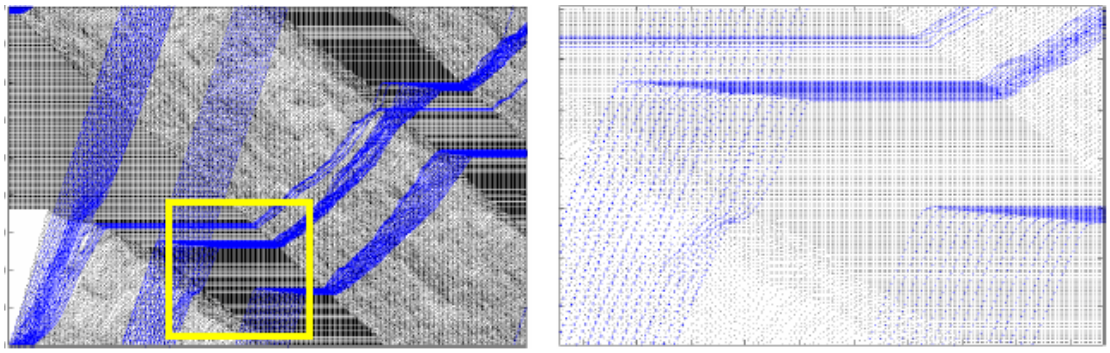

(a) Without motorcycles' transverse crossing.

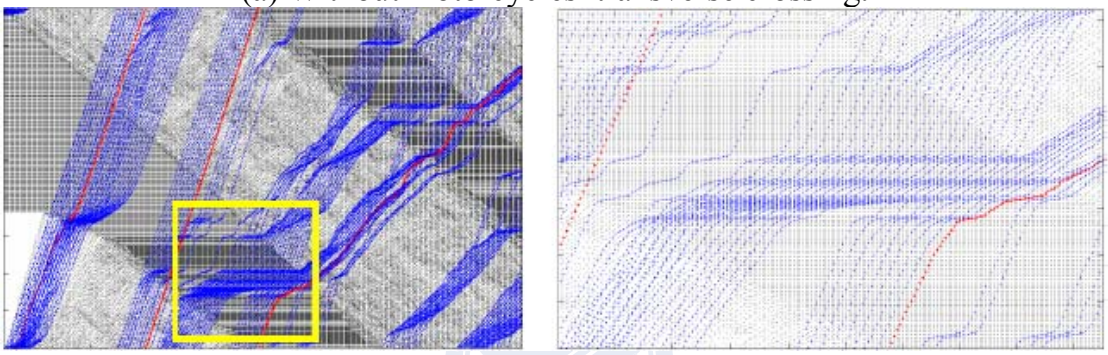

(b) With motorcycles' transverse crossing.

Figure 5-15. *x-t* plots in mixed traffic with and without motorcycles' transverse crossing behaviors *(ρc =100 veh/km/ln*, *ρm = 10 veh/km/ln*). The right panels zoom out the vehicular trajectories in the area marked in the left panels. The designated motorcycle is marked in red.

In Figure 5-15 both trajectories of cars and motorcycles are displayed, either with or without consideration of motorcycles' transverse crossing behaviors. In Figure 5-15(a), one can find that motorcycles break into the traffic jam when arriving at the upstream front as long as there is one empty site available laterally in each lane. However, due to the cars' lateral drift effect, when there is a car blocking the front site, motorcycles will get stuck in traffic jam until the front stationary cars reach the downstream front of traffic jam. In contrast, if motorcycles' transverse crossing behaviors are introduced, as shown in Figure 5-15(b), one can find the similar situation that motorcycles break into the traffic jam from its downstream front. But they are also capable of making transverse crossings to the next or next second sub-lane, even blocked by a stationary car in front, provided that the situations allow. After that,

motorcycles continuously move forward in consecutive time-steps until confronting another stationary car in front that may force them to take another transverse crossing again.

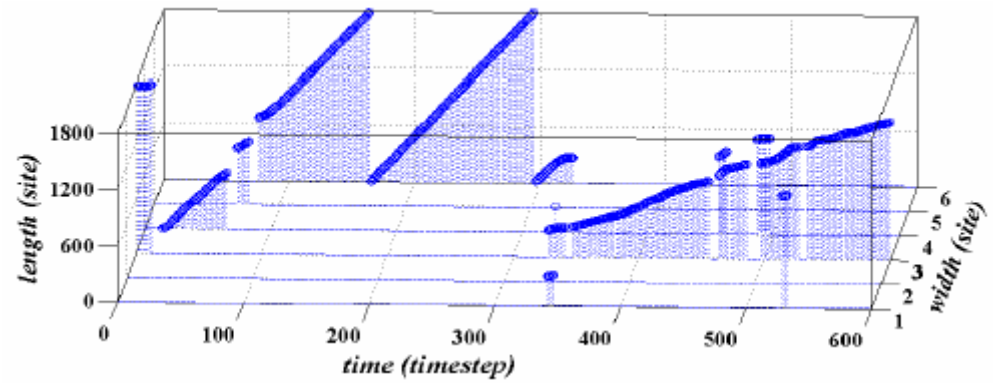

(a) 3-dimensional trajectory of the designated motorcycle.

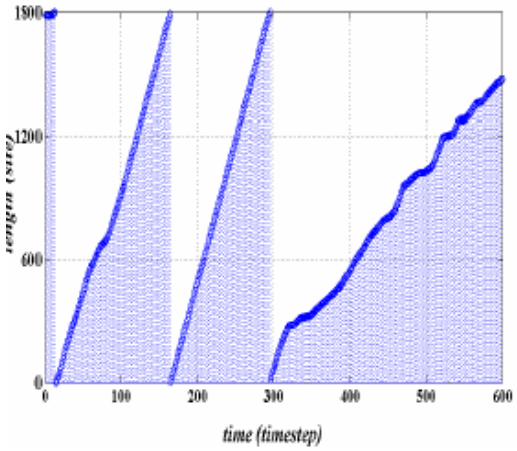

(b) Longitudinal position vs. time

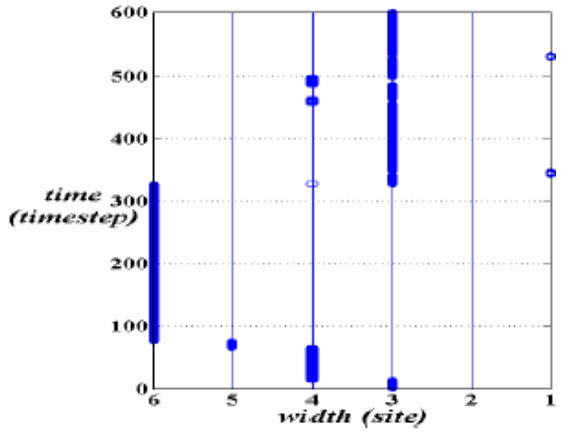

(c) Lateral position vs. time

Figure 5-16. Demonstration of simulated trajectories for the designated motorcycle marked in red in Figure 5-15(b).

Figure 5-16 further demonstrates the trajectory, both the longitudinal and lateral position, of a designated motorcycle marked in red in Figure 5-15(b). According to Figure 5-16, one may find that when simulation initiates, cars line up on the left two sub-lanes from the end of the circular track and leave the right sub-lane empty; therefore, in the early time-steps, motorcycles can easily break into the initial car platoon from its upstream front and smoothly move forward. As a consequence, only few motorcycles' transverse crossings can be observed. As time marches, more frequent car lateral drifts are triggered and henceforth transform into more bottlenecks for motorcycles. This means that there are increasing occasions that motorcycles have to take transverse

crossings through the stationary cars to move as forward as possible in later time-steps. This phenomenon can be supported by the significant difference of number of transverse crossings for the designated motorcycle in the first simulated *150s* and in the latter time-steps (*t=300-600s*). To recap, the simulated results have precisely reflected the real traffic features in mixed traffic contexts. The results also reveal the importance of introducing motorcycles' transverse crossing behaviors into the simulations, especially in congested mixed traffic.

5.3 Comparison of Global and Local Traffic Flows

By end of this chapter, we take comparison between the derived global and local traffic flow, similar to that for pure car traffic simulation. For comparison, in the cases for local traffic flow measurement we deliberately fix the motorcycle density as *93.333 veh/km/ln* and introduce four different car densities ($\rho(S)$= *0.06, 0.12, 0.25* and *0.5*) that represent car density of 1*6, 31, 62 and 125 veh/km/ln* respectively; as to reflect the traffic phenomena of free flow, synchronized flow and jam traffic. A virtual detector is arranged at the mid-way of roadway. Both derived AA and UMA local traffic flow data and global traffic flow are shown in Figure 5-17 and 5-18, respectively.

In both Figure 5-17 and 5-18, one may find that apparently the *1s* local traffic flow is not sufficient to cope with the global traffic flow since that the derived *1s* traffic flow widely scatters on both sides of global traffic curve. This phenomenon duplicates our finding in the previous simulation for pure car traffic, as mentioned in Section 4.7. In addition, the derived maximum traffic flow, the important index for traffic capacity, is also significantly exaggerated, for both cars and motorcycles. This is incurred by the fact that for short time measurement, the impact of local traffic features, either positive or negative, will be amplified; thus the derived maximum traffic flow deviates from reality. Next, as the duration of measurement increases (refer to Figure 5-17(b)-(c) & 5-18(b)-(c)), this amplification effect will be weakened. So the local data span, or say, the standard deviation from the global curve, will gradually converge to the global traffic flow curve, especially for the car flow. However, the maximum traffic flow remains over-estimated.

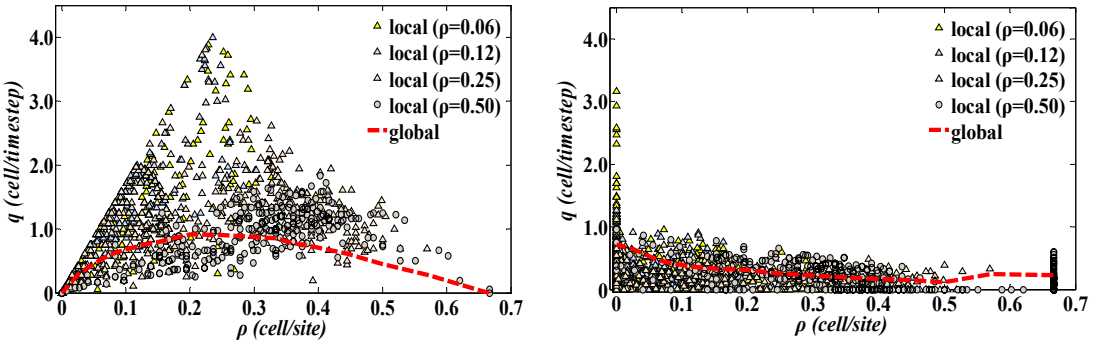

(a) *1s* data

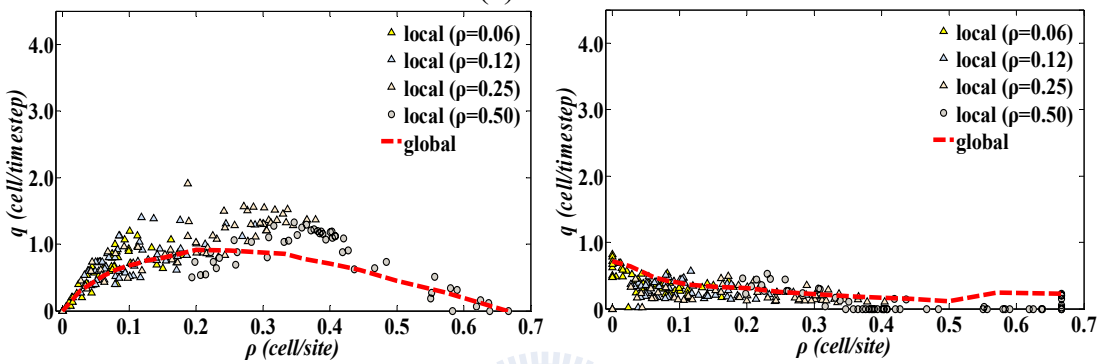

(b) *30s* AA data

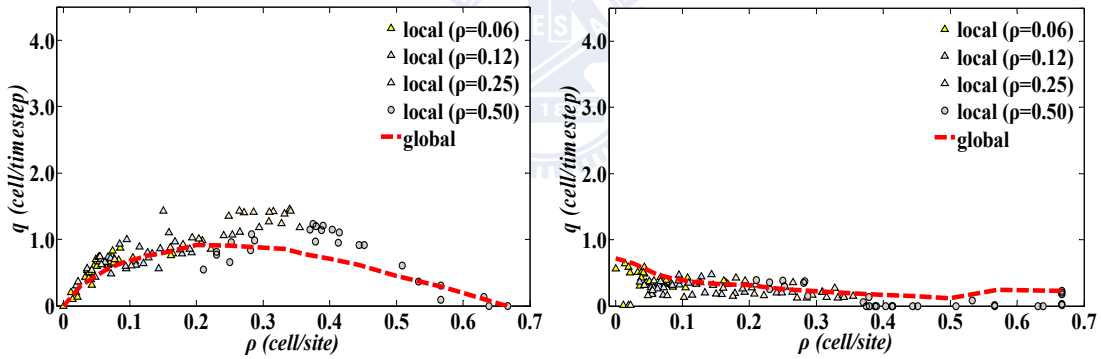

(c) *60s* AA data

Figure 5-17. Comparison of local traffic flow (AA averaged) and global traffic flow. The left panels depict the derived data for cars and the right panels for motorcycles.

Another finding worthy mentioned can be identified when compared simulation fundamental diagram between pure car and mixed traffic scenarios. In pure car case, basically all AA data and major part of UMA data cope with the global curve whereas in congested traffic regime generally speaking both AA and UMA local car flow data scatters below the global counterparts (refer to Figure 4-8 and 4-9). In contrast, in the mixed traffic simulation, most of time the AA and UMA car flow exceeds the global curve (refer to the left panels of

Figure 5-17 and 5-18). This phenomenon again evidences the fact that introduction of erratically moving motorcycles will significantly impair the car flow rate. As the consequence, in mixed traffic local interference raised by randomly moving motorcycles accumulates and finally leads to a lower global car flow rate.

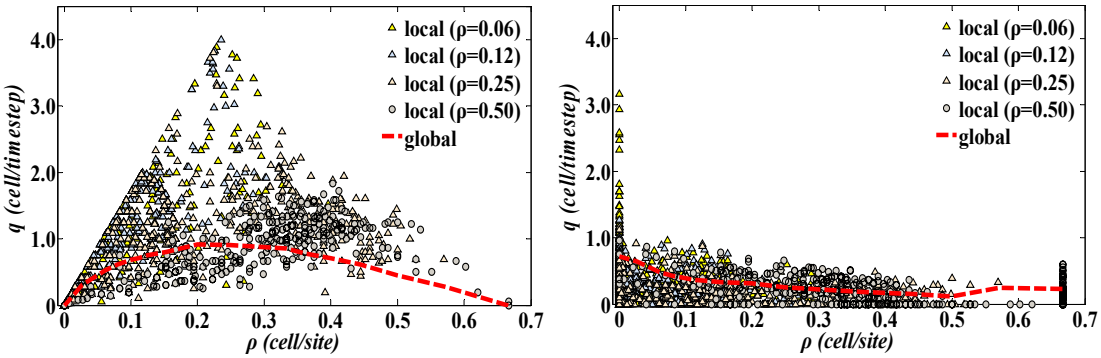

(a) *1s* data

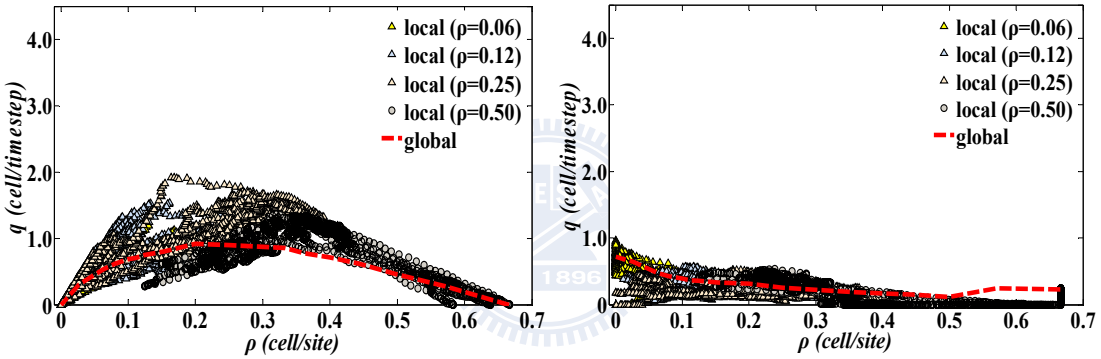

(b) *30s* UMA data

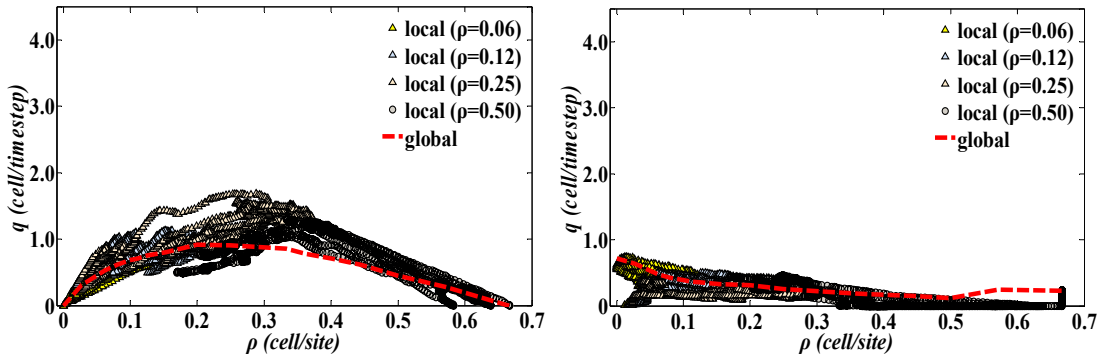

(c) *60s* UMA data

Figure 5-18. Comparison of local traffic flow (UMA averaged) and global traffic flow. The left panels depict the data for cars and the right panels for motorcycles.

It is our experience that the UMA car flow data is efficient in reflecting the local traffic phase transitions (see Chapter 4 for details). However, this

merit will reversely turn into one weakness if we are interested in surveying the global traffic features, both in pure car and mixed traffic simulation. When scrutinize the local traffic data, it is found that the AA data reveals better simulation quality since it scatters in a smaller region in the neighborhood of global curve. It still makes sense since that for AA car flow, the impact of some local noise with short lifetime will be limited to few simulated data because independent time intervals are considered. In contrast, by nature the UMA, a local defect will yield more expansive influence and henceforth force more UMA car flow data biases from the global curve.

As for motorcycles, there is no solid finding can be located between the local flow rate and global traffic curve. Basically local motorcycle data, no matter AA or UMA, presents poor performance for catching the global information. This low performance remains even the duration of measurement increases. (refer to the right panels of Figure 5-17 and 5-18). This result substantiates the high unpredictability of motorcycles' movement. It is our opinion the random nature of motorcycles' movement stands as a serious impediment for defining a clear linkage between local and global motorcycle traffic flow in mixed traffic analysis.

5.4 Simulation on Signalized Intersections

In addition to the analysis of aforementioned mixed traffic comprised by cars and motorcycles, the traffic conditions around signalized intersections may also be simulated. Figure 5-19 shows our preliminary simulation results for pure cars on one closed road section, in which two traffic signals are introduced, with no offset and with *30s* signal offset.

According to Figure 5-19, one may find the stop-and-start behavior, the induced traffic queue is successfully reflected. The speed variation of the randomly designated vehicle in both *x-t* diagrams also cope with the preset deceleration capacity. Figure 5-19 also reveals that the offset of signal timing bring significant influence to vehicles since the speed profile of the designated vehicle varies considerably. It is recommended that additional survey can be analyzed, including the impact of different signal offset, relationship between

the cycle time and the distance between signals. Besides, the dilemma zone can also be considered so as locate the adequate yellow light time.

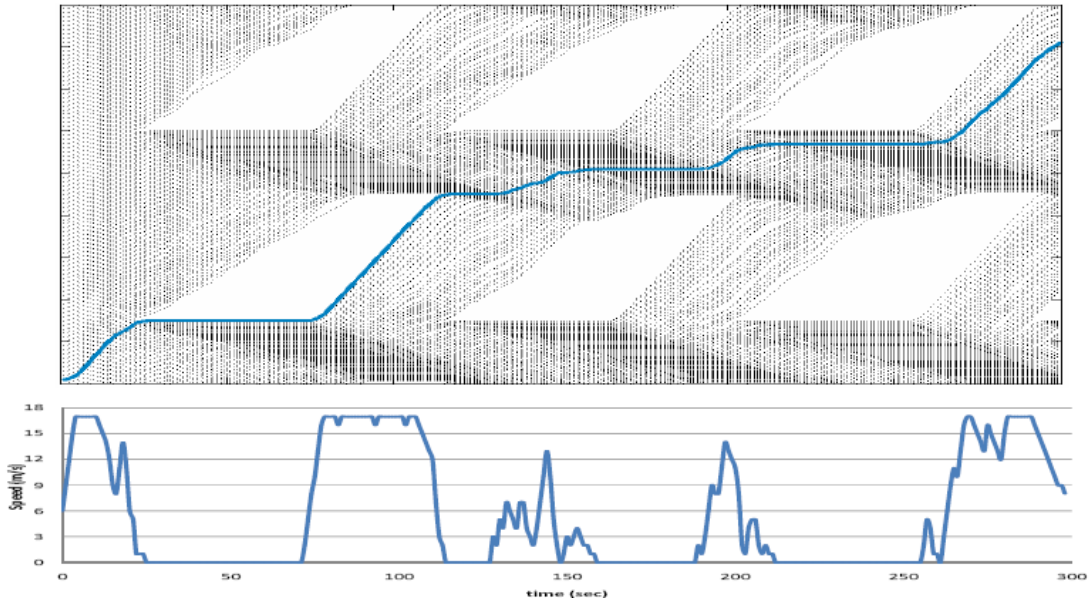

(a) Scenario simulated: pure car traffic, $\rho(S)=0.12$, cycle time=$90s$, $y=3s$,$r=60s$, no offset)

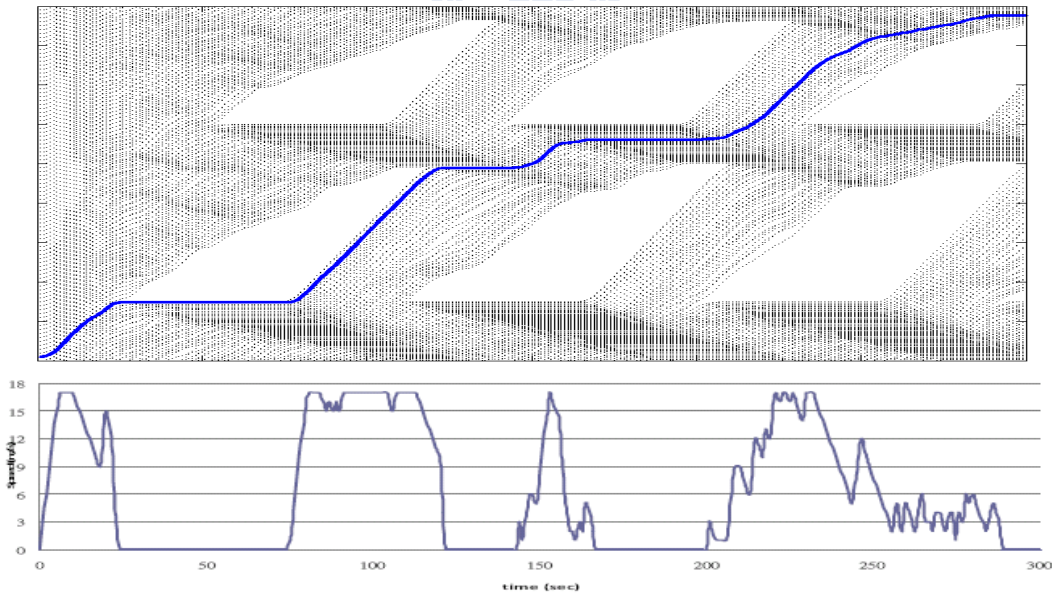

(b) Scenario simulated: pure car traffic, $\rho(S)=0.12$, cycle time=$90s$, $y=3s$,$r=60s$, signal offset =$30s$)

Figure 5-19. Preliminary simulation results of one roadway with two signalized intersections introduced, without and with *30s* signal offset. The upper panels show the simulated *x-t* diagram; the lower panels depict the speed variation of designated vehicle in the upper panels.

5.5 Summary

In this chapter we extend the applicability of the refined CA model by further developing a sophisticated CA model to simulate the mixed traffic comprising cars and motorcycles. Owing to the enhanced resolution of finer cell system, slight speed variations and effects of both the vehicular length and width can be simulated. Most importantly, the frequently observed lateral movements of cars and motorcycles as well as the wide transverse crossing behavior of motorcycles are carefully deliberated with the corresponding CA update rules thereby added. Comparisons with existing studies authenticate the validity of our sophisticated CA model while simulating the pure car traffic scenarios. The simulations show that the unique lateral movements of motorcycles that yet investigated in any existing studies, such as breaking into two moving cars and transverse crossing through two stationary cars in traffic jam, can be precisely illustrated. Our simulations reveal the prevailing motorcycles' transverse crossing behaviors in mixed congested traffic. The maximum car flow decreases with the increase of motorcycle density because the increased interaction among different vehicles will impair the flow efficiency. This conclusion agrees with the study of Meng *et al* (2007).

Besides, our simulation for mixed traffic shows that the derived local traffic car flow, both the AA and UMA ones, inclines to overestimated the reality, this conspicuously opposes to that in our previous simulation for pure car traffic. The lower global traffic flow may be suffered from the fact that it reflects in essence the congregation of frequent interference between cars and motorcycles. As for motorcycles traffic flow, so far no clear linkage between the global and local traffic pattern is found, most likely induced by the erratic nature of motorcycle movement.

CHAPTER 6 CONCLUSIONS AND RECOMMENDATIONS

The objectives of this study are to develop an effective CA model capable of simulating urban traffic with different vehicle kinds and/or sizes introduced. To fulfill this, in this study first the generalized traffic parameters are devised, as to take both vehicular width and roadway width into consideration. Following that, as inspired by grid generation theory that is popular in computational fluid dynamics, the concept of refined grid is also proposed. As such, impact of various vehicle features (e.g., sizes, maximum speed, and acceleration and deceleration ability, etc) can be carefully addressed. Furthermore, for sake of reflecting the realistic deceleration behavior of vehicles, this study further proposes a novel and effective mechanism to rectify the abrupt deceleration behaviors that prevailed in most existing CA models. The methodology for deriving local traffic flow characteristics from the refined CA models are also suggested and discussed in details. Upon these amendments, one important urban traffic scenario yet seldom explored to date—mixed traffic comprised by cars and motorcycles, is investigated. The CA update rules corresponding to the observed lateral movements of cars and motorcycles as well as the wide transverse crossing behavior of motorcycles are thereby carefully deliberated. The following simulations show that the unique lateral movements of motorcycles that yet investigated in any existing studies can be precisely illustrated. The summary of work performed in this study and some important findings arisen since are described in Section 6.1. Recommendations for further research are drawn in Section 6.2.

6.1 Conclusions

1. Our first finding is that the applicability of the common adopted formula for estimating 1-D vehicular average speed *(q=kv*, enclosed as Equation (2-4)) should be carefully re-scrutinized. Equation (2-4) was originally developed by scholars in the field of fluid mechanics upon the fact that fluid flow is continuous. However, traffic flow by nature is no longer continuous but in essence a congregation of discrete particles (vehicles). Besides, by definition the 1-D local traffic flow-*q(x)* is a time-based parameter measured at fixed point whereas the local traffic density-*k(t)* is a space-based traffic parameter

for an certain instant. So Equation (2-4) may be valid under some very restricted conditions, i.e., homogeneous state in which each vehicle equips with identical features (e.g., same headway and identical speed, etc), or in the limit as both the space and time measurement intervals approach zero. If neither of those situations holds, then use of the formula to calculate speed can give misleading results, which would not agree with empirical measurements. This issue is worthy for further survey because Equation (2-4) has often been uncritically applied to situations that exceed its validity.

2. This study endeavors in the development of one novel CA model which is capable of simulating various urban traffic contexts. CA modeling can be categorized as one branch of microscopic approach that interrelationship of individual vehicle movements interacted with other vehicles are described. There are several obvious advantages for selecting CA model for traffic simulations. First, the rule set that describes the update of each vehicle is minimal. Next, the update schedule, being completely parallel, is simple, too. Besides, it is capable of reproducing important entities prevailed in real traffic, e.g., density-flow relation and the traffic jam in congested traffic. The most important and subtle reason is the computation explicitness. It means that data is directly updated and iterations for converging to some predefined residue are never required. The beneficial aspect of using explicit computation is that it minimizes the simulation time and thereby increases likelihood for real-time simulation. Besides, the developed CA model also enjoys an additional advantage—flexibility. Owing the refined grid system devised, the proposed CA model is capable of handling different traffic scenarios and complex mixed traffic that comprised by various vehicle types.

3. Our most important finding is that this study substantiates the criticality of grid system utilized in CA simulation, which in essence represents the resolution (i.e., the degree of detail or the acceptable approximation of traffic phenomena one expects to analyze) may be achieved. The coupled low resolution of existing CA models strictly circumvents their applicability. Aside from their popularity in the past, there is continuous criticism for the significantly limited application of existing CA models to freeway traffic and the deficiency to uncover delicate vehicular behavior from microscopic

viewpoint. This may mainly suffers from the comparatively coarse grid system implemented by most existing CA models, in which each lane is only allowed to be occupied by a single vehicle laterally. It is obvious that such coarse grid system is difficult to implement for mixed traffic simulations where vehicles have different sizes (length and width) and/or possess distinct behavior. The coarse grid system also stands as the crucial barrier for implementing existing CA models into urban traffic simulation in which usually low speed limits prevail and oftentimes vehicles move with slight speed variations. As a matter of fact, few efforts are available hitherto to evaluate the impact of different vehicular width through CA simulation. Consequently, it is comprehensible that a refiner grid system will be the crucial prerequisite for expanding the application of CA modeling to mixed traffic prevailed in urban streets.

4. To contend with such restriction, in this study we first propose a refined 3-D grid system that considers time and both vehicular length and width. As the onset the concept of *"common unit"* (CU), *"cell"* and *"site"* are defined to serve as the universal basis, the basic unit for describing different vehicle sizes and for roadways, respectively. The size of site and cell can be selected in accordance with the scenarios simulated as well as the resolution of simulation required. The sole restriction is that the size of both basic site and basic cell should be identical, i.e., to be the common unit. Besides, to cope with this 3-D grid system, we also extend the 2-D traffic parameters that proposed by Daganzo (1997) to be 3-dimensional. The spatiotemporal traffic flow ($q(S)$ and $\rho(S)$) are therefore defined. Our following simulations evidence the superiority of the proposed novel CA model since that it successfully liberates the above-mentioned restriction and is able to handle the violate traffic phenomena in real world. Based upon the enhanced resolution and the increased flexibility of the proposed CA model, analysis of different traffic contexts, such as such as the mixed traffic comprised by vehicles of various sizes and sophisticated traffic phenomena in urban area, can be performed successfully.

5. Our next effort is to rectify the common defect of existing CA models that vehicles abruptly decelerate when encountered with stationary obstacles or traffic jams. In most existing CA models though the idea of limited

acceleration is implemented; deceleration limitation has seldom been considered. Actually, most CA models simply considered a collision-free criterion explicitly by imposing arbitrarily large deceleration rates, which can be far beyond the practical braking capability under prevailing pavement and tire conditions. Despite simulations through the existing CA models show satisfactory outcome in capturing essential features of traffic flows, most existing CA simulations also revealed that, for sake of collision prevention, a vehicle can take as short as *1s* to come to a complete stop, even from a full speed, apparently exceeding the vehicular deceleration ability. We concur with that existing CA model has led to satisfactory outcome if only long-term average traffic features are concerned or only macroscopic traffic phenomena or global traffic parameters are examined because the effects of locally realistic deceleration have been smoothed out. However, if we scrutinize in detail the microscopic traffic parameters or the neighbourhood of some unexceptional scenarios, such as an accident vehicle or a work zone blocking the partial highway lanes, it is evident that the deceleration rule in existing CA models require further revisions. For this purpose we propose the piecewise-linear movement within each time-step to replace conventional particle-hopping movement adopted in most previous CA models. Upon this adjustment and coupled with refined grid system, the limited deceleration are then introduced which is essence the extension of classic car–following concept proposed by Pipes (1953) and/or Forbes (1958). The main deviation is that appropriate deceleration is determined through Newton's kinematics rather based on a given time headway. The validation simulations show that the proposed novel CA model can fix the unrealistic deceleration behavior, and thus to be more in line with the real world vehicular movement, In addition, the proposed CA model is also capable of revealing Kerner's three-phase traffic patterns and phase transitions among them.

6. Upon all the effort mentioned above, this study further develops a sophisticated CA model to simulate the mixed traffic comprising cars and motorcycles. Owing to the enhanced resolution of the refined cell system, slight speed variations and effects of both the vehicular length and width can be simulated. Most importantly, the frequently observed lateral movements of cars and motorcycles as well as the wide transverse crossing behavior of

motorcycles are carefully deliberated with the corresponding CA update rules thereby added. Comparisons with existing studies authenticate the validity of our sophisticated CA model while simulating the pure car traffic scenarios. The simulations show that the unique lateral movements of motorcycles that yet investigated in any existing studies, such as breaking into two moving cars and transverse crossing through two stationary cars in traffic jam, can be precisely illustrated. Our simulations reveal that maximum car flow decreases with the increase of the motorcycle density since the increased interaction among different vehicles will impair the flow efficiency. Furthermore, the simulations also underline the necessity for introducing motorcycles' transverse crossing behaviors into the simulations of mixed traffic, especially in congested traffic.

7. This study also constructs the methodology for extracting local traffic flow rate and occupancy from the refined grid system. The derived local traffic flow and occupancy, both AA and UMA averaged, is carefully validated through the simulation of selected complex scenarios. The results show that for pure car traffic scenarios, the UMA traffic parameters are efficient in reflecting the complicated traffic phase transitions whereas the AA traffic data is consistent with the three-phase traffic theory. In addition, through the comparison between global and local traffic fundamental diagrams, it is found that in uninterrupted traffic the AA traffic data has potential to be a useful proxy to reflect the global traffic features, though only local traffic information is gathered. In contrast, in mixed traffic comprised by cars and motorcycles, the local traffic data, both AA and UMA averaged, has comparatively poorer performance to reflect the global situation. Another important finding is that the derived local car flow usually is lower in pure car traffic, but higher in mixed traffic cases, than its global counterparts. This may be induced by the random erratic nature of motorcycles' movement in mixed traffic. When introducing more motorcycles in mixed traffic, the local interference raised by randomly moving motorcycles will accumulate and finally leads to a lower global car flow rate. This conclusion again evidenced that introduction of motorcycles will significantly impair the car flow rate.

8. This study serves as the pioneer effort in defining the refined CA model. The proposed novel CA model successfully breaks through the inherent defect of most previous CA models and therefore effectively extends the possible applicability of CA modeling. Thus this study shed some light for the future analysis of traffic modeling. It is looked forward that via the proposed refined CA model different traffic control strategies for separate traffic context can be efficiently evaluated before practical implementation.

6.2 Recommendations

Although this study has taken a gigantic step in the development of CA modeling, some limitations should be noticed to point out and the potential application needs to be addressed for further research.

1. In this study only circular track with periodic boundary is surveyed, for both pure car and mixed traffic. The major advantage therein is that vehicle density can be specified for each simulation. However, in real world roadways are never a close loop but instead, always with open boundaries. So our first recommendation is some CA model with open boundaries should be considered; for instance, that similar to effort by Chiou *et al* (2009). Some potential impediment might be encountered for simulating open boundary scenario, e.g., the measures to handle the enormous data output and the expected high demand for computer performance, since for open boundary traffic scenarios the number of vehicles into simulation will constantly increase. One possible remedy, other than selecting a high performance computer, is a high level implementation of computer memory management.

2. In this study, drivers' heterogeneity is simply simulated via the preset probability. However, it is recommended that more delicate heterogeneity among drivers should be considered. For example, according to field observation, there is significant heterogeneity in the maximum speed among different motorcyclists, which leads to frequent lateral drift behaviors even in non-congested flow. Therefore, the effect of various maximum speeds for motorcycles can be considered in the further study. Besides, in this study it is assumed that all drivers obey the preset safety criteria—always remain an

adequate safety gap to the front. We also assume that all drivers follow the regulatory speed limits. These postulations may deviate from the reality. Therefore, it is recommended that the fuzzy theory that reflects real drivers' behaviors be introduced in the further, similar to the effort by Lan *et al* (2001).

3. Several other avenues can be identified for future study. In this study the car locating away from the lane markings is assumed taking 2 time-steps to make a lane-change. This is deemed a conservative restriction. Moreover, each vehicle only evaluates the traffic conditions around for the next one or two time-steps could also be too conservative. One possible remedy is introducing the anticipation of surrounding conditions with more extended time-steps, according to our field observations. Finally, in real world a car is possible to locate in the center area of each lane, a little different from either left or right two sub-lanes as described in this study. This may further discourage the aside motorcycles from sharing the same lane. To deal with this phenomenon, implementation of more refined cell system might be necessary. It, however, will significantly increase the computation burden and require more simulation time. A trade-off between simulation efficiency and realism of simulation deserves further evaluation.

4. It is understood that oftentimes drivers will not follow the lateral movement update rules prescribed in this study. Some aggressive drivers will try to take lane change even there is no allowable backward gap in the target lane. This phenomenon is commonly observed in congested traffic, for example, in the on-ramp zone during rush hours. Nevertheless, it is still possible the turn signal will be turned on before they take lane change. As the consequence, it is recommended that the effect of turn signal should be considered when construct the lateral movement update rules.

5. In this study, the roadway section under simulation each lane is always set as 3.75 meter in width, for both freeway and urban street scenarios. However, in real world the lane widths of urban streets oftentimes are lesser. In these cases, inevitably smaller site/cell size must be considered. For instance, for a narrow street lane with width close to 3 meters, it can be set with 3 sites laterally with site width of 1 meter. Also the cell size can be selected in light

of the various lengths and widths of different vehicle types. Besides, according to field observation, for motorcyclists the perceived gap between two still cars that allowing for passing through may not be a fixed value. When approaching the upstream front of traffic jams, motorcycles with high speeds will be more hesitated to break inside the traffic jams since moving with high speed raises the possibility of hitting the still cars aside when passing through them. Therefore, it is proposed that for future study when a motorcycle determines if a breaking inside the traffic jam should be taken, the concept of *"effective gap"* that introducing the effect of magnitudes of motorcycle's velocity may be considered.

6. Our simulations reveal that the local AA traffic flow has the potential to serve as the proxy for reflecting realistic traffic flow (i.e., its global counterpart), especially for uninterrupted traffic. However, the adequate time interval for taking AA average is not identified yet. It is recommended further research in this regard might be considered, since in light of the difficulty for global traffic measurement, the local traffic feature is much easier and cheaper to be located.

NOTATION TABLE

Variable/ parameter	Definition
a	*Acceleration*
a_k	*Maximum acceleration capacity of k-type vehicle*
D	*Maximum deceleration capacity of k-type vehicle*
$\ddot{x}$	*Second time derivative of displacement*
A	*Two-dimensional domain under consideration with size* $L \times T$
$\lvert A \rvert$	*'Area' of A*
AA	*Arithmetic average*
d	*Space headway*
$d(S)$	*The total distance traveled by all cells in domain S*
d_m	*Preset deceleration capacity*
d_n^{eff}	*Effective distance of* n^{th} *vehicle*
g	*Distance (Gap)*
$H_i(t)$	*Head location of vehicle i at instant t*
$l(A)$	*Averaged vehicular length*
L	*Longitudinal length of area A and/or domain S*
L_d	*Detection zone length*
ms	*Location of virtual detector*
S_0	*Original front gap at instant t*
S_1	*Front gap at instant t+1*
S_{final}	*Evaluated front gap after time steps* t_{req}
$T_i(t)$	*Tail location of vehicle i at instant t*
W	*Transverse width of roadway, counted in sites*
VL	*Vehicular length, counted in cells*
VW	*Vehicular width, counted in cells*
x	*Position of* n^{th} *vehicle*
h	*Time headway*
k	*Traffic density*
N	*Total number of sites arranged in domain S*
$N_0(t)$	*Total number of sites occupied by cells (vehicles) at the instant t*
NC	*Number of cars in mixed traffic of given* $\rho(S)$
NM	*Number of motorcycles in mixed traffic of given* $\rho(S)$

$O(t)$	*Accumulated local occupancy at instant t*
P	*Probability:*
P_b	*Probability accounting for impact of decelerating vehicle in near front*
P_0	*Probability reflecting delay-to-start behaviors of vehicles that stuck in traffic jam*
P_d	*Probability for other situations*
P_{lc}	*Probability of lane-change*
P_{ld}	*Probability of lateral drift*
q	*Traffic flow rate*
$q(A)$	*Two dimensional traffic flow over area A*
$q(S)$	*Generalized traffic flow over domain S*
$q(t)$	*Accumulated local traffic flow at instant t*
$rand()$	*Randomly generated number*
S	*Spatiotemporal domain under consideration with size* $L \times W \times T$
$\|S\|$	*'Volume' of S*
S_n	*Status identifier of* n^{th} *vehicle, representing its brake light status*
t	*Time:*
h_k	*Preset time threshold of vehicle of type k for reflecting effect of synchronized distance*
$t(A)$	*Accumulated time of* $N_0(t)$ *spent in area A for all times simulated*
$t(S)$	*Accumulated time of* $N_0(t)$ *spent in S for all times simulated*
$t_h = d_n / v_n(t)$	*Time headway of* n^{th} *vehicle to front*
$t_s=min(v_n(t),h_k)$	*Final time threshold for initiating the consideration of front brake light effect, taking vehicular speed into consideration*
t_{st}	*Accumulated time of* n^{th} *vehicle that stuck in traffic jam*
$t_{k,c}$	*Time threshold of vehicle of type k for initiating delay-to-start behavior*
τ	*Safe time gap for collision prevention*
T	*Observed time period*
UMA	*Un-weighted moving average*
v	*Speed*
c_n	*Safe speed of* n^{th} *vehicle*

$v(S)$	*Generalized space-mean speed over domain S*
V_0	*Original speed at instant t*
V_1	*Updated speed at instant t+1, per Equation (3-10)*
$\dot{x}$	*First time derivative of displacement (Speed)*
ρ	*Density*
$k(A)$	*Generalized density over area A*
$\rho(S)$	*Generalized density over domain S*
ρc	*Generalized density of car in mixed traffic over domain S*
ρm	*Generalized density of motorcycle in mixed traffic in domain S*
Δ	*Minimum clearance for the follower*
Suffix	
anti	*Anticipated (speed)*
k	*Type of vehicles: k=0, motorcycle; k=1, car*
ma	*Un-weighted moving average*
max	*The maximum value*
n	*The n^{th} vehicle*
n+1	*Vehicle in front*
req	*Time required for deceleration*
t	*Instant t*
Superscript	
1(2)	*The next (the next second) site considered for a lateral movement*
b	*Downstream*
f	*The nearby upstream in the next or next second site*
eff	*Effective*
opt	*Optimum*
r(l)	*The right (left) lane or site considered for lane change or lateral drift*

REFERENCES

1. Ahmed, K.I, Ben-Akiva, M.E., Houtsopoulos, H.N. & Mishalani, R.G. (1997) Models of freeway lane changing and gap acceptance behavior. *Proceedings of the 13th International Symposium on the Theory of Traffic Flow and Transportation*.
2. Aron, M. (1988) Car following in an urban network: simulation and experiments. *Proceeding of Seminar D 16th PTRC Meeting*, pp. 27-39.
3. Bando, M., Hasebe, K., Nakayama, A., Shibata, A. & Sugiyama, Y. (1995) Dynamical model of traffic congestion and numerical simulation. *Physical Review E,* Vol. 51, pp. 1035-1042.
4. Bando, M., Hasebe, K., Nakanishi, K., Nakayama, A., Shibata, A. & Sugiyama Y. (1998) Analysis of optimal velocity model with explicit delay. *Physical Review E,* Vol. 58, pp. 5429-5435.
5. Barlovic, R., Santen, L., Schadschneider, A. & Schreckenberg, M. (1998) Metastable states in cellular automata for traffic flow. *Eur. Phys. J. B*, Vol. 5, pp. 793-800.
6. Benjamin, S.C., Johnson, N.F., & Hui, P.M. (1996) Cellular Automaton Models of Traffic Flow Along a Highway Containing a Junction. *Journal of Physics A: Mathematical & General,* Vol. 29, pp. 3119-3127.
7. Bham, G.H. & Benekohal, R.F. (2004) A high fidelity traffic simulation model based on cellular automata and car-following concepts. *Transportation Research Part C*, Vol. 12, pp. 1-32.
8. Bick, J. H., Newll, G.F. (1960) A continuum model for two-directional traffic flow. *Q. Applied Mathematics*, Vol. 18, pp. 191-204.
9. Brackstone, M. & McDonald, M. (1999) Car-following: a historical review. *Transportation Research Part F*, Vol. 2, pp. 181-196.
10. Burghout, W. (2004) Hybrid microscopic-mesoscopic traffic simulation. Doctoral Dissertation. *Royal Institute of Technology, Stockholm, Sweden* 2004.
11. Cremer, M. & Ludwig, J. (1986) A fast simulation model for traffic flow on the basis of Boolean operations. *Mathematics and Computers in Simulation*, Vol. 28, pp. 297-303.
12. Chakroborty, P. & Kikuchi, S. (1999) Evaluation of the general motors

based car-following models and a proposed fuzzy inference model. *Transportation Research Part C*, Vol. 7, pp. 209-235.

13. Chandler, R.E., Herman, R. & Montroll, E.W. (1958) Traffic dynamics: studies in car following. *Operations Research,* Vol. 6, pp. 165-184.
14. Chiou, Y.C., Lan, L.W., Chung, J.C., Hsu, C.C. & Lin, Z.H. (2009) Two-stage fuzzy logic control for ramp metering with cellular automaton simulation. J*ournal of Chinese Institute of Transportation*, Vol. 21, pp. 1-24.
15. Chowdhury, D., Santen, L. & Schadschneider, A. (2000) Statistical physics of vehicular traffic and some related systems. *Physics Reports,* Vol. 329, pp.199-329.
16. Chowdhury, D. & Schreckenberg, M. (1999) Self-organization of traffic jams in cities-Effects of stochastic dynamics and signal periods. *Physical Review E*, Vol. 59, R1311-1314.
17. Chowdhury, D., Wolf, D.E. & Schreckenberg, M. (1997) Particle-hopping models for two-lane traffic with two kinds of vehicles: effects of lane-changing rules. *Physica A*, Vol. 235, pp. 417-439.
18. Cooper, P. J. & Zheng, Y. (2002) Turning gap acceptance decision-making: the impact of driver distraction. *Journal of Safety Research*, Vol. 33, pp. 321-335.
19. Daganzo, C.F. (1993) The cell-transmission model. Part I: A simple representation of highway traffic. *Research report UCB-ITS-PRR-93-7, Institute of Transportation Studies,* University of California, Berkeley.
20. Daganzo, C.F. (1994) The cell transmission model: a dynamic representation of highway traffic consistent with the hydrodynamic theory. *Transportation Research Part B*, Vol. 28, pp. 269-287.
21. Daganzo, C.F. (1995) A finite difference approximation of the kinematic wave model of traffic flow. *Transportation Research Part B,* Vol. 29B, pp. 261-276.
22. Daganzo, C.F. (1997) *Fundamentals of Transportation and Traffic Operations*. Elsevier Science Ltd. Pergamon.
23. Daganzo, C.F. (1999) The lagged cell-transmission model. *International Symposium on Transportation and Traffic Theory,* Ceder, A. (Ed.), New York, Pergamon.
24. Daganzo, C.F. (2002) A behavioral theory of multi-lane traffic flow. Part I:

Long homogeneous freeway sections. *Transportation Research Part B*, Vol. 36, pp. 131-158.

25. Ebersbach, A., Schneidery, J., Morgensterny, I. & Hammwohner, R. (2000) The influence of trucks on traffic flow- An investigation on the Nagel-Schreckenberg model. *International Journal of Modern Physics C,* Vol. 11, pp. 837-842.
26. Edie, L.C. (1960) Car following and steady state theory for non-congested traffic. *Operations Research*, Vol. 9, pp. 66-76.
27. Evans, L. & Rothery, R. (1973) Experimental measurement of perceptual thresholds in car following. *Highway Research Record*, Vol. 64, pp. 13-29.
28. Ez-Zahraouy, H., Jetto, K. & Benyoussef, A. (2004) The effect of mixture lengths of vehicles on the traffic flow behavior in one-dimensional cellular automaton. *European Physical Journal B*, Vol. 40, pp. 111-117.
29. Forbes, T.W., Zagorski, H.J., Holshouser, E.L. & Deterline, W.A. (1958) Measurement of driver reactions to tunnel conditions. *Highway Research Board, Proceedings,* Vol. 37, pp. 345-357.
30. Fukui, M. and Ishibashi, Y. (1996) Traffic flow in 1D cellular automaton model including cars moving with high speed. *Journal of the Physical Society of Japan*, Vol. 65, pp. 1868-1870.
31. Gazis, D., Herman, R. & Maradudin, A. (1960) The problem of the amber signal light in traffic flow. *Operations Research,* Vol. 8, pp. 112-132.
32. Gazis, D.C., Herman, R. & Potts, R.B. (1959) Car following theory of steady state traffic flow. *Operations Research,* Vol. 7, pp. 499-505.
33. Gazis, D.C., Herman, R. & Rothery, R.W. (1961) Nonlinear follow the leader models of traffic flow. *Operations Research,* Vol. 9, pp. 545-567.
34. Gipps, P.G. (1981) A behavioral car following model for computer simulation. *Transportation Research Part B*, Vol. 15, pp. 105-111.
35. Hamed, M.M., Easa, S.M. & Batayneh, R.R. (1997) Disaggregate Gap-Acceptance Model for Unsignalized T-Intersections. *J. Transportation. Engineering*, Vol. 123, pp. 36-42.
36. Helly, W. (1959) Simulation of bottlenecks in single lane traffic flow. *Proceedings of the Symposium on Theory of Traffic Flow*, Research Laboratories, General Motors, pp. 207-238.
37. Ho, F.S. & Ioannou, P. (1996) Traffic flow modeling and control using

artificial neural networks. *IEEE Control Systems Magazine*. Vol. 16, pp. 16-26.

38. Hoogendoorn, S.P. (1999) Multi-class continuum modeling of multilane traffic flow. *PhD thesis, Delft University of Technology*, The Netherlands.
39. Hsu, C.C., Lin, Z.S., Chiou, Y.C. & Lan, L.W. (2007) Exploring traffic features with stationary and moving bottlenecks using refined cellular automata. *Journal of the Eastern Asia Society for Transportation Studies,* Vol. 7, pp. 2246-2260.
40. Jia, B., Jiang, R., Wu, Q.S. & Hu, M.B. (2005) Honk effect in the two-lane cellular automaton model for traffic flow. *Physica A*, Vol. 348, pp. 544-552.
41. Jiang, R. & Wu, Q.S. (2003) Cellular automata models for synchronized traffic flow. *Journal of Physics A: Mathematical & General,* Vol. 36, pp. 381–390.
42. Jiang, R. & Wu, Q.S. (2004) Spatial–temporal patterns at an isolated on-ramp in a new cellular automata model based on three-phase traffic theory. *Journal of Physics A: Mathematical & General,* Vol. 37, pp. 8197–8213.
43. Jiang, R. & Wu, Q.S. (2006) A stopped time dependent randomization cellular automata model for traffic flow controlled by traffic light. *Physica A*, Vol. 364, pp. 493-496.
44. Kerner, B.S. (1998) Experimental features of self-organization of traffic flow. *Physical Review Letter*, Vol. 81, pp. 3797-3800.
45. Kerner, B.S. (2004) *The Physics of Traffic*. Springer-Verlag, Berlin Heidelberg.
46. Kerner, B.S. (2005) Control of spatiotemporal congested traffic patterns at highway bottlenecks. *Physica A*, Vol. 355, pp. 565-601.
47. Kerner, B.S. & Klenov, S.L. (2002) A microscopic model for phase transitions in traffic flow. *Journal of Physics A: Mathematical & General,* Vol. 35, pp. 31-43.
48. Kerner, B.S., Klenov, S.L. & Wolf, D.E. (2002) Cellular automata approach to three-phase traffic theory. *Journal of Physics A: Mathematical & General*, Vol. 35, pp. 9971-10013.
49. Kerner, B.S. & Klenov, S.L. (2004) Spatiotemporal patterns in heterogeneous traffic flow with variety of driver behavioral characteristics

and vehicle parameters. *Journal of Physics A: Mathematical & General,* Vol. 37, pp. 8753-8788.

50. Kerner, B.S. & Rehborn, H. (1996) Experimental features and characteristics of traffic jams. *Physical Review E*, Vol. 53, pp. 1297-1300.
51. Kikuchi, S. & Chrkroborty, P. (1993) Car-following model based on fuzzy inference system. *Transportation Research Record*, Vol. 1365, pp. 82-91.
52. Klar, A. & Wegener, R. (1999) A hierarchy of models for multilane vehicular traffic I & II: modeling. *SIAM Journal of Applied Mathematics*, Vol. 593, pp. 983-1001.
53. Knospe, W., Santen, L., Schadschneider, A. & Schreckenberg, M. (1999) Disorder effects in cellular automata for two-lane traffic. *Physica A,* Vol. 265, pp. 614-633.
54. Knospe, W., Santen, L., Schadschneider, A. & Schreckenberg, M. (2000) Towards a realistic microscopic description of highway traffic. *Journal of Physics A: Mathematical and General,* Vol. 33, pp. 477-485.
55. Knospe, W., Santen, L., Schadschneider, A. & Schreckenberg, M. (2002) A realistic tow-lane traffic model for highway traffic. *Journal of Physics A: Mathematical and General,* Vol. 35, pp. 3369–3388.
56. Kometani, E. & Sasaki, T. (1959) Dynamic behavior of traffic with a nonlinear spacing-speed relationship. *Proceedings of the Symposium on Theory of Traffic Flow*, Research Laboratories, General Motors, pp. 105-119.
57. Krauss, S. & Wagner, P. (1997) Metastable states in a microscopic model of traffic flow. *Physical Review E,* Vol. 55, pp. 5597-5602.
58. Lan, L.W. & Chang, C.W. (2003) Moving behaviors of motorbikes in mixed traffic: particle hopping model. *Journal of the Eastern Asia Society for Transportation Studies*, Vol. 5, pp. 23-37.
59. Lan, L.W. & Chang, C.W. (2005) Inhomogeneous cellular automata modeling for mixed traffic with cars and motorcycles. *Journal of Advanced Transportation*, Vol. 39, pp. 323-349.
60. Lan, L.W. & Hsu, C.C. (2005) Using cellular automata to explore spatiotemporal traffic patterns. *Proceedings, 10th International Conference of Hong Kong Society for Transportation Studies*, pp. 210-219.
61. Lan, L.W. & Hsu, C.C. (2006) Formation of spatiotemporal traffic patterns

with cellular automaton simulation. *Transportation Research Board, 85th Annual Meeting,* Washington, DC, in CD-ROM.

62. Lan, L.W. & Yeh, H.H. (2001) Car following behavior for drivers with non-identical risk aversion: ANFIS approach. *Journal of the Chinese Institute of Civil and Hydraulic Engineering*, Vol. 13, pp. 427-434.
63. Lan, L.W., Chiou, Y.C., Hsu, C.C. & Lin, Z.S. (2007) Spatiotemporal mixed traffic patterns with revised cellular automaton simulation. *Proceedings, 12th International Conference of Hong Kong Society for Transportation Studies*, pp. 133-142.
64. Lan, L.W., Chiou, Y.C., Lin, Z.S. & Hsu, C.C. (2008) A new cellular automaton model in traffic simulation at a highway work zone. *Proceedings, 10th International Conference on Applications of Advanced Technologies in Transportation,* Athens, in CD-ROM.
65. Lárraga, M.E., del Río, J.A. & Alvarez-lcaza, L. (2005) Cellular automata for one-lane traffic flow modeling. *Transportation Research Part C*, Vol. 13, pp. 63-74.
66. Leclercq, L. & Moutari, S. (2007) Hybridization of a class of "second order" models of traffic flow. *Simulation Modeling Practice and Theory*, Vol. 15, pp. 918-934.
67. Lee, H.K., Barlovic, R., Schreckenberg, M. & Kim, D. (2004) Mechanical restriction versus human overreaction triggering congested traffic states. *Physical Review Letter,* Vol. 92, pp. 238702-1~238702-4.
68. Leonard, D.R., Power, P. & Taylor, N.B. (1989) CONTRAM: structure of the model. *Transportation Research Laboratory,* Crowthorn.
69. Lertworawanich, P. & Elefteriadou, L. (2001) Capacity estimations for Type B weaving areas based on gap acceptance. *Transportation Research Record*, Vol. 1776, pp. 23-34.
70. Leung, S. & Starmer, G. (2005) Gap acceptance and risk-taking by young and mature drivers, both sober and alcohol-intoxicated, in a simulated driving task. *Accident Analysis and Prevention*, Vol. 37, pp. 1056–106.
71. Lighthill, M.H. & Whitham, G.B. (1955) On kinematic waves: a theory of traffic flow on long crowed roads. *Proceedings of the Royal Society, Series A*, No. 229, pp. 317-345.
72. Liu, G., Lyrintzis, A.S. & Micahalopoulus, P.G. (1998) Improved high-order

model for freeway traffic flow. *Transportation Research Record*, Vol. 1644, pp. 37-46.

73. Mahmassani, H. & Sheffi, Y. (1981) Using gap sequences to estimate gap acceptance functions. *Transportation Research Part B*, Vol. 15, pp. 143-148.
74. Mallikarjuna, C. & Ramachandra Rao, K. (2006) Area Occupancy characteristics of heterogeneous traffic. *Transportmetrica*, Vol. 2, pp. 223-236.
75. Mallikarjuna, C. & Ramachandra Rao, K. (2008) Cellular Automata Model for Heterogeneous Traffic. *Journal of Advanced Transportation,* Vol. 43, pp. 321-345.
76. May, A.D. (1990) *Traffic Flow Fundamentals*. Prentice-Hall Inc., New Jersey.
77. Meng, J.P., Dai, H.Q., Dong, L.Y. & Zhang, J.F. (2007) Cellular automaton model for mixed traffic flow with motorcycles. *Physica A,* Vol. 380*,* pp. 470-480.
78. Michaels, R.M. (1963) Perceptual factors in car following. *Proceedings of the Second International Symposium on the Theory of Road Traffic Flow,* pp. 44-59.
79. Munial, P.K. & Pipes, L.A. (1971) Propagation of on-ramp density perturbations on unidirectional two and three-lane freeways. *Transportation Research*, Vol. 5, pp. 241-255.
80. Nagel, K. & Schreckenberg, M. (1992) A cellular automaton model for freeway traffic. *Physics I*, Vol. 2, pp. 2221-2229.
81. Nagel, K. (1996) Particle-hopping models and traffic flow theory. *Physical Review E*, Vol. 53, pp. 4655-4672.
82. Nagel, K. (1998) From particle-hopping models to traffic flow theory. *Transportation Research Record*, Vol. 1644, pp. 1-9.
83. Nagel, K., Wolf, D.E., Wagner, P. & Simon, P. (1998) Two-lane traffic rules for cellular automata: A systematic approach. *Physical Review E*, Vol. 58, pp. 1425-1437.
84. Payne, H.J. (1971) Model of freeway traffic and control. *Mathematics of Public Systems*, Vol. 1, pp. 51-61.
85. Pipes, L.A. (1953) An operational analysis of traffic dynamics. *Journal of*

Applied Physics, Vol. 24, pp. 74–281.

86. Pollatscheka, M.A., Polus, A. & Livneh. M. (2002) A decision model for gap acceptance and capacity at intersections. *Transportation Research Part B*, Vol. 36, pp. 649-663.
87. Pottmeier, A., Barlovic, R., Knospe, W. & Schadschneider, A. (2002) Localized defects in a cellular automaton model for traffic flow with phase separation. *Physica A*, Vol. 308, pp. 471-482.
88. Reiter, U. (1994) Empirical studies as basis for traffic flow models. *Proceedings of the Second International Symposium on Highway Capacity*, Vol. 2, pp. 493-502.
89. Rickert, M., Nagel, K., Schreckenberg, M. & Latour, A. (1996) Two lane traffic simulations using cellular automata. *Physica A*, Vol. 231, pp. 534-550.
90. Richards, P.I. (1956) Shock waves on highway. *Operations Research,* Vol. 4, pp. 42-51.
91. Sheu, J.B. (2008) A quantum mechanics-based approach to model incident-induced dynamic driver behavior. *Physica D*, Vol. 237, pp. 1800-1814.
92. Simon, P. & Nagel, K. (1998) Simplified cellular automaton model for city traffic. *Physical Review E*, Vol. 58, pp. 1286-1295.
93. Sprott J. C. (2003) *Chaos and time-series analysis*. Oxford University Press, New York.
94. Spyropoulou, I. (2007) Modeling a signal controlled traffic stream using cellular automata. *Transportation Research Part C,* Vol. 15, pp. 175-190.
95. Takayasu, M. & Takayasu, H. (1993) 1/f Noise in a traffic model. *Fractals,* Vol. 1, pp. 860-866.
96. Teodorović D. (1994) Fuzzy sets theory applications in traffic and transportation. *European Journal of Operational Research*, Vol. 74, pp. 379-390.
97. Transportation Research Board (2000) *Highway Capacity Manual,* National Research Council, Washington D.C.
98. Wagner P., Nagel, K. & Wolf, D.E. (1997) Realistic multi-lane traffic rules for cellular automata. *Physica A,* Vol. 234, pp. 687-698.
99. Wang, B.H., Wang, L., Hui, P.M. & Hu, B. (2000) The asymptotic steady

states of deterministic one-dimensioned traffic flow models. *Physica B*, Vol. 27, pp. 237-239.

100. Wang, R., Jiang, R., Wu, Q.S. & Liu, M. (2007) Synchronized flow and phase separations in single-lane mixed traffic flow. *Physica A,* Vol. 378, pp. 475-484.

101. Watanabe, M.S. (2003) Dynamical behavior of a 2D cellular automaton with signal processing - Effect of signal period. *Physica A,* Vol. 328, pp. 251-260.

102. Wolf, D.E. (1999) Cellular automata for traffic simulations. *Physica A*, Vol. 263, pp. 438-451.

103. Wong, G.C.K. & Wong, S.C. (2002) A multi-class traffic flow model – an extension of LWR model with heterogeneous drivers. *Transportation Research Part A*, Vol. 36, pp. 827-841.

104. Wang, R., Jiang, R., Wu, Q.S. & Liu, M. (2007) Synchronized flow and phase separations in single-lane mixed traffic flow. *Physica A*, Vol. 378, pp. 475-484.

105. Xing, J. (1995) A parameter identification of a car following model. *Proceedings of the Second World Congress on ATT,* Yokohama, November, pp. 1739-1745.

106. Yamg, M.L., Liu, Y.G. & You, Z.S. (2007) A new cellular automata model considering finite deceleration and braking distance. *Chinese Physics Letters*, Vol. 24, pp. 2910-2913.

107. Yin, H., Wong, S.C., Xu, J. and Wong, C.K. (2002) Urban traffic flow prediction using a fuzzy-neural approach. *Transportation Research Part C,* Vol. 10, pp. 85-98.

108. Zhang, H.M. (1998) A theory of nonequilibrium traffic flow. *Transportation Research Part B*, Vol. 32, pp. 485-498.

109. Zhang, H.M. & Kim, T. (2005) A car-following theory for multiphase vehicular traffic flow. *Transportation Research Part B*, Vol. 39, pp. 385-399.

110. Zhu, H.B., Lei, L. & Dai, S.Q. (2009) Two-lane traffic simulations with a blockage induced by an accident car. *Physica A*, Vol. 388, pp. 2903-2910.

APPENDIX

Publications related to dissertation research

A. Refereed Papers

1. Lan, L.W., Chiou, Y.C., **Lin, Z.S.** and Hsu, C.C. (2010) Cellular automaton simulations for mixed traffic with erratic motorcycles behaviors. *Physica A*, Vol. 389, pp. 2077-2089. (**SCI**, 2009 Impact Factor: 1.562)
2. 邱裕鈞、藍武王、鐘仁傑、許志誠、**林日新** (2010) 兩階段模糊邏輯控制之匝道儀控細胞自動機模擬 *運輸學刊* 第二十二卷第二期，pp. 159-184. (**TSSCI**).
3. Lan, L.W., Chiou, Y.C., **Lin, Z.S.** and Hsu, C.C. (2009) A refined cellular automaton model to rectify impractical vehicular movement behavior. *Physica A*, Vol. 388, pp. 3917-3930.(**SCI**, 2009 Impact Factor: 1.562)
4. Hsu, C.C., **Lin, Z.S.**, Chiou, Y.C. and Lan, L.W. (2007) Exploring traffic features with stationary and moving bottlenecks using refined cellular automata. *Journal of the Eastern Asia Society for Transportation Studies,* Vol. 7, pp. 2246-2260. (**Yasoshima Prize**: Best paper award out of 507 accepted papers)

B. Conference Papers

1. Lan, L.W., Chiou, Y.C., **Lin, Z.S.** and Hsu, C.C. (2008) A new cellular automaton model in traffic simulation at a highway work zone. *Proceedings, 10th International Conference on Applications of Advanced Technologies in Transportation, Athens.*
2. Lan, L.W., Chiou, Y.C., Hsu, C.C. and **Lin, Z.S.** (2007) Spatiotemporal mixed traffic patterns with revised cellular automaton simulation. *Proceedings, 12th International Conference of Hong Kong Society for Transportation Studies*, pp. 133-142.

C. Research Reports

1. 藍武王、邱裕鈞、許志誠、**林日新** (2009)，異質混合車流細胞自動機模式之研究 (III)：市區道路環境測試與驗證，國科會研究報告，計畫編號：NSC 95-2211-E-451-015-MY3。

2. 藍武王、邱裕鈞、許志誠、**林日新** (2008)，異質混合車流細胞自動機模式之研究 (II)：高速公路環境測試與驗證，國科會研究報告，計畫編號：NSC 95-2211-E-451-015-MY3。
3. 藍武王、邱裕鈞、許志誠、**林日新** (2007)，異質混合車流細胞自動機模式之研究(I)：細胞自動機基本規則與車輛時空特性之關係，國科會研究報告，計畫編號：NSC 95-2211-E-451-015-MY3。

林日新 簡歷

教育

國立台灣師大附中	(1981)
國立成功大學航空工程系 學士	(1985)
國立成功大學航空太空工程研究所 碩士	(1987)
國立交通大學交通運輸研究所 博士	(2010)

考試與證照

期貨人員考試	(1996)
專技人員高考 航空工程技師	(1997)
民航人員特考 三等航務科	(2006)

獲獎

東亞運輸協會(EASTS)年會 最佳論文獎(Yasoshima Prize)	(2007)

經歷

國防部中山科學研究院第二研究所 助理研究員	(1988~1996)
遠東航空公司機務處 工程師	(1997)
交通部航空器設計製造適航驗證中心 正工程師	(1998~2005)
交通部民航局飛航標準組 飛航安全檢查員	(2006)
交通部民航局台南航空站航務組 航務員	(2007)
交通部民航局飛航標準組 技士	(2008~)